Pilot study concerning the behaviour of coastal supply on the Dutch Wadden Island of Terschelling

M.Sc. Thesis Report, Part 1

August 1995

N.F. Kersting

TU Delft
Delft University of Technology

Faculty of Civil Engineering
Hydraulic and Geotechnical Engineering Division
Hydraulic Engineering Group

This work was carried out as part of the NOURTEC project. It was funded jointly by Delft University of Technology, Rijkswaterstaat and the Commission of the European Communities, Directorate General for Science, Research and Development, under contract MASTII-CT93-0049

Summary

In 1993 an artificial sand nourishment was carried out at the coast of Terschelling. The total amount of supply was deposited in a trough between two breaker bars, up to a level of about NAP -5m.

The present report gives a prediction of the development of the coast in the next 10 years.

For this, a mathematical model has been used, in which the coast is characterized by 3 lines, roughly representing the beach, the inshore and the area between NAP-6m and NAP-9m. The model simulates the diffusion of the supply in longshore and cross-shore direction.

Two extremes cases are considered:

1. cross shore diffusion without longshore diffusion

2. cross shore diffusion with longshore diffusion

   The diffusitivity is determined by the wave climate and by a sand transport formula (the Svašek variation of the CERC formula, (Bijker & Svašek, 1969)).
   As the effect of the curvature of the inshore on the curvature of the beach is not included in this case, the diffusitivity of sand along the beach will be rather overestimated.

Starting from the assumptions, given in section 2.2, the computations give the result that the present erosion of the beach, estimated as 2.75 m/year, will be compensated for 13 years in case 1 and for 7 years in case 2. The values of the longshore diffusitivity constants have apparently a rather high influence on the results of the computations.

The effect on the beach of the supply between NAP-9m and NAP-6m is found to be approximately one third of the result with the supply at the inshore (between NAP-6m and NAP-3m). The recommendation is therefore to carry out the supply as high as economically attractive.

Contents **page**

List of figures

Number **page**

List of symbols

c_b	wave celerity at the breaker line
d_1	depth of separation plane between zone 1 and 2
d_2	depth of separation plane between zone 2 and 3
d_3	depth of lower limit of zone 3
g	acceleration of gravity
h_1	height of zone 1
h_2	height of zone 2
h_3	height of zone 3
h_b	breaker depth
$H_{b,sig}$	significant wave height at the breaker line
i	counter of steps in x-direction
j	number of zone
L_1	characterizing mean line of the beach zone
L_2	characterizing mean line of the inshore zone
L_3	characterizing mean line of the deeper part
n	counter of time steps
n_b	ratio (group velocity / phase velocity) at the breaker line
S_1	longshore transport in the beach zone
S_2	longshore transport in inshore zone
S_3	longshore transport in the deeper part
S_{y1}	cross-shore transport from the beach zone (1) to the inshore (2)
S_{y2}	cross-shore transport from inshore (2) to the deeper part (3)
S_x	sediment transport in longshore direction
Δt	timestep
T	wave period
x	coordinate along the coast
y_1	distance to initial equilibrium position of line 1
y_2	distance to initial equilibrium position of line 2
y_3	distance to initial equilibrium position of line 3
y_∞	total accretion if nourishment is equally distributed over the profile
y(z)	distance of profile to a reference line
z	height above the y-axis
Δx	step in x-direction
φ_0	angle of wave approach at deep water
φ_b	angle of wave approach at the breaker line

1 Introduction

The Northern part of the Dutch coast consists of a chain of barrier islands (Figure 1). On the island of Terschelling the central part of the North Sea coast is eroding over the last decades.

As for other eroding parts of the Dutch coast, artificial nourishment was proposed as remedy. In this particular case a special type of nourishment has been proposed and executed in 1993, namely a shore-face nourishment. Instead of a sandsupply on the beach, the total amount of sand was deposited in a trough between two breaker bars.

Apart from protecting the area by compensating for the erosion, the nourishment is a study object and is therefore meticulously monitored and reported. The project has been carried out as part of the NOURTEC project in which investigators of the Netherlands, Germany and Denmark participate in the scope of the MASTII EU project. In order to answer several questions concerning the planning and behaviour of the nourishment Rijkswaterstaat has commissioned various institutions to compute predictions with the COMOR and UNIBEST-models and with the n-line modelling. The latter will be described in the present report and results will be presented.

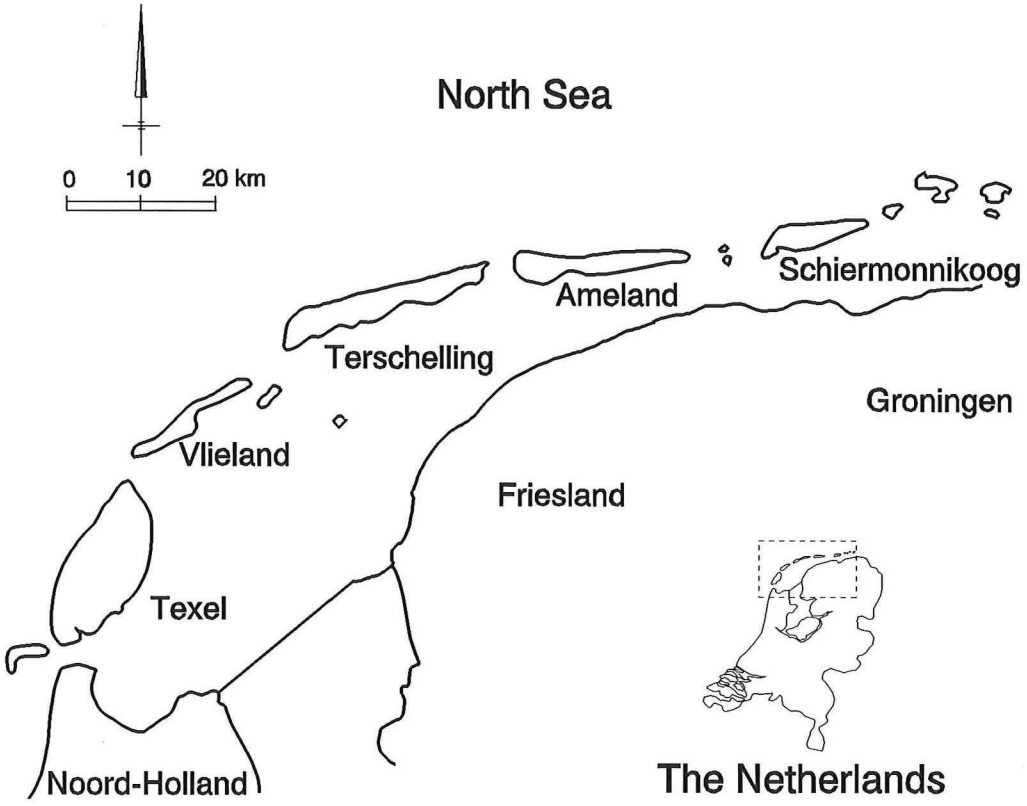

Figure 1 *The location of Terschelling.*

2 Description of Terschelling and assumptions

§2.1 Description of situation.

The study area is located between the ranges km 10 and km 24 of the RSP-line (?). In this area a nourishment has been carried out in 1993 between beachpole km 14.8 and km 19.8 involving an amount of 2 million m^3 sand.

Volumetric measurements and computations show natural sandlosses between 1982 and 1991 of 0.117 million m^3 each year (Van Vessem, 1992) between the levels NAP[1] +3 m and NAP -5.25 m. Another study (Noordstra, 1992) gives an amount of 0.106 million m^3/year. These values show a linear trend. Depth averaged (between NAP +3m and NAP -5.25m) over the distance between km 14.8 and km 19.8, this may be interpreted as a coastal retreat of about 2.75 m/year.

To compensate for the erosion in 10 years normally a beach nourishment would be carried out with a total amount of about 1 million m^3. With a shoreface nourishment twice as much material is needed to obtain the same lifetime expectation of 10 years. However, still the latter way of supply is anticipated to be economic, because the sand can be dumped directly at the site.

Along the North Sea coast of Terschelling three parallel breaker bars exist which propagate in a seaward direction. The outer bar decreases in height during this seaward motion and disappears after roughly 10 years; thus the motion can be considered as periodical with a 10-year period.

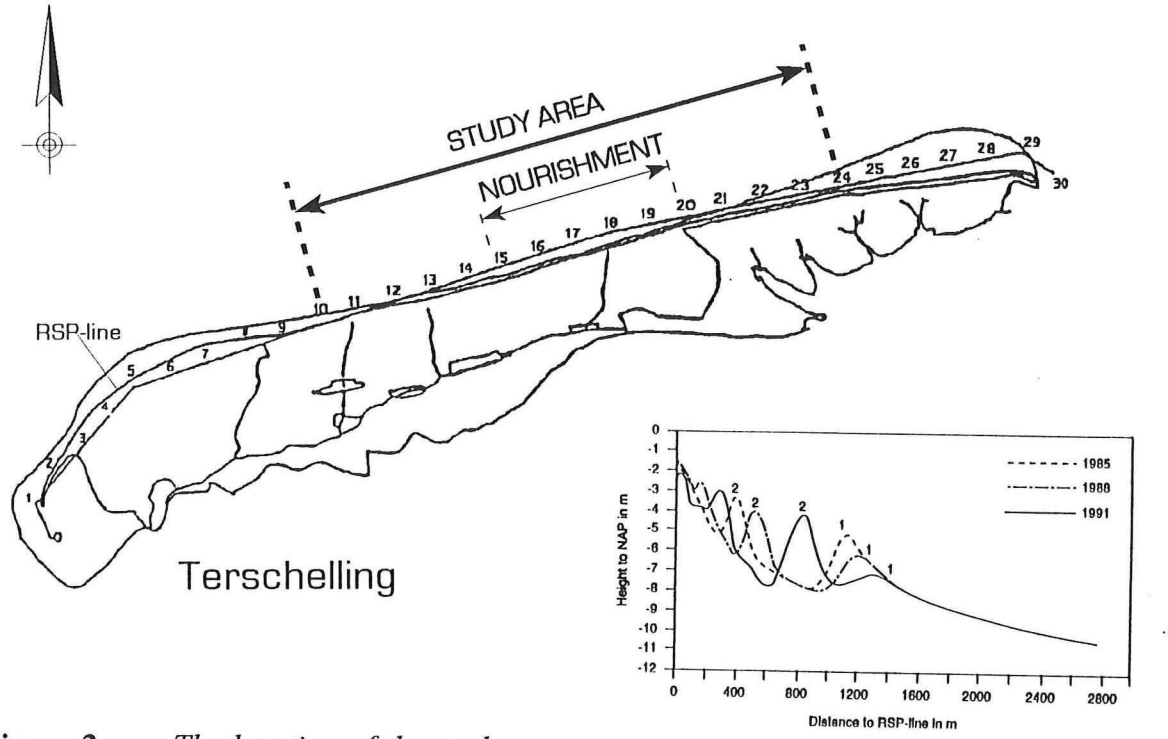

Figure 2 *The location of the study area.*

[1] *NAP = Normaal Amsterdams Peil = Dutch Ordnance Level*

§2.2 Assumptions

It's necessary to schematize the coastal behaviour to characteristic values, which are used in the n-line modelling. For this goal the following assumptions are made:

1. The motion of the breaker bars is periodical with a return period of 10 years. In this period a breaker bar moves seaward to a lower level.

2. In 1993 (t=0) the levels of the breaker bars are assumed to be at NAP -6, -3 and 0 m. The outer breaker bar moves down to NAP -9 m where this bar disappears. The distance between the breaker bars is 500m.

3. According to Smit (1987) the timescale of the cross shore transport between the area above NAP -9m and below this height, is of another magnitude than the timescale of the cross shore transport in the area above NAP -9m. The losses of sand due to cross shore transport to the area below NAP -9m, therefore are assumed to be not significant for the period of ten years and have been neglected in the computations. The fluctuations of the sand amount above NAP +3m are assumed to have a minor influence on the coastal behaviour of the area between NAP -9m and NAP +3m for the period of ten years and are therefore neglected in the computations.

4. Over one return period the motion as such causes no net resulting cross-shore transports. After a return period the same situation as on t=0 occurs in case of no other influences.

5 The disturbance of a bar due to the sand supply affects the nearest bars by a diffusion process.

6. The amount of supply is uniform in longshore direction. In various reports a supply between 400 and 800 m^3/m' is mentioned. In the present report a supply of 600 m^3/m' has been taken.

7. The profile displays a stationary autonomous behaviour which can be assumed to be constant at the time scale of decades. It is characterized by an erosion of approximately 2.75 m/year for the zone between NAP -9m and NAP +3 m.

8. The longshore transport rates can be determined with the CERC-formula and the assumptions of Svašek and Bijker (1969). These assumptions will be referred to in chapter 4.

3 Three-line modelling

§3.1 Principles of the three-line model.

In the three-line model the coastal zone is schematized in three zones (Figure 3). In each zone it is assumed that all contour lines remain parallel and that the profile of this zone only moves horizontally. It is sufficient to compute only an average line in each zone , because it characterizes this zone. There is assumed to be a horizontal separation plane between the zones.

The sediment transport between the lines is assumed to be proportional to the difference between the equilibrium distance and the actual distance between the characterizing lines.

In literature like Smit (1988) or Van der Velden (1990) these characterizing lines each have a distance to a reference line which can be defined as:

$$L_1 = \frac{1}{h_1}\int_{-d_1}^{0} y(z)dz \qquad \textit{beach line}$$

$$L_2 = \frac{1}{h_2}\int_{-d_2}^{-d_1} y(z)dz \qquad \textit{inshore line} \qquad (3.1)$$

$$L_3 = \frac{1}{h_3}\int_{-d_3}^{-d_2} y(z)dz \qquad \textit{line of deeper part}$$

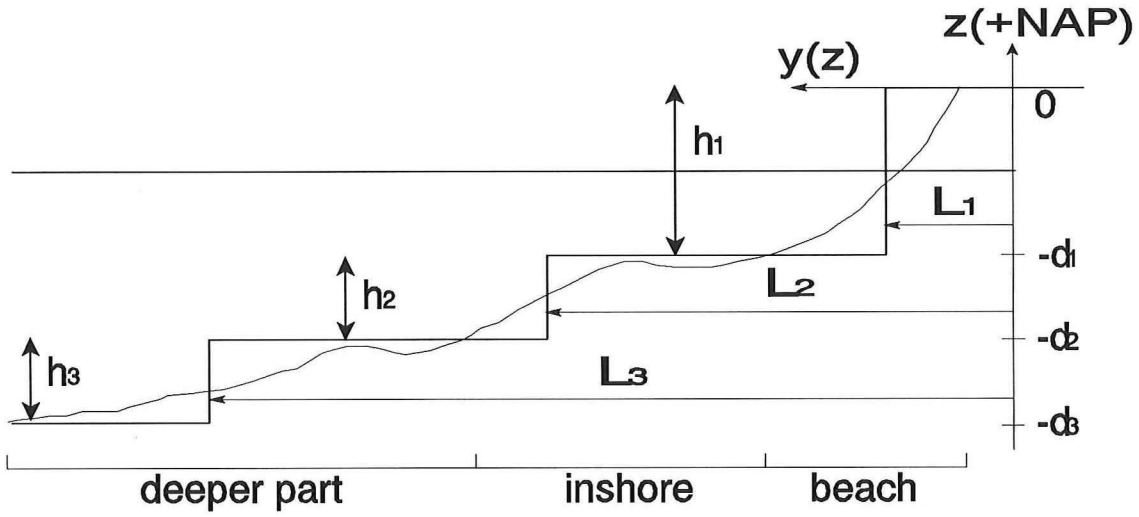

Figure 3 *Schematisation of the cross-section.*

The parameters mentioned in the equations and Figure 3 mean:

d_1 = depth of separation plane between zone 1 and 2
d_2 = depth of separation plane between zone 2 and 3
d_3 = depth of lower limit of zone 3
h_1 = height of zone 1
h_2 = height of zone 2
h_3 = height of zone 3
L_1 = characterizing mean line of the beach zone
L_2 = characterizing mean line of the inshore zone
L_3 = characterizing mean line of the deeper part
y(z) = distance of profile to a reference line
z = height above the y-axis

The same principle but with another schematization is used in this study. To simplify the equations another references axes have been used to avoid the use of the equilibrium distances W_1 and W_2 (Smit, 1987). Instead of the distances L_1, L_2 and L_3 of the lines to a reference axis, use has been made of the distances y_1, y_2 and y_3 to the lines of the equilibrium profile. The difference (L_2-L_1) to the equilibrium distances between the lines now have been replaced by the distances (y_2-y_1). and (L_3-L_2) and (y_3-y_2).

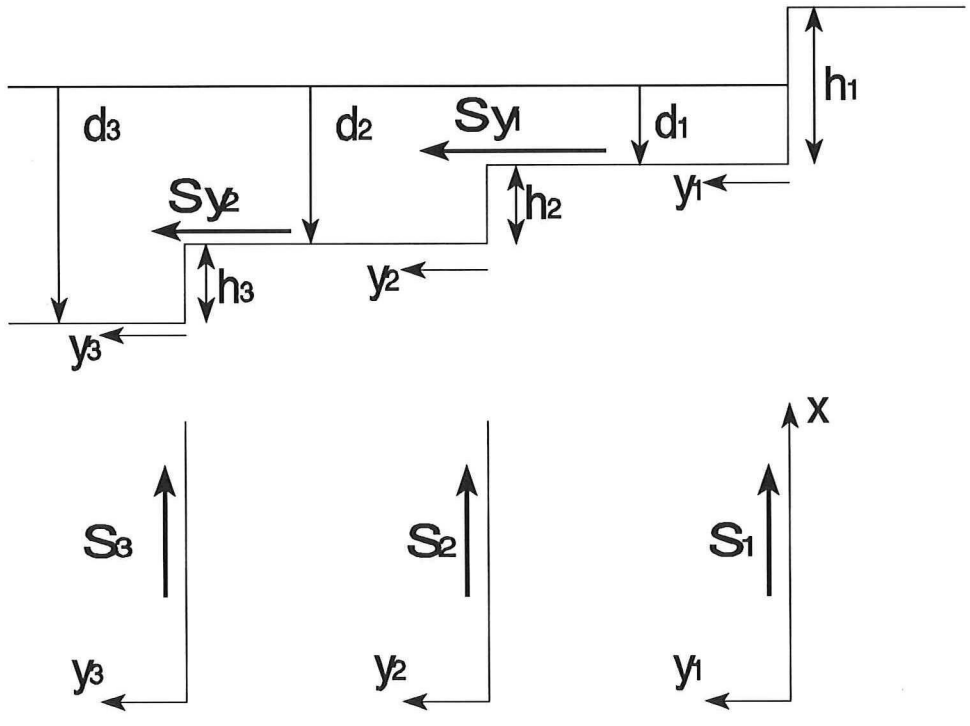

Figure 4 *The cross-section and the upperview of the three-line schematization.*

The parameters of Figure 4 mean:

S_1 = longshore transport in the beach zone
S_2 = longshore transport in inshore zone
S_3 = longshore transport in the deeper part
S_{y1} = cross-shore transport from the beach to the inshore zone
S_{y2} = cross-shore transport from the inshore to the deeper part
y_1 = distance to the initial equilibrium position of the beach
y_2 = distance to the initial equilibrium position of the inshore
y_3 = distance to the initial equilibrium position of the deeper part

In the theory an initial position (before any supply takes place) is assumed where the lines L_1, L_2 and L_3 are straight, parallel to the x-axis and where the zones are in equilibrium position (Figure 5). Distances y_1, y_2 and y_3 are the deviations of the lines of the beach, inshore and deeper part, compared with this initial position. In case of $y_1 = y_2 = y_3$ the profile is assumed to have an equilibrium shape, because the difference (y_2-y_1) and (y_3-y_2) are both zero and no resulting cross-shore transport is assumed to occur.

The y-value is computed by dividing the surplus volume in a zone (with respect to the initial situation) by its height. In Figure 5 the schematisation is shown of the "initial situation" directly after supply and of an example of distribution of the sand after a while.

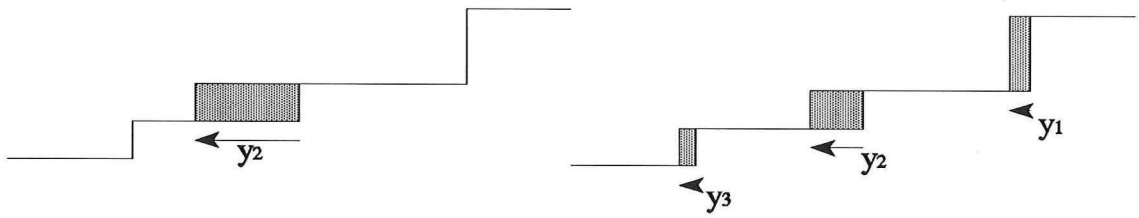

Figure 5 *Example of schematization.*

To come to the equations, which determine the development of the three lines, first the influence of cross shore transport and later on the influence of longshore transport will be derived.

If the transport rates S_{y1} and S_{y2} are assumed to be proportional to the difference (y_1-y_2) for S_{y1} and (y_2-y_3) for S_{y2}, then the following dynamical equations can be derived:

$$S_{y_1} = s_{y_1} * (y_1-y_2) \qquad m^3/m'/s \qquad (3.2)$$

$$S_{y_2} = s_{y_2} * (y_2-y_3) \qquad m^3/m'/s \qquad (3.3)$$

The parameters s_{y1} and s_{y2} are the proportionality constants.

Assuming no effect of longshore transport for a moment, continuity gives:

$$S_{y_1} = -h_1 * [\frac{dy_1}{dt}]_{cross}$$

$$S_{y_2} = +h_3 * [\frac{dy_3}{dt}]_{cross} \qquad (3.4)$$

$$y_1 * h_1 + y_2 * h_2 + y_3 * h_3 = constant$$

Substitution of S_{y1} and S_{y2} yields:

$$\begin{aligned} [\frac{dy_1}{dt}]_{cross} &= -\frac{s_{y_1}}{h_1} * (y_1 - y_2) \\ [\frac{dy_2}{dt}]_{cross} &= -\frac{s_{y_2}}{h_2} * (y_2 - y_3) + \frac{s_{y_1}}{h_2} * (y_1 - y_2) \\ [\frac{dy_3}{dt}]_{cross} &= +\frac{s_{y_2}}{h_3} * (y_2 - y_3) \end{aligned} \qquad (3.5)$$

These equations give the influence of cross-shore transport.

For the basic ideas concerning longshore transport in coastal dynamics there is referred to, for instance Van der Velden (1990). The idea originates from Bossen and it was first published by Pelnard Considère (1954), who gave proofs by experiments. Because the matter is of crucial importance for understanding the present report, the outline will be given below.

As the principle holds for as well S_1 and S_2 in this abstract the longshore transport will be characterized by the symbol S_x and the subscripts of h_1, h_2, y_1 and y_2 will be omitted.

For the longshore transport Van der Velden states the following equation of continuity:

$$\frac{\partial S_x}{\partial x} + h * \frac{\partial y}{\partial t} = 0 \qquad (3.6)$$

with h as the thickness of the layer over which the eroding or accreting takes place. The gradient of sediment transport ($\partial S_x/\partial x$), determining the changes of the coastline, is mainly due to changes in wave height or in angle of wave approach φ (Figure 6) along the coast. The coast is curved and assumed to have an equilibrium profile.

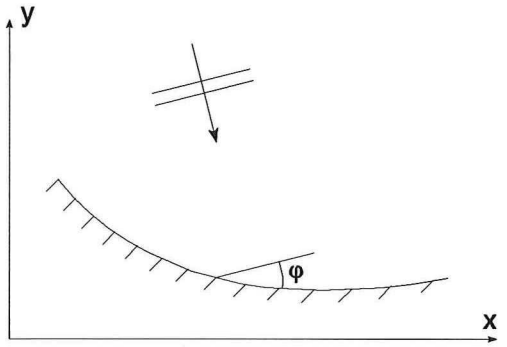

Figure 6 *Definition of angle of wave approach.*

The wave climate is assumed to be constant along the coast. The change of angle of wave approach therefore determines the gradient. With small changes of the angle, the gradient is assumed to be constant:

$$\frac{\partial S_x}{\partial \varphi} = s_x \tag{3.7}$$

The chain rule gives:

$$\frac{\partial S_x}{\partial x} = \frac{\partial S_x}{\partial \varphi} * \frac{\partial \varphi}{\partial x} \tag{3.8}$$

Substituting yields:

$$\frac{\partial S_x}{\partial \varphi} * \frac{\partial \varphi}{\partial x} + h * \frac{\partial y}{\partial t} = 0 \tag{3.9}$$

For the gradient ($\partial S_x/\partial \varphi$) the constant s_x can be substituted. Assuming small angles:

$$\frac{\partial}{\partial x}(\varphi) = \frac{\partial}{\partial x}\left(-\frac{\partial y}{\partial x}\right) = -\frac{\partial^2 y}{\partial x^2} \tag{3.10}$$

The resulting equation then becomes:

$$-s_x * \frac{\partial^2 y}{\partial x^2} + h * \frac{\partial y}{\partial t} = 0 \qquad \textbf{(3.11)}$$

The change of the coastline ($\partial y/\partial t$) thus appears to be proportional to the curvature of the coastline. This also applies if the profile is divided into several zones. The equations for the zones then become:

$$\begin{aligned}
[\frac{dy_1}{dt}]_{long} &= \frac{s_1}{h_1} * \frac{\delta^2 y_1}{\delta x^2} \\
[\frac{dy_2}{dt}]_{long} &= \frac{s_2}{h_2} * \frac{\delta^2 y_2}{\delta x^2} \\
[\frac{dy_3}{dt}]_{long} &= \frac{s_3}{h_3} * \frac{\delta^2 y_3}{\delta x^2}
\end{aligned} \qquad \textbf{(3.12)}$$

The following remarks on this derivation should be made:

- The assumption of unidirectional waves is not essential (in some way). If one assumes that the transport depends on ($-\partial y/\partial x$), the same result is obtained.
- In anticipation on chapter 4, it is pointed out, that refraction of the waves on the deeper part (not taken into account in the considerations above) is neglected.

Combination of both physical processes with linear addition gives:

$$\frac{dy_1}{dt} = \frac{s_1}{h_1} * \frac{\delta^2 y_1}{\delta x^2} - \frac{s_{y_1}}{h_1} * (y_1 - y_2)$$

$$\frac{dy_2}{dt} = \frac{s_2}{h_2} * \frac{\delta^2 y_2}{\delta x^2} + \frac{s_{y_1}}{h_2} * (y_1 - y_2) - \frac{s_{y_2}}{h_2} * (y_2 - y_3) \qquad \textbf{(3.13)}$$

$$\frac{dy_3}{dt} = \frac{s_3}{h_3} * \frac{\delta^2 y_3}{\delta x^2} + \frac{s_{y_2}}{h_3} * (y_2 - y_3)$$

In these equations the longshore transport is determined by the constants s_1, s_2 and s_3 and the cross-shore transport by the constants s_{y1} and s_{y2}.

These three equations determine the development of y_1, y_2 and y_3 in time and position along the coast.

§3.2 Schematization of the Terschelling case

The levels of the breaker bars (assumptions, §2.2, page 3) are used to schematize the profile into three zones:

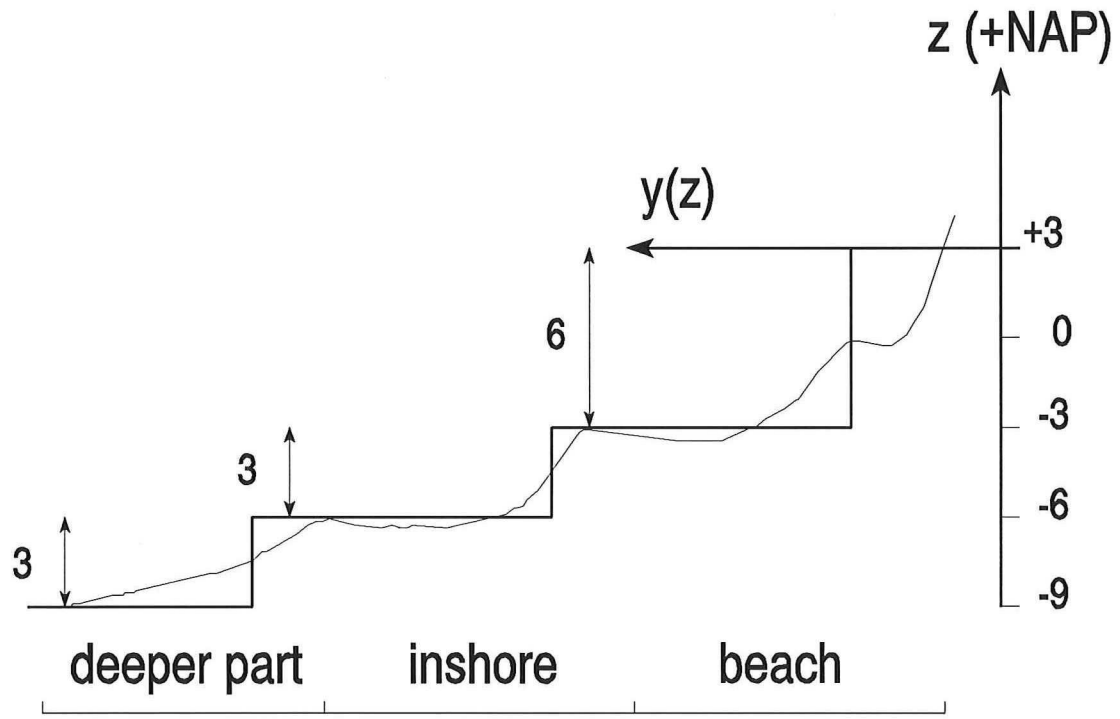

Figure 7 *The schematization of the cross profile of the coast of Terschelling.*

The unit of the numbers in Figure 7 is meter.

The lower two zones have a height of 3 meter and the beach zone has a thickness of 6m (NAP -3m to NAP +3m).

Because of variables, not taken into account in this theory (for instance the gradients of transports by tidal current), the "initial situation" before supply, being stable in theory, is not stable in practice.

It is assumed, that the effect of the supply, as follows from theory, may be superimposed with the present coastal evolution. The present erosion is schematized, to compare the results with, to a coastal retreat of 2.75 meter/year for the area above NAP-6m, and none below that level.

§3.3 Analytical solution; determination of cross shore constants

The Manual on Beach Nourishment (1988) only gives analytical solutions for more simple situations than the present one: for a two-line schematization only for some particular situations a solution is found. The manual recommends, if use is made of more lines, to find a numerical solution rather than spending too much time finding an analytical solution.

However Smit (1987) has made an effort and succeeded to find, a solution in case of three lines without longshore transport. Smit found expressions for y_1 and y_2. The third line y_3, Smit found simply by a continuity equation, because the volume in a cross-section remains constant:

$$y_1 * h_1 + y_2 * h_2 + y_3 * h_3 = constant \qquad \textbf{(3.14)}$$

To translate Smit's solutions (Appendix A) to the schematisation mentioned in §3.1, page 5, some remarks and assumptions are made. The assumptions are presented below.

1. In case of no longshore transport the total average accretion due to the nourishment will be the total amount of sand deposited (§2.2, assumption 6) divided by the height of the active zone (see Figure 7):

$$y_\infty = \frac{600 \ (m^3/m')}{(6+3+3) \ (m)} = 50 \ m \qquad \textbf{(3.15)}$$

2. In the solutions of Smit (Appendix A) three timescales of diffusitivity are mentioned:

   T_{01}, which determines the smoothing speed of distortions if no lower third zone would exist (i.e.: when a two-line model (beach/inshore) would be used).

   T_{02}, which determines the smoothing speed of distortions if no higher third zone would exist (i.e. only inshore and deeper part).

   T_0, which determines the smoothing speed, when all mentioned zones are taken into account. It results from interaction between the various zones.

3. The solutions of Smit are a sum of two negative exponential processes from which the one with the longest timescale will rule the solution over a longer period.

4. The propagation period of a seaward bar motion is 10 years, i.e. in 10 years a bar is replaced by the landward neighbouring bar. From the equations of Smit it can be derived that in a period T_{01} the process of spreading the supply evenly over the profile is completed for almost 80%. It does not seem illogical to assume, that a diffusion process to a similar rate is accomplished during the propagation period. The period T_{01} and T_{02} are therefore chosen both equal to ten years.

5. With the equations of Smit the values of s_{y1} and s_{y2} follow from:

$$s_{y_1} = \frac{1}{T_{01}} * (\frac{h_1 * h_2}{h_1 + h_2}) = 0.2 \quad m/year \tag{3.16}$$

$$s_{y_2} = \frac{1}{T_{02}} * (\frac{h_2 * h_3}{h_2 + h_3}) = 0.15 \quad m/year \tag{3.17}$$

and therefore:

$$s_{y_1} = \frac{4}{3} * s_{y_2} \tag{3.18}$$

The cross-shore coefficient s_{y1} is in this way thus assumed to be one third higher than s_{y2}. This seems to be reasonable; larger s_{y1} means larger diffusitivity on the upper side of the profile. At NAP -3m the energy dissipation of waves will cause larger diffusitivity than at the lower side, at NAP -6m.

The solutions of Smit then become:

$$y_1(t) = y_\infty * [\ (\frac{1}{2\sqrt{3}} - \frac{1}{2}) * e^{(-1+\frac{1}{\sqrt{3}})*\frac{t}{T_0}} - (\frac{1}{2\sqrt{3}} + \frac{1}{2}) * e^{-(1+\frac{1}{\sqrt{3}})*\frac{t}{T_0}} + 1\ ] \tag{3.19}$$

$$y_2(t) = y_\infty * [\ (\frac{5-3\sqrt{3}}{2\sqrt{3}}) * e^{(-1+\frac{1}{\sqrt{3}})*\frac{t}{T_0}} - (\frac{5+3\sqrt{3}}{2\sqrt{3}}) * e^{-(1+\frac{1}{\sqrt{3}})*\frac{t}{T_0}} + 1\ ] \tag{3.20}$$

$$y_3(t) = \frac{1}{h_3} * (600 - y_1(t) * h_1 - y_2(t) * h_2) \tag{3.21}$$

With these equations computations have been made to compare the results with those of numerical computations without longshore transport. After drawing a comparison between these results, computations have been made with the numerical method with longshore transport. The numerical method is described in the next section (§3.4). The tests and

results are presented in chapter 5.

§3.4 Numerical solution

The numerical method used is: 'Euler explicit'. That is a Time Forward, Central Space method.
To be solved is a system of three coupled partial equations:

$$\frac{\partial Y}{\partial t} = A * \frac{\partial^2 Y}{\partial x^2} + B * Y \tag{3.22}$$

with:

$$Y_i = \begin{pmatrix} y_{i,1} \\ y_{i,2} \\ y_{i,3} \end{pmatrix} \tag{3.23}$$

and

$$A = \begin{pmatrix} \frac{s_1}{h_1} & 0 & 0 \\ 0 & \frac{s_2}{h_2} & 0 \\ 0 & 0 & \frac{s_3}{h_3} \end{pmatrix} \tag{3.24}$$

and

$$B = \begin{pmatrix} -\frac{s_{y_1}}{h_1} & \frac{s_{y_1}}{h_1} & 0 \\ \frac{s_{y_1}}{h_2} & -\frac{(s_{y_1}+s_{y_2})}{h_2} & \frac{s_{y_2}}{h_2} \\ 0 & \frac{s_{y_2}}{h_3} & -\frac{s_{y_2}}{h_3} \end{pmatrix} \tag{3.25}$$

A is the matrix with the longshore constants and B is the matrix with the cross shore constants.

The differentials can be approximated with:

$$\frac{\partial y}{\partial t} = \frac{y_i^{n+1} - y_i^n}{\Delta t}$$
$$\frac{\partial^2 y}{\partial x^2} = \frac{y_{i-1}^n - 2*y_i^n + y_{i+1}^n}{\Delta x^2} \qquad \textbf{(3.26)}$$

Substituting these approximations in (3.22) yields :

$$\frac{Y_i^{n+1} - Y_i^n}{\Delta t} = A * (\frac{Y_{i-1}^n - 2*Y_i^n + Y_{i+1}^n}{\Delta x^2}) + B * Y_i^n \qquad \textbf{(3.27)}$$

with

$$Y_i^n = \begin{pmatrix} y_{i,1} \\ y_{i,2} \\ y_{i,3} \end{pmatrix}^n \qquad \textbf{(3.28)}$$

where

j	= number of zone
i*Δx	= x-coordinate
n*Δt	= moment
Δt	= timestep
Δx	= step in x-direction

To be found is an expression for each y-value at x=(i*Δx) at the next moment t=(n+1)*Δt. With the equations it can be derived that:

$$y_{i,j}^{n+1} = [\ y_{i,j} + \Delta t * (B \cdot Y_i)_j + a_{jj} * \frac{\Delta t}{\Delta x^2} * (y_{(i-1),j} - 2 * y_{i,j} + y_{i+1,j})\ ]^n \qquad \textbf{(3.29)}$$

For each equation there is a stability restriction :

$$\frac{a_{jj} * \Delta t}{\Delta x^2} < \frac{1}{2} \qquad \textbf{(3.30)}$$

The accuracy is sufficient if :

$$\frac{a_{jj} * \Delta t}{\Delta x^2} < \frac{1}{6} \qquad \textbf{(3.31)}$$

The latter 'restriction' has been used in the program 3LINES.PAS written in Turbo Pascal 7.0. For every combination the stability rate has been computed. This program computes the behaviour of the nourishment with the above mentioned numerical equations. The results are visualized on the screen and the data are put into an output file.

4 Longshore coastal constants

§4.1 Principle and assumptions

To determine the longshore constants for the line modelling use is made of the CERC-formula and the assumptions of Svašek (1968). The following assumptions have been made:

1. The total sediment transport in the breaker zone in longshore direction caused by waves is proportional to the longshore component of the energy flux of the waves at the breaker line (Figure 8).

2. The energy flux can be determined by the linear refraction theory.

3. The energy losses of a wave only take place by breaking and take place in the breaker zone.

4. The breaker wave height $H_{b,rms}$ is proportional to the breaker depth h_b.

5. The longshore transport within two contour-lines is proportional to the longshore component of the decrease of energy flux between these two lines. For a detailed description is referred to Bakker (1969), Bakker, ten Hoopen and Grieve (1972), ten Hoopen and Bakker (1974), Bakker and Delver(1986) and to Bakker, v.d. Kerk & de Vroeg (1988).

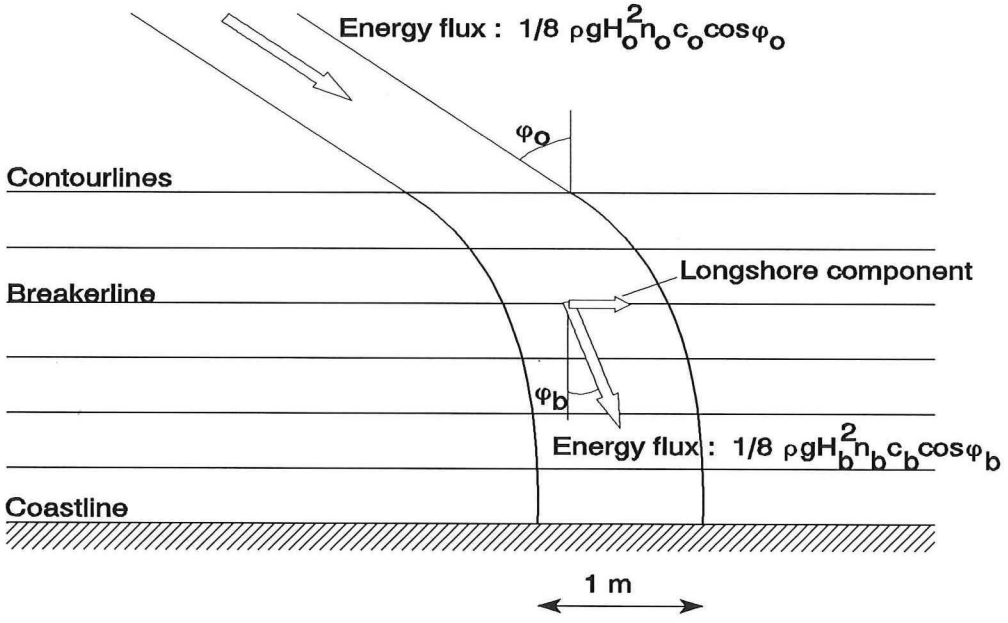

Figure 8 *The longshore component of the energy flux at the breakerline determines the longshore transport.*

§4.2 Formulae

The basic longshore transport formula that has been used is the CERC formula:

$$S_x = 0.040 * H_{b,sig}^2 * n_b * c_b * \cos(\varphi_b) * \sin(\varphi_b) \qquad (4.1)$$

where

S_x = sediment transport in longshore direction
$H_{b,sig}$ = significant wave height
φ_b = angle of wave at the breaker line
c_b = wave celerity at the breaker line
n_b = ratio (group velocity / phase velocity) at the breaker line

After substituting

$$H_{b,sig}^2 = 2 * H_{b,rms}^2$$
$$H_{b,rms} = \gamma * h_b \qquad (4.2)$$

the CERC formula becomes:

$$S_x = 0.080 * (\gamma * h_b)^2 * n_b * c_b * \cos(\varphi_b) * \sin(\varphi_b) \qquad (4.3)$$

with:

$$n_b = \frac{1}{2} + \frac{kh_b}{\sinh(2kh_b)}$$
$$c_b = c_o * \tanh(kh_b)$$
$$L = \frac{gT^2}{2\pi} * \tanh(kh_b) \qquad (4.4)$$
$$k = 2\pi/L$$

where

g = acceleration of gravity
T = wave period
h_b = breaker depth

The latter term, tanh(kh), has been computed numerically with the Newton-Raphson method.

To determine the coastal constants, s_1 and s_2, a series of computations have been made to determine the effect of a small change of angle of the parallel contour lines in one zone to the transport in this zone. After these computations, the gradient $\partial S_x/\partial\varphi$ has been computed (page 21) and therefore also the longshore constants.

The angle φ_b has been determined in the following way using Snel's law with the schematization according to Figure 9.

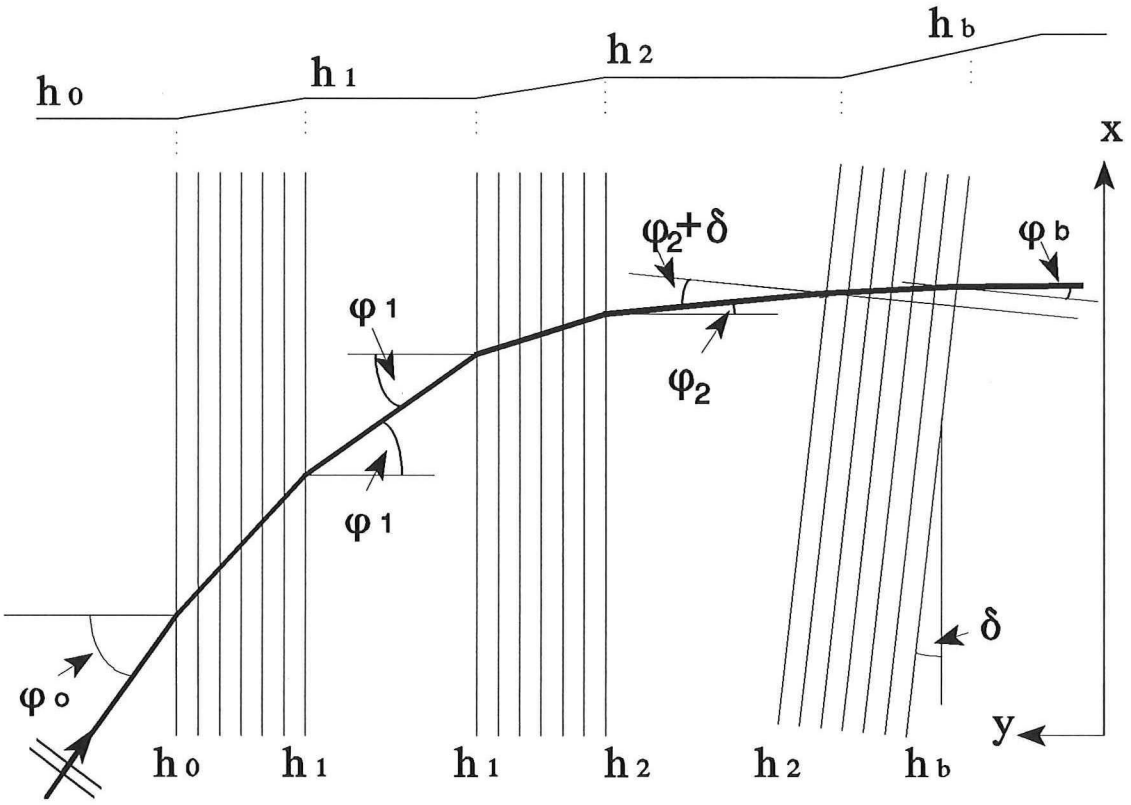

Figure 9 *The schematized coastal zone (cross-section and upperview).*

With Snel's Law the angle φ_b can be expressed in φ_0, c_b and c_o :

$$\frac{\sin(\varphi_o)}{c_o} = \frac{\sin(\varphi_2)}{c_2} \tag{4.5}$$

$$\frac{\sin(\varphi_2 + \delta)}{c_2} = \frac{\sin(\varphi_b)}{c_b} \tag{4.6}$$

Hence, to compute the value φ_b first the value φ_2 has to be computed. All parameters mentioned in the CERC-formula are now determined with (4.4),(4.5) and (4.6) can be computed directly or via an iteration method.

The way of assigning some part of the transport to the beach zone and another part to the inshore zone will not be treated here; there is referred to the literature named in §4.1.

To determine the coastal constants several computations were made with the wave climate made available by Rijkswaterstaat (Roskam, 1988). The wave and water level measurements are from SON, a measurement station in the neighbourhood of Schiermonnikoog.

The data consists of tables of the probability of occurrence of a particular combination of wave height and wave period and tables with the combination of wave height and water level. The wave height is split into 16 classes, the wave period and water level both in 6 classes.

The tables give the information on wave classes of 30 degrees. The mean value of angle in each segment has been taken as the angle determining the angle of approach of each possible wave from that segment. For each combination of angle of approach, wave height, wave period and water level the longshore transport has been computed. After this computation the computed transport has been multiplied by the probability of occurrence of this particular combination of φ_o, H_o, T_o and water level dh (the latter relative to NAP).

Because of the orientation of the coast of Terschelling and the classification of segments use is made of 7 segments (Figure 11).

To obtain the coastal constants for each direction two extra computations were made with a positive and an equally negative δ. This angle δ denotes the angle between the parallel depth contours of one zone and the other zones. Due to refraction the angle φ_b is already small. A little δ gives therefore a relative large difference in transport.

The results of the computations are presented graphically in Figure 10 where Table 1 gives the computed results. When the breaker depth is larger than the depth of the level of separation between the inshore and the deeper part, the longshore transport is distributed over the three zones according to the method of Svašek (1969). In the same way, when the breaker point is in the inshore zone, the transport is distributed over the beach and the inshore zone.

For every direction segment the values of transport are displayed. For both S_1 and S_2 a negative and a positive angle δ of 2 degrees have been used (hatched arrows in Figure 10) and a computation without this angle (black arrows) has been carried out. It is obvious that the segments of +60° and +30° give the largest transport rates due to waves. The right most column of Figure 10 and Table 1 gives the total transport, $S_i(\varphi)$, for beach, inshore and deeper part respectively. Neglecting the longshore transport in the deeper zone is substantiated by these results.

The (volumes of the) arrows in Figure 10 correspond with the numbers in Table 1. For both beach and inshore zone, the longshore transport has been computed three times for every direction. The angles (+2°, 0° and -2°) mentioned in the left column of Table 1 represent the angle δ between the contour lines. The numbers are the computed transport, $S_i(\varphi)$, for each direction for a certain zone and angle δ, multiplied with the probability of occurrence.

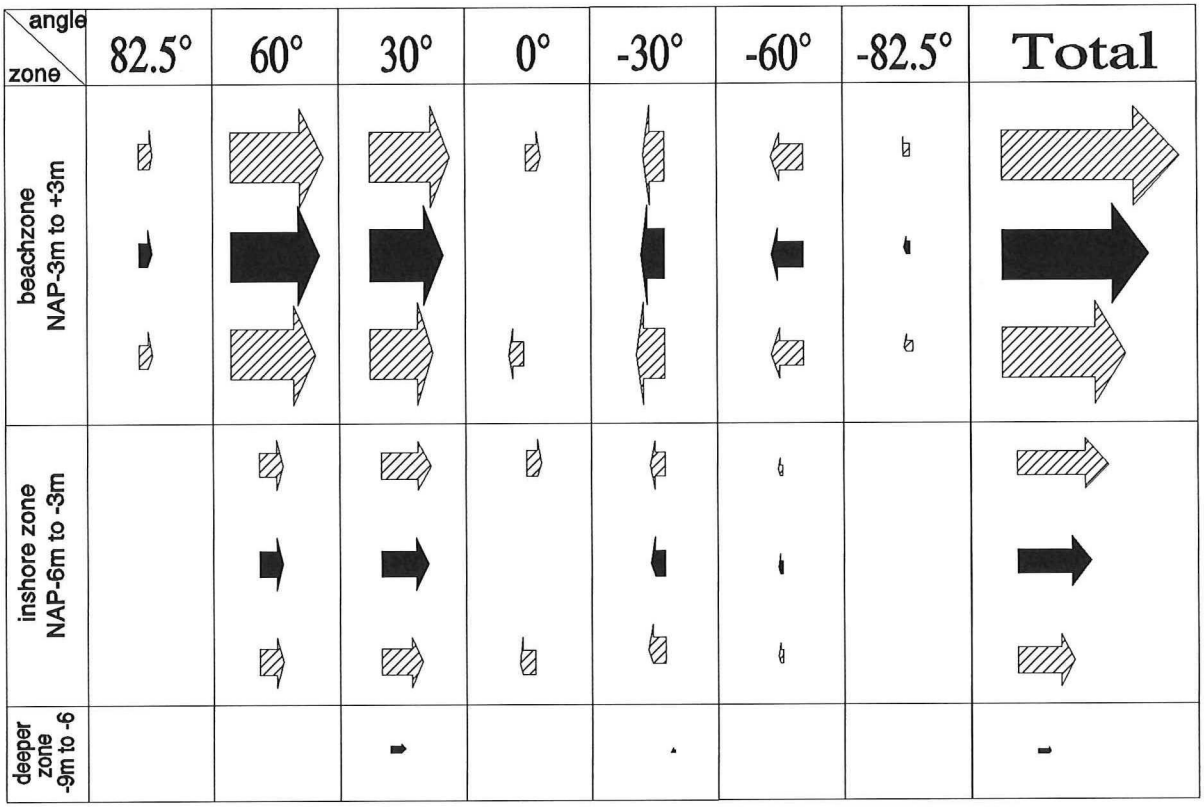

Figure 10 *The transport rates along the three zones as function of the angle of approach of the wave at deep water and the extra angle delta. The volumes of the arrows are proportional to the numbers in Table 1.*

	82.5°	60°	30°	0°	-30°	-60°	-82.5°	ΣS
+2°	41.42	500.4	431.4	40.53	-114.6	-84.83	-10.14	804.2
0°	40.55	478.3	387.3	0	-128.7	-87.91	-10.25	679.3
-2°	39.46	453.8	341.2	-40.53	-142.1	-90.54	-10.30	551.0
+2°	0.004	68.36	161.9	15.22	-38.16	-8.830	0	198.5
0°	0.004	67.57	148.5	0	-41.98	-8.818	0	165.3
-2°	0.004	66.30	134.4	-15.22	-45.56	-8.732	0	131.2
0°	0	0	5.518	0	-1.428	0	0	4.09

Table 1 *The numbers are the transport rates in thousands m^3/year computed with the Pascal program CERC.PAS.*

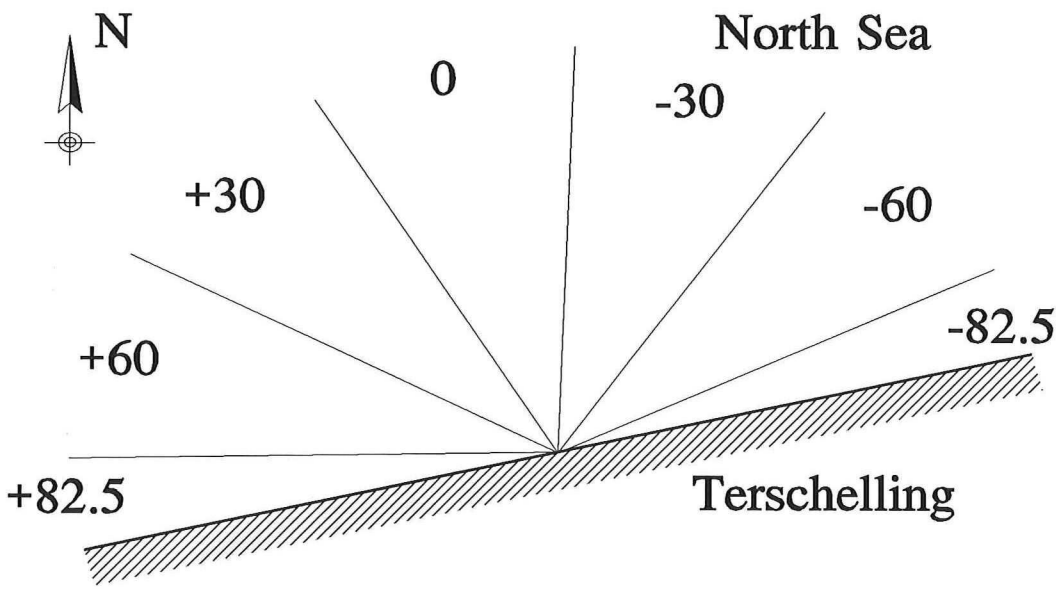

Figure 11 *The schematized coastline of Terschelling with the mean directions of wave-approach of each segment relative to the perpendicular on the coast.*

The coastal constants s_1 ($\partial S_1/\partial\varphi$) and s_2 ($\partial S_2/\partial\varphi$) have been computed with:

$$s_i = \frac{\sum_{+82.5^\circ}^{-82.5^\circ} [S_i(\varphi_i+\delta) - S_i(\varphi_i-\delta)]}{2*\delta}$$

$$s_1 = \frac{804.2 - 551}{2*2*\frac{\pi}{180}} * 10^3 = 3.63\ 10^6 \quad m3/year/rad \qquad (4.7)$$

$$s_2 = \frac{198.5 - 131.2}{2*2*\frac{\pi}{180}} * 10^3 = 0.964\ 10^6 \quad m3/year/rad$$

For the total longshore transport has been computed:

$$S_x = (679.3 + 165.3 + 4.09) * 10^3 = 848.7\ 10^3 \quad m3/year \qquad (4.8)$$

To determine the influence of the chosen angle (δ=2°), also some computations with an angle of 1° has been used. The results gave almost the same values for the constants.

The constant s_l seems to be rather high compared with the values mentioned in "Determination of coastal constants in mathematical line models, "Bakker et al (1988). The reason is discussed in chapter 7, item 2. However, in the following computations this constant will be used. The results will therefore show a longshore distribution of the supply along the beach, which probably will be too fast. The effect of the supply computed with this method and constants will therefore give an pessimistic estimate of the real effect.

5 Results

§5.1 Description of computed cases

The following cases have been computed:

1. Supply (as mentioned: 600 m^3/m') between NAP-6m and NAP-3m with longshore and with cross-shore transport, numerically computed.

2. The same as 1. however neglecting longshore transport, numerical and analytical.

3. The same as 1. however with supply between NAP-9m and NAP-6m

4. The same as 1. with a distributed supply: 300 m^3/m' between NAP-9m and NAP-6m and the same amount between NAP-6m and NAP-3m.

5. The same as 1. without cross-shore transport to the zone lower than NAP-6m. In fact this is a two-line schematisation.

In the next section the results are presented in several graphs:

1. The visualized results during the computation of case 1 are presented in the next 8 pictures of Figure 12 . In addition Figure 13 to Figure 15 show the development in time of y1, y2 and y3 in longshore direction, concerning case 1. Only half of the schematized coastline is shown in the figures, because due to the line schematization, which has been used, the development of the coastlines will be symmetric to the centre of the supply.

2. In Table 2 the results of case 1 and case 2 are presented to compare the results of the numerical method and the analytical method in case of no longshore transport. It also shows the results of the analytical method in case of no longshore transport and the numerical method with longshore transport. Figure 16 shows the latter comparison in a graph.

3. In Figure 17 the results of a computation of case 3 are presented. A comparison between the coastal shape, respectively with or without longshore transport, can be made.

4. The results of case 4 with a supply of sand distributed equally between NAP-9m and NAP-3m and the results of the shoreface nourishment as high as possible (case 1), both with longshore transport are presented in Figure 18.

5. Finally Figure 19 and Figure 20 show the results of a computation with only two lines. In this case the cross-shore transport to a level lower than NAP-6m has been taken zero.

It has to be reminded, that the autonomous erosion (horizontal lines in Figure 13 and 14) has to be subtracted from the accretion, indicated in the figures and the table.

§5.2 Graphs

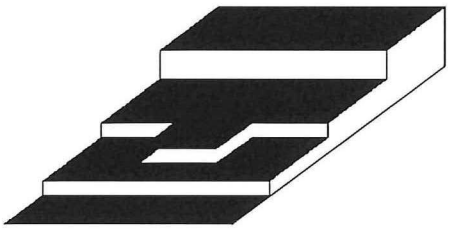

The situation at t=0.

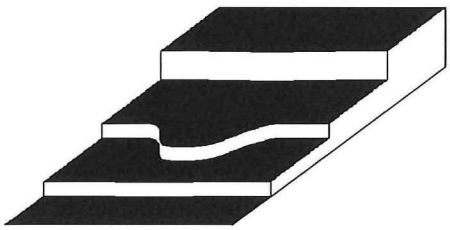

The situation after 1 year

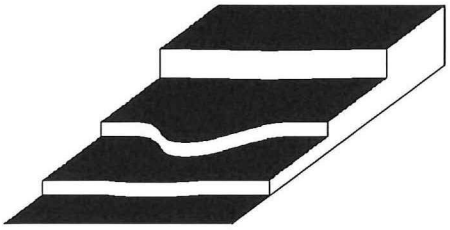

The situation after 2 years

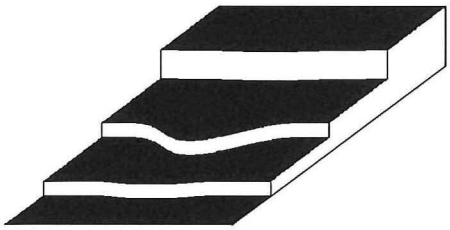

The situation after 3 years

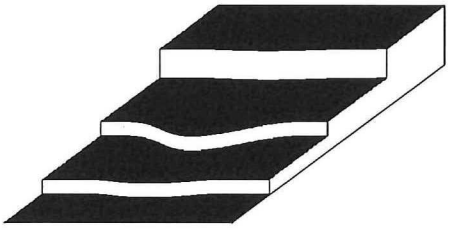

The situation after 4 years

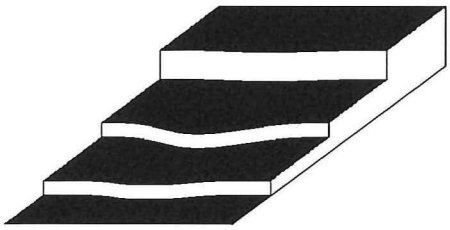

The situation after 6 years

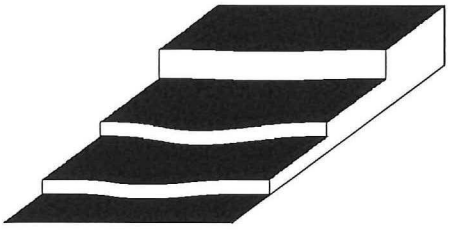

The situation after 8 years

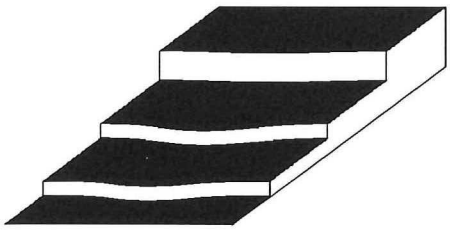

The situation after 10 years

Figure 12 *During the computations these pictures occur on the screen to visualize the results.*

In Figure 12 is shown how the diffusion of sand in cross shore and longshore direction takes place. After the supply has been carried out, the supply is schematized by the rectangular increase of the inshore line (y2) at t=0.

Figure 13 to Figure 15 show the development in time of the beach line (y1), the inshore line (y2) and the line of the deeper part (y3). On the vertical axis at the right side, the autonomous erosion is displayed.

Several remarks can be made:

- After ten years on the inshore an accretion of 40 to 60 meter is what remains of the supply. This compensates the autonomous erosion of 27.5 meter.

- Without the autonomous erosion, at the beach after ten years, an accretion would result of 17 to 21 meter. However, the autonomous erosion will dominate after about 7 years. The effect of the supply due to cross shore transport to the beach diminishes due to the large longshore transport.

- Due the longshore transport a rather high amount of sand is transported out of the supply area and benefits especially the beach and inshore in the neighbouring area. At the beach the amount of sand which is still in the area after ten years is about 50%. At the inshore this amount is about 65% and at the deeper zone still 70%.

- The accretion in meter, due to the cross shore transport, is higher at the deeper part than at the beach. The beach zone is although twice as high as the deeper zone. The total amount of sand in cubic meter is therefore higher at the beach due to the higher value of the cross shore transport constant s_{y1}.

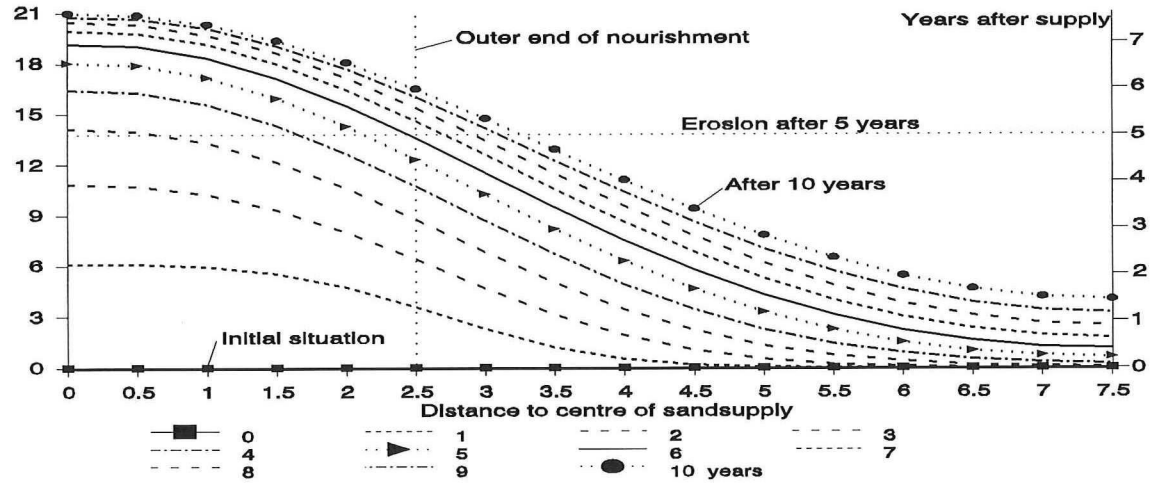

Figure 13 *The line of beach, y_1, in case of three lines with longshore transport.*

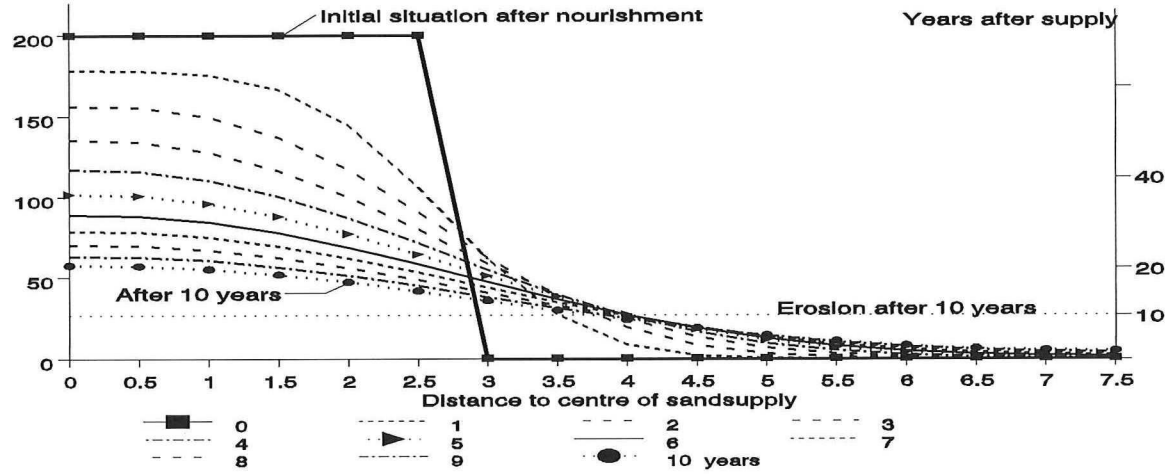

Figure 14 *The inshore line, y_2, in case of three lines with longshore transport.*

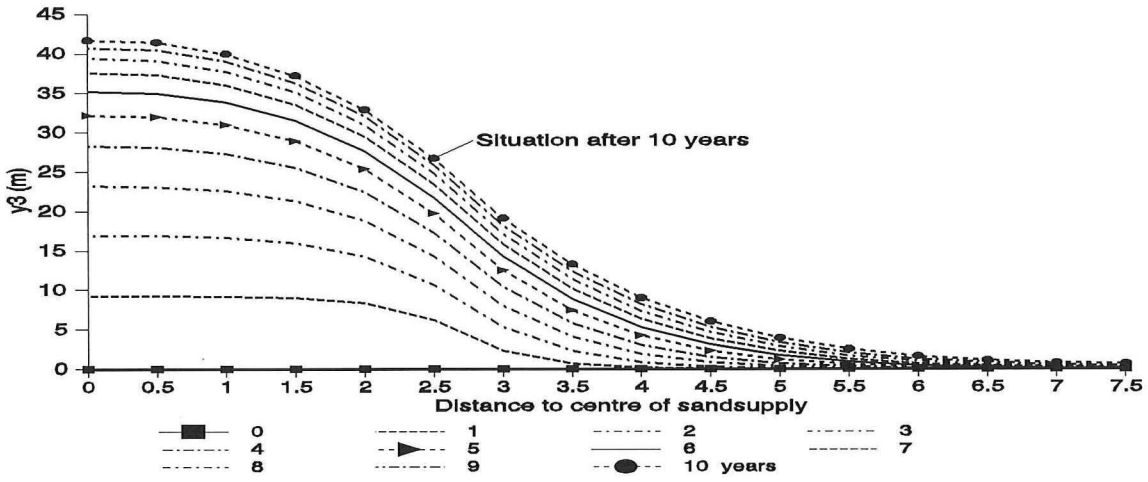

Figure 15 *Line of deeper part, y_3, in case of three lines with longshore transport.*

	line of beach			line of inshore			line of deeper part		
0	0.00	0.00	0.00	200	200	200	0	0	0
1	6.15	6.20	6.20	178.2	178.4	178.4	9.15	9.21	9.21
2	10.8	11.54	11.54	156.3	159.9	159.9	16.95	17.00	17.00
3	14.10	16.13	16.13	135.2	144.2	144.1	23.25	23.58	23.57
4	16.50	20.10	20.10	116.9	130.7	130.7	28.20	29.12	29.12
5	18.00	23.54	23.52	101.6	119.2	119.2	32.10	33.78	33.78
6	19.20	26.51	26.49	89.10	109.3	109.3	35.25	37.70	37.00
7	19.95	29.07	29.07	78.75	100.9	100.9	37.50	40.98	40.98
8	20.55	31.31	31.31	70.35	93.68	93.69	39.30	43.73	43.71
9	20.85	33.24	33.26	63.45	87.51	87.53	40.65	46.01	45.99
10	21.00	34.94	34.94	57.60	82.23	82.26	41.70	47.88	47.88

Table 2 *Comparison of the development of the lines in the middle of the supply in the course of time in three different cases.*

Table 2 gives the values of y1, y2 and y3 in the centre of the supply for each year in case of supply between NAP-6m and NAP-3m.

The first column for each line gives the values computed numerically taking longshore transport into account.

The third column gives the numerically computed values without taking longshore transport into account. The second column gives the values computed analytically with the solutions of Smit, without the longshore transport, to compare the values of third column with.

The conclusion can be made that the differences between the analytically computed values and the numerical ones (both without longshore transport) are negligible. In Figure 16 the results are shown in a graph.

Because the results of the computations without the longshore transport with the analytical and the numerical way, are the same, only the results of the computation with the analytical equations ("anal") are shown.

The results of the numerical way to compute the development of the lines with the longshore transport, is shown to visualize the influence of the longshore constants.

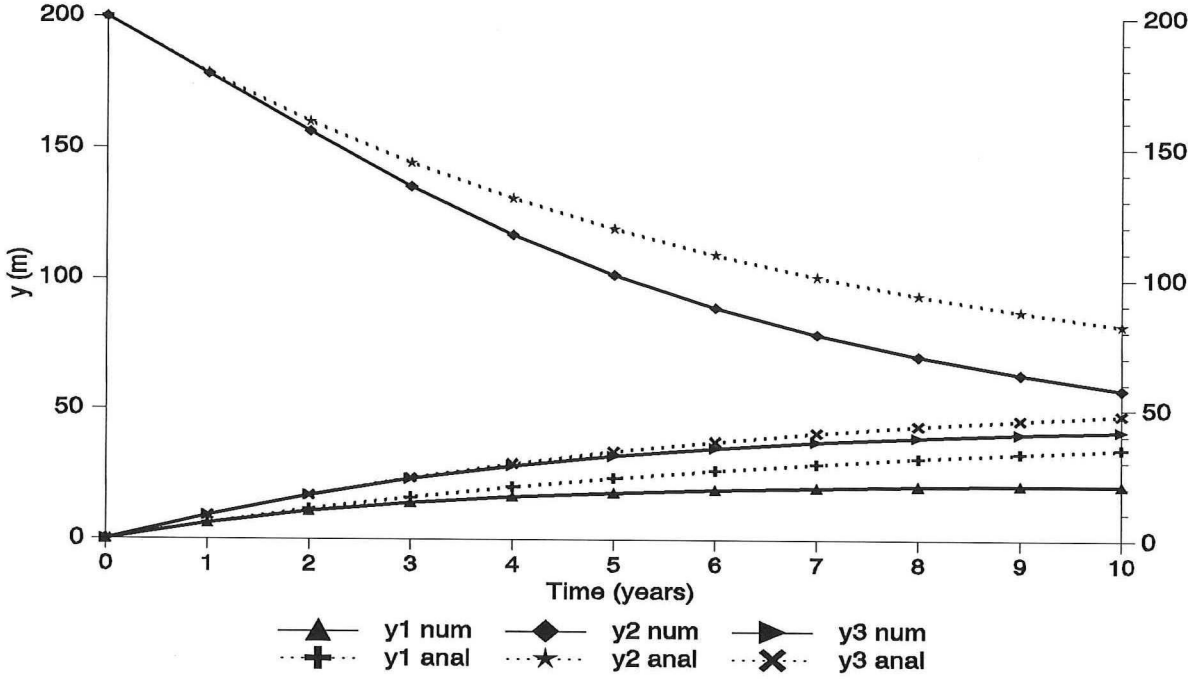

Figure 16 *Development of the lines of beach, inshore and deeper part in the centre of the supply, if carried out between NAP-6m and NAP-3m, with longshore transport ("num") and without longshore transport ("anal").*

Figure 16 and Table 2 show that the accretion of the beach, inshore and of the deeper part is remarkable less, if the longshore transport has been taken into account. The accretion of the beach is 40% less, at the inshore 30% and at the deeper part 15%. The influence of the high value of the longshore constants is a rather large decrease of the effect of the supply at the beach and inshore, in comparison with the case with only cross shore transport taken into account. The decrease of the effect is at the outer ends of the supply even bigger.
In case 2, where longshore transport is neglected, the accretion of the beach in the middle of the supply is about 35 meter and compensates an erosion of about 13 years. The supply remains longer on the inshore due to the fact that no longshore transport has been taken into account.

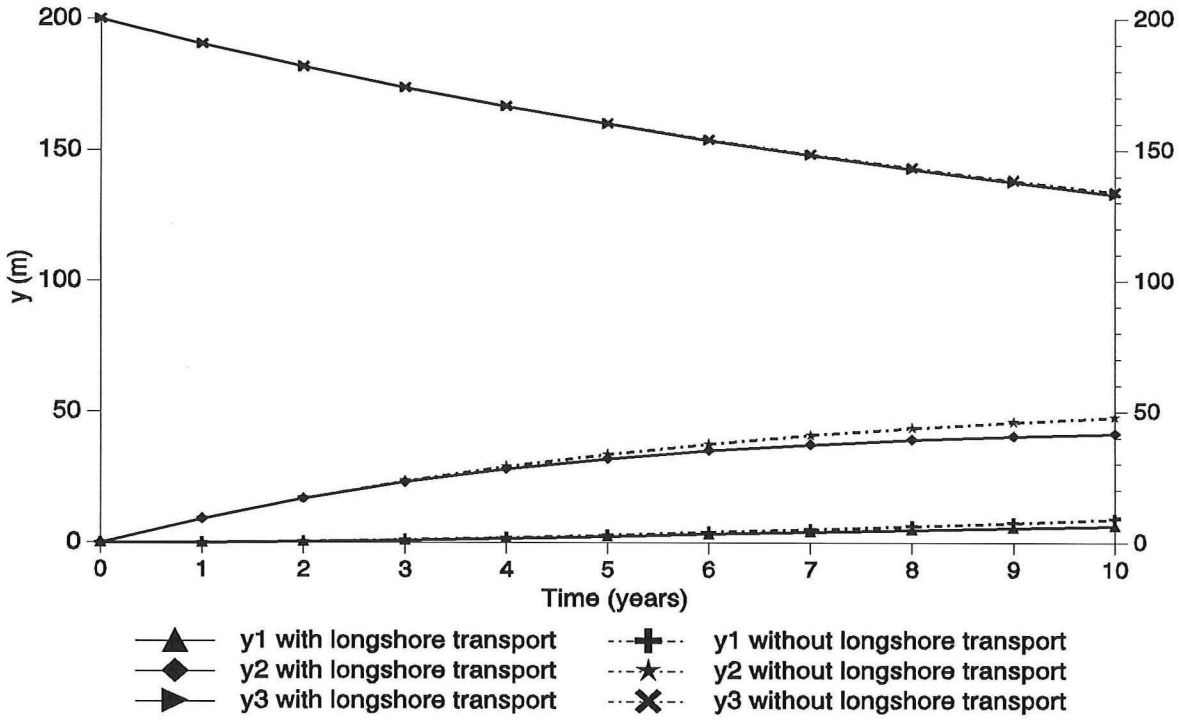

Figure 17 *Development of the lines of beach (y_1), inshore (y_2) and deeper part (y_3) in case of supply between NAP-9m and NAP-6m, with and without longshore transport.*

In Figure 17 the effect of the supply is shown if this has been carried out on the deeper part, between NAP-9m and NAP-6m. Comparing this with the results computed with a supply between NAP-6m and NAP-3m, several remarks can be made:

- Only 30% of the supply has been spread over the profile from the deeper part to the rest of the profile, compared to 70% of the sand if this has been supplied to the inshore.

- The effect on the beach of the supply at the deeper part is found to be about 1/3 of the effect with the supply at the inshore. The accretion at the inshore after ten years is 7/10 of the effect with the supply at the inshore.

- Only an accretion of the beach of about 7 meter is found. This is far too low to compensate the erosion for several years.

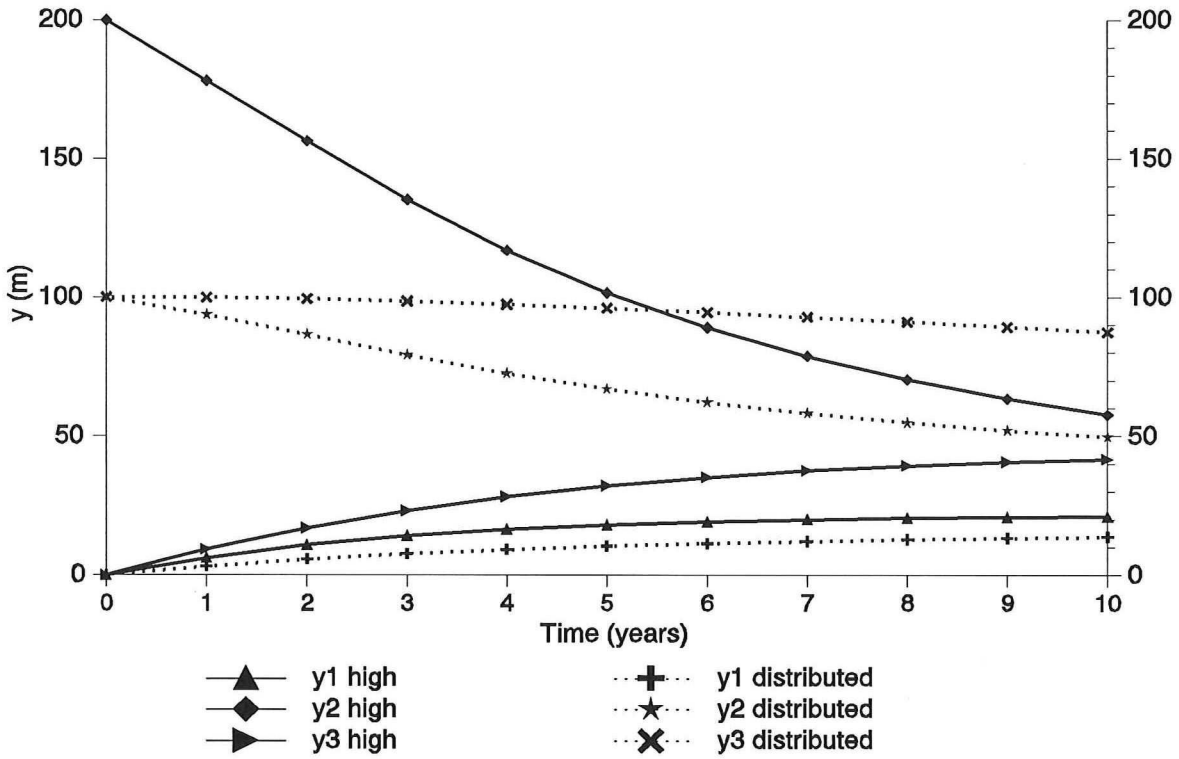

Figure 18 *The development of y_1, y_2 and y_3 with supply between NAP-6m and NAP-3m (high) and the same amount of sand equally distributed between NAP-6m and NAP-3m and NAP-9m and NAP-6m (distributed).*

Figure 18 shows the effect of a supply which is partly carried out between NAP-9m and NAP-6m (300 m^3/m') and between NAP-6m and NAP-3m (also 300 m^3/m'). This already gives large differences compared to a supply with the same total amount of sand between NAP-6m and NAP-3m. Comparing this with the results computed with a supply between NAP-6m and NAP-3m, several remarks can be made:

- Only 12% of the supply has been spread over the profile from the deeper part to the rest of the profile and 50% from the inshore, over against 70% of the supply if this has been carried out at the inshore.

- The effect on the beach with the distributed supply is found to be about 2/3 of the effect with supply at the inshore. The accretion at the inshore after ten years is 7/10 of the effect of the supply at the inshore.

- The supply in the third zone has hardly influence on the beach. It does of course influence the zone NAP-6m to NAP-3m, because there is no transport from this zone to a lower level.

In Figure 19 and Figure 20 the effect is shown if no transport to the deeper part would take place. The accretion of the beach and inshore are both about 25% higher compared with the results in case of cross shore transport to the deeper part.

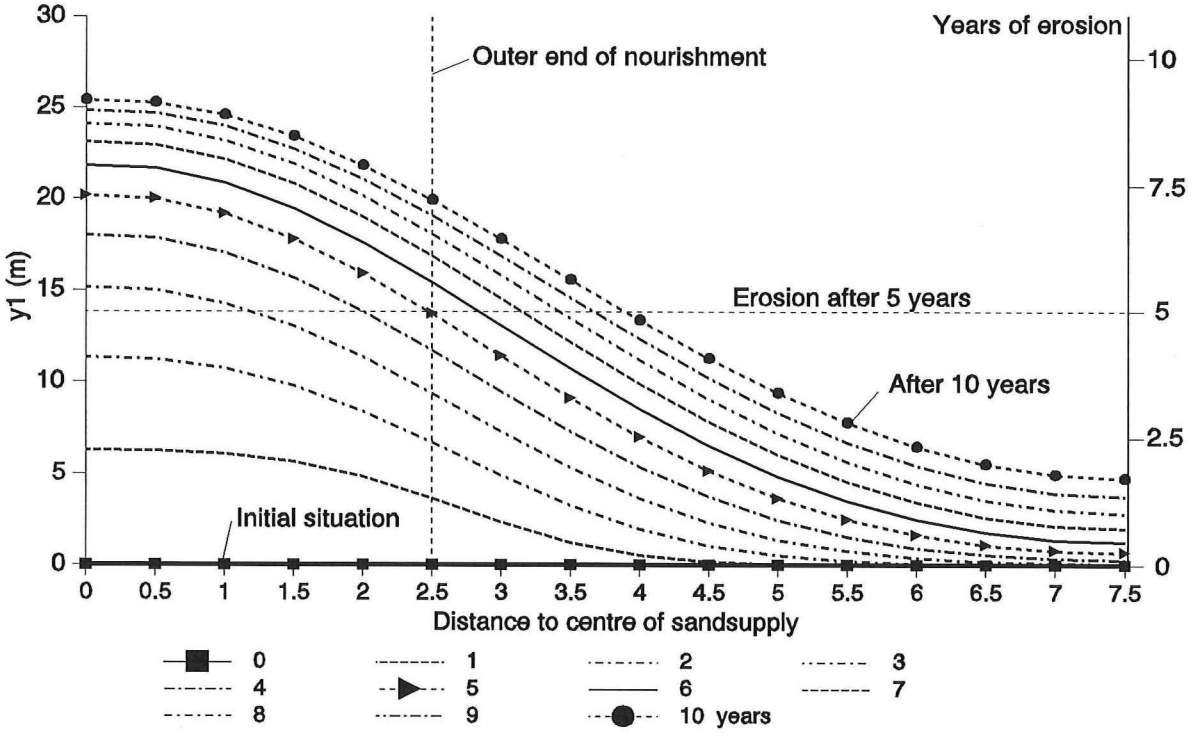

Figure 19 *Line of beach, y_1, in case of two lines with longshore transport.*

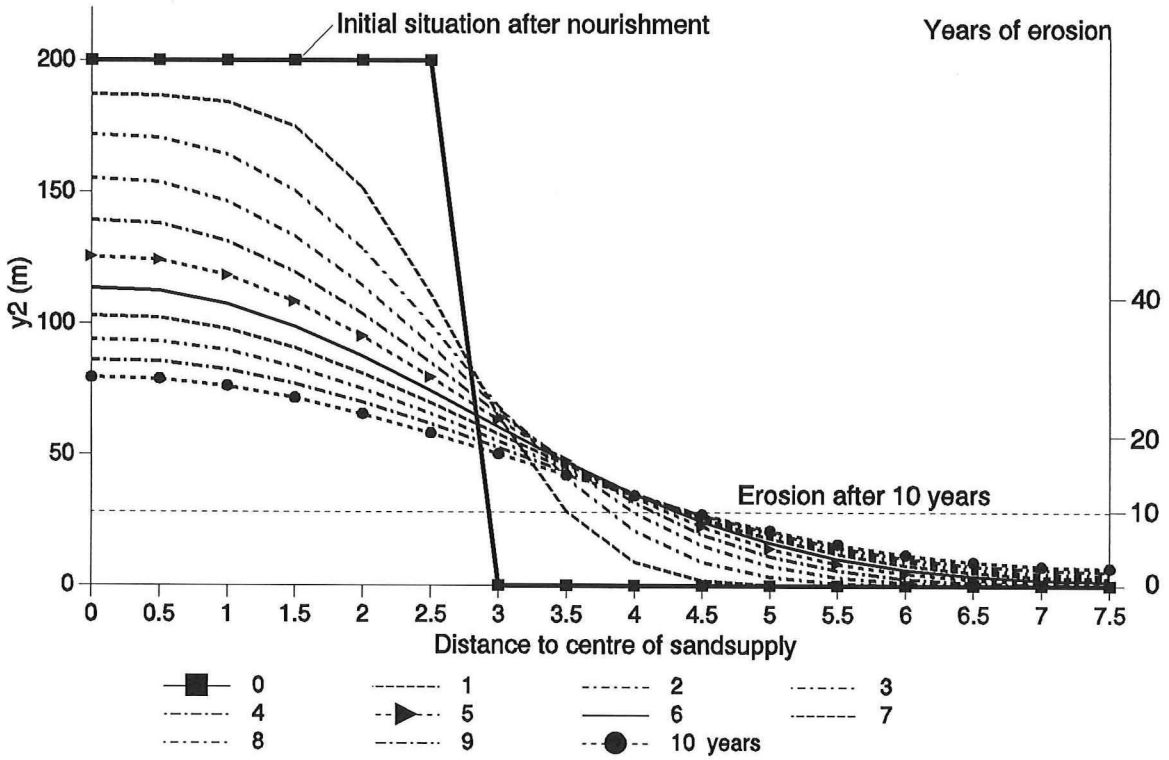

Figure 20 *Line of inshore, y_2, in case of two lines with longshore transport.*

6 Discussion

§6.1 Deviation between theory and reality

Evidently the only thing the present model pretends, is giving a very rough impression of the processes, occurring in reality. It is hoped and supported by checks on natural situations (see for instance CUR et al (1988)) that the diffusion processes on the beach or inshore nourishment can be reproduced.
Long lists of deviations between theory and reality can be made. Only the most important features will be emphasized:

- Effect of sand transport caused by tide is neglected. It is the impression of the author that the effect of diffusion will dominate, however some shift in eastward direction of the site of the point of maximum disturbance of the profile in the course of time can be expected.

- The present report does not explain the cause of the erosion occurring in the present situation. This would require an investigation of its own.

- The causes of existence of breaker bars is treated neither.

- The motion of the breaker bars is assumed to be periodically. After ten years the position of the breaker bars of that moment is assumed to be the same. The motion of the breaker bars during the ten years has not been taken into account. In the computations is not accounted for the short term effects of the motion of the bars. Only after the return period of ten years, a good evaluation can be made.

- The amount of supply varies between 400 to 800 m^3/m' and stretches over an area of 5 km. The schematization as "600 m^3/m' over 5 km" overestimates in a way the total amount of supply and thus its positive effect.

- In the computation the simplifying assumption has been used, that the curvature of the inshore does not affect the transport along the beach. This is a very unfavourable assumption. Bakker & Delver (1986) even considerably reduce the coastal constant s_1 for this reason. In the present report the option has been chosen to show both extremes: the case with no diffusion in longshore direction and the case with a maximum diffusion in longshore direction.

- In practice there has to be accounted for the possibility of backscour i.e. development of longshore troughs on the beach, discharging water driven by tide or water originating from swash.

§6.2 Sensitivity of conclusions for assumed values of constants

The various computations of chapter 5 give an impression of the sensitivity of the results for the way of schematization. It is the impression of the author , that the two cases considered ("no diffusitivity" and "large diffusitivity") give a reasonable idea of the extremes which have to be considered.

In the present report, s_{y1} and s_{y2}, have not been varied. The time scale of the process in the final stage is determined by λ in Smit's solutions. Halving the values of T_{01}, T_{02} and T_0 would give the same results after five years as the ones in Table 2 after ten years. Evidently, the magnitude of s_{y1} and s_{y2} should be subject of future research.

§6.3 Comparison with other computations

In Groenendijk & Uit den Boogaard (1992) computations have been made with the model UNIBEST-TC. The wave climate in that report is schematized to two directions and computations have been made with a storm wave climate and a rather calm wave climate. The results have been averaged by taking the probability of occurrence into account.

A longshore transport due to waves has been found of approximately 400,000 m^3/year. In the present report a longshore transport of about 850,000 m^3/year has been computed (page 21). The difference is a factor two, which is rather usual in coastal practice, when various ways of computations are applied. The resulting longshore transport is often a result of a relative small difference of rather large amounts of sand moving in both directions along the coast.

The conclusion of the UNIBEST report that the supply should be carried out as high as possible at the inshore is sustained by the results of the present report.

7 Conclusions

1 Depending on the assumptions (of which the extremes are "only cross shore diffusitivity" and "cross shore plus an unfavourable high value for longshore diffusitivity") a "lifetime" of the supply can be estimated, which varies respectively between 13 (Figure 16) and 7 years (Figure 17) if the erosion is estimated as 2.75 m/year.
Referring as well to other aspects, mentioned in chapter 6, it must be emphasized that the cross shore diffusitivity constants only have been estimated by "engineering judgement". More research on these constants is carried out at present.

2 The idea of the designers, that the supply on the inshore should be placed as high as possible is supported by the results of the computations (Figure 17 and Figure 18).
If the supply had been sited between the lines of NAP-6m and NAP-9 m, the reduction of the erosion of the beach by the supply would have been only (according to the computations) one third of the one in case of supply at the inshore (NAP-6m to NAP-3m).

3. Assuming a supply of 600 m^3/m (the average of the amounts, mentioned in the Technical Annex of NOURTEC, i.e. 400 and 800 m^3/m) over a length of 5 km, the computations yield a reduction of the erosion of the beach of 2.1 m/year (Figure 13) if the unfavourable high value for the longshore coastal (diffusitivity) constant is used. Without the longshore diffusitivity the erosion would be reduced with 3.5 m/year (Figure 16). In the latter case an accretion of 7.5 meter should result after ten years.

4. The supply is favourable for a rather broad coastal stretch of the beach, whereas the diffusion of sand on the inshore is less pronounced.
One should take this feature into account, even admitting the rather high longshore diffusitivity constants, which are at the basis of the computation.

5. The basic assumptions of the simple mathematical model do not involve specific detailed features, which still might occur in practice and still have to be accounted for.

8 Future research

- The effect of the supply has been computed apart from the autonomous behaviour of the North Sea coast of Terschelling. The position and motion of the breaker bars has been used to schematize the profile and to determine the cross shore constants. The present erosion is schematized to a mean value of 2.75 m/year. In the future it would be useful to implement in the computations the changes in volume of the beach and inshore, due to the motion of breaker bars.

- As been mentioned in chapter 7, the cross shore constants are determined by "engineering judgement". It has to be recommended to carry out research concerning these constants.

- No effort has been made to reproduce the present coastal behaviour with the aid of line modelling. A serious effort (an investigation on its own) could lead, by calibration on coastal measurements, to values of as well the cross shore as the longshore diffusitivity constants, which could be compared with the values found in the present report.

9 References

Bakker, W.T.
Gidsstudie naar het gedrag van een vooroeversuppletie op het eiland Terschelling. (in Dutch)
Rijkswaterstaat, Dienst Getijdewateren, internal report
Okt 1992.

Bakker, W.T.
Berekening van het langstransport door golven met de methode van evenwijdige dieptelijnen.
Rijkswaterstaat, Dir. Waterhuishouding en waterbeweging.
Studierapport WWK 69-7. (in Dutch)
1969.

Bakker, W.T.; ten Hoopen, H.G.H.; Grieve, G.R.H.
Berekening van het zandtransport volgens de methode Svašek bij een strand en een vooroever die een hoek met elkaar maken. (in Dutch)
Rijkswaterstaat, Dir.Waterhuishouding en Waterbeweging, Studierapport WWK 71-18;
Juni 1972.

Bakker, W.T. & Delver, G.,
Coastal changes, caused by a shallow water sanddam in front of the Delfland coast.
Technical University of Delft; Coastal Engineering Group.
Sept 1986.

Bakker, W.T. ; van de Kerk, C.P.T. ; de Vroeg, J.H.
Determination of coastal constants in mathematical line-models.
Second European Workshop on Coastal Zones, Loutraki.
1988.

Banning, G.K.F.M.
Shoreface Nourishment Terschelling
Numerical model simulation.
Delft Hydraulics, Report H1823
1993

Casteleyn, J.A.
Numerieke berekeningen van de verandering van kustvormen onder invloed van golfaanval. 1975. (in Dutch)
Deel 1 De berekening van kustconstanten bij kusten onder invloed van een golfklimaat met refracterende en diffracterende golven.
Deel 2 De berekening van kustvormen uit kustconstanten volgens de éénlijn theorie.
Technische Universiteit Delft; Vakgroep Kustwaterbouwkunde; Technisch Rapport 75-1 & 2

CUR, Rijkswaterstaat, Waterloopkundig Laboratorium
Manual on Artificial Beach Nourishment.
1988.

Dijkman, M.J., Bakker, W.T. & de Vroeg,J.H.,
Prediction of coastline evolution for specific parts of the Holland coast.
The Dutch coast; Report of a session on the 22nd ICCE, Delft.
1990.

Groenendijk, F.C., Uit den Boogaard, L.
UNIBEST-berekeningen t.b.v. ontwerp onderwateroeversuppletie Terschelling. Concept werkdocument; (in dutch)
Rijkswaterstaat, Dienst Getijdewateren.
1992

Noordstra, P.
Kustsuppletie Terschelling 1993.
Rijkswaterstaat, Directie Friesland.
Rapport ANW 92.20. (in Dutch)
1992.

Pelnard Considère, R.
Essai de theory de l'evolution de formes de rivages en plages de sable et de galets.
Quatrième Journees de l'Hydraulique, Paris
Les Energies de la Mer, Question III, June 1954

Roskam, A.P.
Golfklimaten langs de Nederlandse kust. (in Dutch)
Rijkswaterstaat, Dienst Getijdewateren (RIKZ).
1988.

Smit, E.S.P.,
De rol van sedimentdwarstransport in de ontwikkeling van de Hollandse kust vanaf het begin van de grote kustuitbouw (ca 5000 jaar geleden).
Notitie in het kader van het project Kustgenese.(in Dutch)
April 1987.

Svašek, J.N.
Invloed van brekende golven op de stabiliteit van zandige kusten.
Rijkswaterstaat, Deltadienst, Waterloopkundige Afdeling
Nota W 68.083.
1968.

Svašek, J.N. ; Bijker, E.W.
Two methods for determination of morphological changes induced by coastal structures.
XXIInd Int. Nav. Congress Paris, section II, item 4.
1969

Syllabus symposium "Lijnmodellen in kustdynamica".(in Dutch)

Velden, E.T.J.M. van der
Coastal Engineering.
Technical University of Delft; Coastal Engineering Group.
dec 1990.

Vessem, P. van
Morfologische analyse kustvak Terschelling, raai 13.00 tot 20.00.
Rijkswaterstaat, Dienst Getijdewateren.
Concept werkdocument. (in Dutch)
1992.

Zwiers, M
Kustdynamiek van vooroeversuppleties.
Onderzoek naar de vooroeversuppleties uitgevoerd op het badstrand van Vlissingen.(in Dutch)
Juni 1990.

Appendix A Smits analytical solutions.

In deze appendix wordt het drie-lijnenmodel (bij een stationaire waterstand) analytisch uitgewerkt; als resultaat worden de functies $y_i(t)$ $(i=1,2,3)$ verkregen.

In figuur h1 wordt een definitieschets gegeven van de gebruikte schematisering.

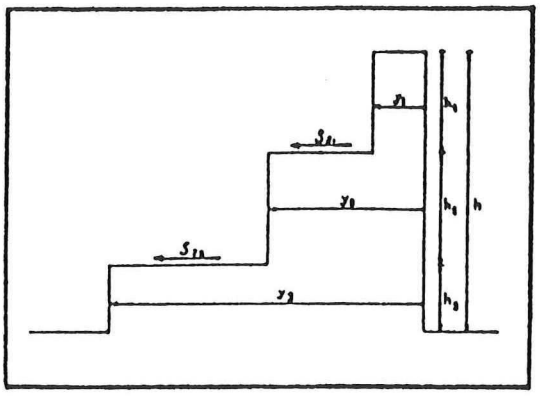

Figuur h1.
Definitieschets drie-lijnenmodel.

Overeenkomstig het twee-lijnenmodel kunnen de volgende twee bewegingsvergelijkingen worden opgesteld:

$$S_{y_1} = s_{y_1} \cdot (y_1 - y_2 + W_1) \qquad (h1^a),$$

$$S_{y_2} = s_{y_2} \cdot (y_1 - y_3 + W_2) \qquad (h1^b).$$

Ook geldt:

$$S_{y_1} = - h_1 \cdot \frac{dy_1}{dt} \qquad (h2^a),$$

$$S_{y_2} = + h_3 \cdot \frac{dy_3}{dt} \qquad (h2^b).$$

En:

$$h_1 \cdot y_1 + h_2 \cdot y_2 + h_3 \cdot y_3 = \text{oppervlak (opp)} = \text{constant} \qquad (h3).$$

Combinatie van $(h1^a)$, $(h2^a)$ en (h3) levert:

$$\frac{dy_1}{dt} = - \frac{s_{y_1}}{h_1} \cdot \left(\frac{h_1+h_2}{h_2} \cdot y_1 + \frac{h_3}{h_2} \cdot y_3 + W_1 - \frac{opp}{h_2} \right) \qquad (h4^a).$$

Combinatie van $(h1^b)$, $(h2^b)$ en (h3) levert:

$$\frac{dy_3}{dt} = + \frac{s_{y_2}}{h_3} \cdot \left(- \frac{h_1}{h_2} \cdot y_1 - \frac{h_2+h_3}{h_2} \cdot y_3 + W_2 + \frac{opp}{h_2} \right) \qquad (h4^b).$$

De vergelijkingen $(h4^a)$ en $(h4^b)$ vormen een gekoppeld stelsel differentiaalvergelijkingen:

$$\begin{bmatrix} \frac{dy_1}{dt} \\ \frac{dy_3}{dt} \end{bmatrix} = \begin{bmatrix} a & b \\ c & d \end{bmatrix} \cdot \begin{bmatrix} y_1 \\ y_3 \end{bmatrix} + \begin{bmatrix} - \frac{s_{y_1}}{h_1} \cdot (W_1 - \frac{opp}{h_2}) \\ + \frac{s_{y_2}}{h_3} \cdot (W_2 + \frac{opp}{h_2}) \end{bmatrix} \qquad (h5),$$

met: $$a = -\frac{s_{y_1}\cdot(h_1+h_2)}{h_1\cdot h_2} = -s_{y_1}^{\circ} = -\frac{1}{T_{o_1}}$$

$$\left.\begin{aligned} b &= -\frac{s_{y_1}\cdot h_3}{h_1\cdot h_2} \\ c &= -\frac{s_{y_2}\cdot h_1}{h_2\cdot h_3} \end{aligned}\right\} \quad b\cdot c = \frac{s_{y_1}\cdot s_{y_2}}{h_2^2} = \frac{1}{T_o^2}$$

$$d = -\frac{s_{y_2}\cdot(h_1+h_3)}{h_2\cdot h_3} = -s_{y_2}^{\circ} = -\frac{1}{T_{o_2}}$$

De oplossing van dit stelsel differentiaalvergelijkingen luidt als volgt:

$$Y_1(t) = K\cdot\exp(\lambda_1\cdot t) + M\cdot\exp(\lambda_2\cdot t) + Y_{1\infty} \qquad (h6^a),$$

$$Y_3(t) = \frac{1}{b}\cdot\left(\lambda_1+\frac{1}{T_{o_1}}\right)\cdot K\cdot\exp(\lambda_1\cdot t) + \frac{1}{b}\cdot\left(\lambda_2+\frac{1}{T_{o_1}}\right)\cdot M\cdot\exp(\lambda_2\cdot t) + Y_{3\infty} \qquad (h6^b).$$

Hierin is: $$Y_{1\infty} = \frac{1}{h}\cdot(opp - (h_1+h_3)\cdot W_1 - h_3\cdot W_2)$$

$$Y_{3\infty} = \frac{1}{h}\cdot(opp + h_1\cdot W_1 + (h_1+h_2)\cdot W_2)$$

en: $$\lambda_1 = -\frac{1}{2\cdot T_{o_1}} - \frac{1}{2\cdot T_{o_2}} - \sqrt{\frac{1}{4}\cdot\left(\frac{1}{T_{o_1}}-\frac{1}{T_{o_2}}\right)^2 + \frac{1}{T_o^2}}$$

$$\lambda_2 = -\frac{1}{2\cdot T_{o_1}} - \frac{1}{2\cdot T_{o_2}} + \sqrt{\frac{1}{4}\cdot\left(\frac{1}{T_{o_1}}-\frac{1}{T_{o_2}}\right)^2 + \frac{1}{T_o^2}}$$

Invulling van deze resultaten in (h3) geeft:

$$Y_1(t) = \left(-\frac{h_1}{h_2} - \frac{h_3}{h_2}\cdot\frac{1}{b}\cdot\left(\lambda_1+\frac{1}{T_{o_1}}\right)\right)\cdot K\cdot\exp(\lambda_1\cdot t) + \left(-\frac{h_1}{h_2} - \frac{h_3}{h_2}\cdot\frac{1}{b}\cdot\left(\lambda_2+\frac{1}{T_{o_1}}\right)\right)\cdot M\cdot\exp(\lambda_2\cdot t) + Y_{1\infty} \qquad (h6^c).$$

Hierin is: $$Y_{1\infty} = \frac{1}{h}\cdot(opp + h_1\cdot W_1 - h_3\cdot W_2)$$

K en M volgen uit de beginvoorwaarden:
als geldt: $Y_1(t=o) = Y_{1_b}$
en: $Y_3(t=o) = Y_{3_b}$,
dan volgt voor K en M:

$$K = -\frac{b}{\lambda_2-\lambda_1}\cdot(Y_{3_b}-Y_{3\infty}) - \frac{\lambda_2+\frac{1}{T_{o_1}}}{\lambda_2-\lambda_1}\cdot(Y_{1\infty}-Y_{1_b}) \qquad (h7^a),$$

$$M = +\frac{b}{\lambda_2-\lambda_1}\cdot(Y_{3_b}-Y_{3\infty}) + \frac{\lambda_1+\frac{1}{T_{o_1}}}{\lambda_2-\lambda_1}\cdot(Y_{1\infty}-Y_{1_b}) \qquad (h7^b).$$

Appendix B1 Example of table with distribution of wave height and wave period of one wave direction sector.

STATION : SCHIERMONNIKOOG-NOORD (SON)

PERIOD : 21-11-1979 T/M 31-12-1991
3-HOURS INTERVAL MEASUREMENTS SERIES

WIND DIRECTION SEKTOR : 205 - 235

WAVE HEIGHT Hmo IN CLASSES OF 50 CM (VERTICAL)
WAVE PERIOD Tmo IN CLASSES OF 2.0 SEC (HORIZONTAL)
FREQUENCIES IN PERCENTS

NUMBER OF VALUES IN THIS SECTOR = 3723.

	<1.0	1-2.9	3-4.9	5-6.9	7-8.9	>=9.0	ALL	Tmean	CUM.
0-49	0	1.397	11.362	0.833	0	0	13.591	3.71	100
50-99	0	0.269	31.91	4.244	0.107	0	36.53	4.08	86.409
100-149	0	0	23.127	5.963	0	0	29.089	4.53	49.879
150-199	0	0	8.783	5.855	0.054	0	14.692	4.94	20.79
200-249	0	0	1.155	3.492	0.081	0.027	4.754	5.37	6.097
250-299	0	0	0	0.86	0.107	0	0.967	5.95	1.343
300-349	0	0	0	0.188	0.081	0	0.269	6.32	0.376
350-399	0	0	0	0.054	0.027	0	0.081	6.7	0.107
400-449	0	0	0	0	0.027	0	0.027	7.9	0.027
450-499	0	0	0	0	0	0	0	0	0
500-549	0	0	0	0	0	0	0	0	0
550-599	0	0	0	0	0	0	0	0	0
600-649	0	0	0	0	0	0	0	0	0
650-699	0	0	0	0	0	0	0	0	0
700-749	0	0	0	0	0	0	0	0	0
>750	0	0	0	0	0	0	0	0	0
ALL	0	1.665	76.336	21.488	0.483	0.027	100	4.38	100
Hmean	0	38.9	95.5	149.3	233.1	235	106.8		

Appendix B2 Example of table with distribution of wave height and water level of one wave direction sector.

STATION : SCHIERMONNIKOOG-NOORD (SON)

PERIOD : 21-11-1979 T/M 31-12-1991
3-HOURS INTERVAL MEASUREMENTS SERIES

WIND DIRECTION SEKTOR : 205 - 235

WAVE HEIGHT Hmo IN CLASSES OF 50 CM (VERTICAL)
WATER LEVEL IN CLASSES OF 50 CM (HORIZONTAL)
FREQUENCIES IN PERCENTS

NUMBER OF VALUES IN THIS SECTOR = 3723.

	<-100	-100 -50	-50 -1	0 +49	+50 +99	>= +100	ALL	WL mean	CUM.
0-49	2.901	1.853	1.612	2.498	4.136	0.591	13.59	-8	100
50-99	6.608	5.748	4.996	6.473	10.556	2.149	36.53	-5	86.409
100-149	4.19	5.238	4.136	5.345	7.843	2.337	29.09	-1	49.879
150-199	1.504	2.337	2.444	2.417	4.163	1.826	14.69	11	20.79
200-249	0.161	0.645	0.886	1.128	1.155	0.779	4.75	26	6.097
250-299	0	0.188	0.215	0.215	0.134	0.215	0.97	27	1.343
300-349	0	0	0.054	0	0.081	0.134	0.269	89	0.376
350-399	0	0	0.027	0.027	0	0.027	0.081	32	0.107
400-449	0	0	0	0	0.027	0	0.027	87	0.027
450-499	0	0	0	0	0	0	0	0	0
500-549	0	0	0	0	0	0	0	0	0
550-599	0	0	0	0	0	0	0	0	0
600-649	0	0	0	0	0	0	0	0	0
650-699	0	0	0	0	0	0	0	0	0
700-749	0	0	0	0	0	0	0	0	0
>750	0	0	0	0	0	0	0	0	
ALL	15.364	16.009	14.37	18.104	28.096	8.058	100	0	100
Hmean	90.9	108	114.1	106.7	104.1	132	106.8		

Evaluation of a combined inshore and beach nourishment at the German Wadden Island of Norderney

M.Sc. Thesis Report, Part 2

August 1995

N.F. Kersting

TU Delft

Delft University of Technology

Faculty of Civil Engineering
Hydraulic and Geotechnical Engineering Division
Hydraulic Engineering Group

The author gratefully acknowledge that the volume data from profile measurements used in this report have been made available by Dr.-Ing. H.J. Stephan of the Coastal Research Station Norderney (CSR).

Furthermore, the collaboration with the Rijkswaterstaat, National Institute for Coastal and Marine Management/RIKZ, direct commissioner of the project and with the CSR in general is memorized with great acknowledgement.

This work was carried out as part of the NOURTEC project. It was funded jointly by Delft University of Technology, Rijkswaterstaat and the Commission of the European Communities, Directorate General for Science, Research and Development, under contract MAS2-CT93-0049.

Summary

In the scope of the NOURTEC project, offshore nourishment at the German Wadden island of Norderney has been evaluated with the use of line-modelling.

In past and present times the island of Norderney suffers from severe erosion of its West coast. Problems and solutions, which have been found in the present and in the past are described.
Specially, the attention is drawn to the various artificial sand supplies of which the last one, contained in available data, took place in 1992.
The available data concerning volumes of sand, enclosed in groyne fields at various times is visually displayed. A rough analysis of the observed phenomena is given.

"Coastal constants", which give information on the way a distinct coastal shape (as for instance caused by sand supply) diffuses in longshore and cross-shore direction are derived in two ways: a theoretical way and a phenomenological way. Knowledge of these constants enables coastal morphological predictions and evaluation of alternatives.

The theoretical way for finding the coastal constants starts from wave climate and from sand transport formulae; a transformation from offshore wave climate to local wave climate is necessary.
This transformation is rather complicate because of the shelter of the considered area at the Norderney West coast by the outer delta and the presence of nearshore tidal channels. Furthermore high waves mostly are combined with storm surges and thus in a sense hop over the outer delta.

The phenomenological way considers initial conditions and boundary conditions of a coastal stretch. The coastal constants are matched in such a way, that the observed coastal behaviour is reproduced.

Results, found in theoretical and phenomenological way are compared (also with results found elsewhere) and discussed.
High diffusitivity constants are found as well for the longshore diffusion in the upper beach area and for the cross-shore diffusion.

This gives numerical support to the German "Fingerspitzengefühl" that offshore supply between the groynes is feasible.

Contents **page**

List of figures

List of Tables

List of abbreviations

FSK	Forschungsstelle Küste; Coastal Research Station.
KFKI	Kuratorium für Forschung im Küsteningenieurswesen; German Committee on Coastal Engineering Research.
MAST II	Marine Science and Technology, part two; EU research program.
MTHW	Mittleres Tidehochwasser; Mean High Water Level.
MTNW	Mittleres Tideniedrigwasser; Mean Low Water Level
NCK	Nederlands Centrum voor Kustonderzoek; Netherlands Centre for Coastal Research.
NLÖ	Niedersächsische Landesamt für Ökologie; Lower Saxonian Central Board for Ecology.
NN	Normal Null; German geodetic reference datum, equals nearly the mean sea level.
NOURTEC	Innovative Nourishments Techniques Evaluation; part of MAST-project.
STAIK	Staatliches Amt für Insel- und Küstenschutz Norden; Local Board for island and coastal protection in Norden, East Frisia.

1 Introduction

The island of Norderney is one of the East Frisian Islands in the state of Lower Saxony, Germany (Figure 1). The shape of these islands changed in the past due to migration of tidal inlets (Homeier, 1962). Due to the migration of the tidal channel towards the western shore of Norderney severe dune erosion occurred during the last two centuries.

A similar development would have been accepted in the past and people would simply build their houses on a site at the island which at that time was expected to be stable and therefore safe.

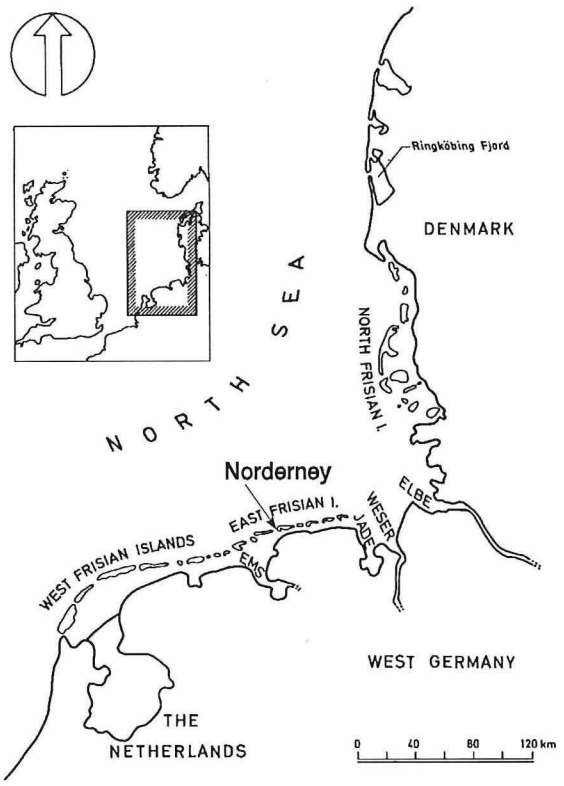

Figure 1 *The location of Norderney*

At Norderney, however, a health resort had developed since the end of the 18th century. A large number of buildings had been built on the western part of Norderney which afterwards were endangered by erosion.

In 1858 the first solid coastal protection structures were erected. These consist of revetments and groins. Since then these structures have been extended over a total length of approximately 6 km (Figure 2). Most groins were meant to stabilize the

beach, but around 1900, groins were built on the western side of Norderney, which are extended to a depth of 18 m in order to prevent future channel migration more eastward.

All these structures were successful in keeping the shoreline, but these were not able to maintain stable beaches. To protect the structures against undermining and weakening, in 1951 and in 1952 the first artificial nourishments in Europe were carried out at Norderney. A total of approximately 1.25 million cubic meter sand was used for recovery of the beaches. Since then several beach fills were carried out.

Largely based on cost effectiveness, artificial nourishment is selected as the measure to secure the island, instead of the extension of the solid structures. The structures, however, are the real protection of the most densely populated part of the island against storm surges. The main goal of the nourishments is therefore to reduce damage to the structures and their function is considered as a maintenance measure (Arbeitsgruppe Norderney, 1952).

The second important reason to carry out nourishments is the recreational function of the beaches, which is of a great importance for the economy of Norderney.

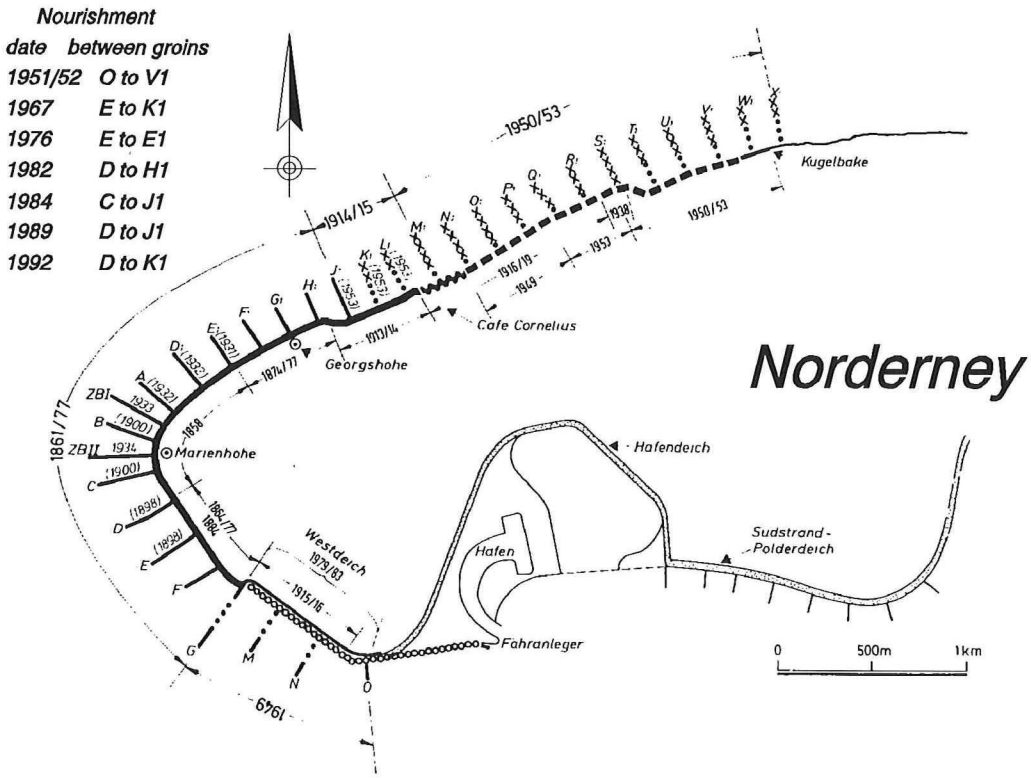

Figure 2 *Coastal protection at Norderney.*

In 1988 an intensive monitoring program was started to investigate the effects of the nourishment to be carried out in 1989, including field measurements of hydrodynamical parameters, surveys of the beach and inshore and sediment sampling. The main results were :

a) the nourishments are indeed an appropriate solution to protect the existing structures from failure during storm surges.
b) to achieve lower losses of nourished material the beach should not be nourished higher than to achieve the protection goals (Kunz & Stephan, 1992)
Above a 'critical beach profile' the losses of nourished material out of the groinfields increase considerably with height.

The application of an inshore nourishment was therefore regarded as a suitable alternative to the conventional beach nourishment (Niemeyer, 1992). In 1992 a combination of beach and inshore nourishment has been carried out in order to find the most economical way of nourishment.

The project will be evaluated as part of the NOURTEC project in which investigators of the Netherlands, Germany and Denmark participate in the scope of the MASTII EU program. Rijkswaterstaat commissioned the Technical University of Delft to compute predictions with the aid of the n-line modelling technique and to evaluate the development of the nourishment of 1992.

The following chapter 2 presents the results of a literature study about the situation of Norderney. This concerns the historical development of the tidal inlet of Norderney and several important aspects of the various sand supplies.

Chapter 3 gives, as a first impression, a visualisation of the data gathered during the various supplies. Furthermore it gives a rough phenomenological analysis.

Chapter 4 focuses on boundary conditions, waves and tides, causes of sand transport. The object of chapter 5 is the mechanism of sand transport; characteristics of it are derived from the boundary conditions, described in ch.4.

Chapter 6 refers to chapter 3: the data on sand volumes in groin sections in course of time is converted to its essentials, i.e. to three characteristic lines. These are: a line of the beach, a line of the inshore and a line of the deeper zone. The behaviour of these lines as found from the data is compared with the results of computations with three-line modelling (compare fig.31 with fig.32 and fig.33 with fig.34).

In three-line modelling diffusitivity constants ("coastal constants") in longshore and cross-shore direction are important. These can be calibrated in order to match natural development (as happens in ch.6) or can be found from wave data, as happens in ch.4 and 5. A comparison is given in ch.7, which also gives the conclusions.

2 Description of Norderney

2.1 Description of morphology

Regarding the hydrodynamical classification of tidal inlets according to Hayes (1979), the inlet 'Norderneyer Seegat' can be classified as a mixed energy type with a tide

dominance, based on the mechanism of the tidal inlet system. This can be supported by historical knowledge about the area. In the case of Norderney the morphological development in the past is very well known (Figure 3). From study of maps the behaviour of the tidal inlet has been reconstructed (Homeier, 1962, 1964).

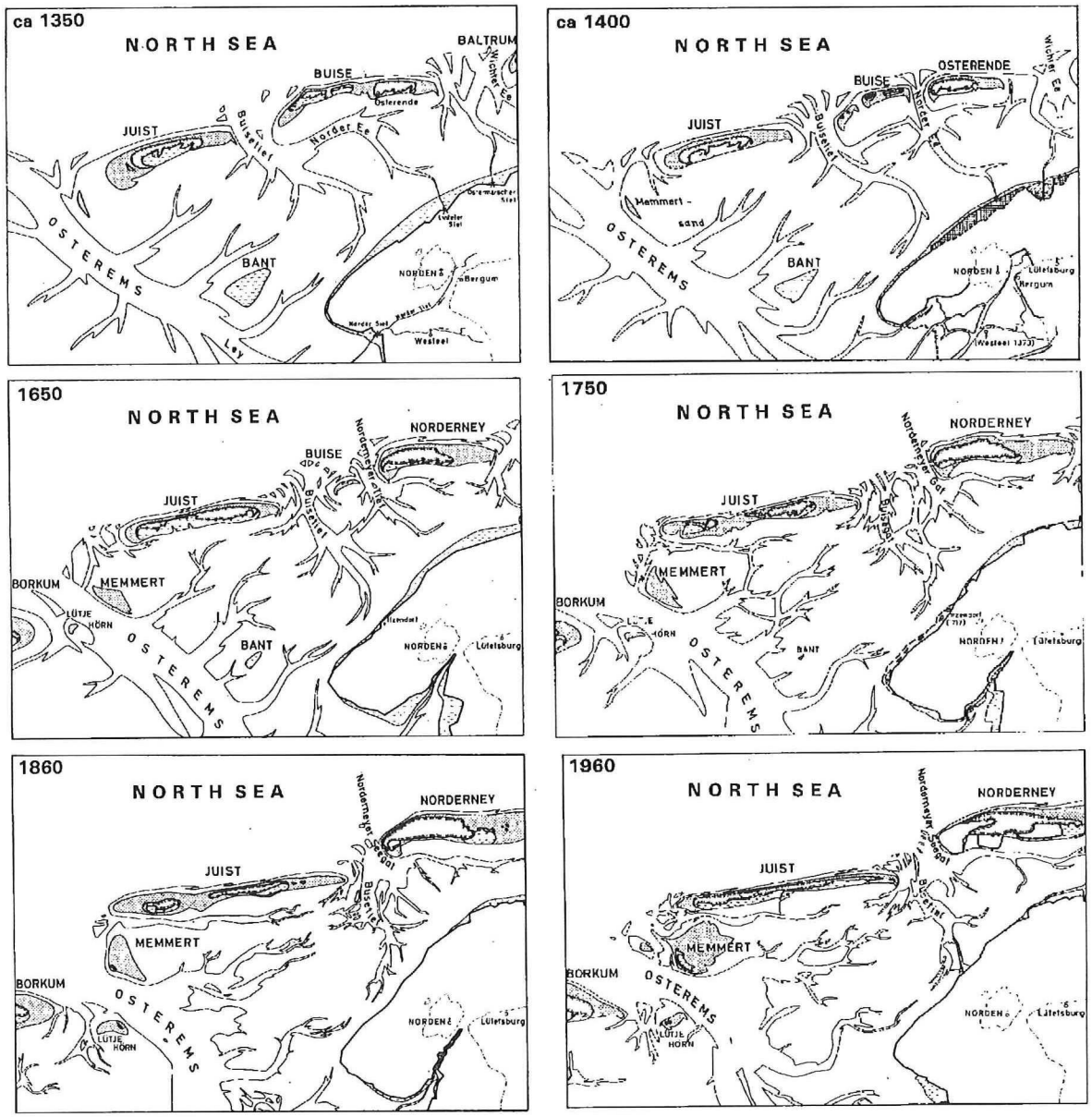

Figure 3 *Morphological development of Norderney in the past.*

A cyclic bypassing process has been recognized (Luck, 1977), consisting of six phases (Figure 4). The tidal inlet system has nowadays developed to phase IV of a one-throat system with one ebb-delta which extends furthermore seaward due to an increasing tidal volume through the deep tidal channel, which is situated on the downdrift eastward side of the tidal inlet (Figure 4). The longshore sediment transport due to the eastward directed littoral drift bypasses the inlet in the form of large, migrating swash bars.

The "landfall" (Niemeyer, 1990), i.e., the place where the swash bars "land" on the coastline, at Norderney is downdrift at about 5 km distance of the western end of Norderney. The beaches updrift of the landfall get almost no sand supply due to littoral drift and erode due to a gradient in longshore transport. This erosion, in combination with the shoreline protection by solid structures, has led to narrow, steep beaches without bars.

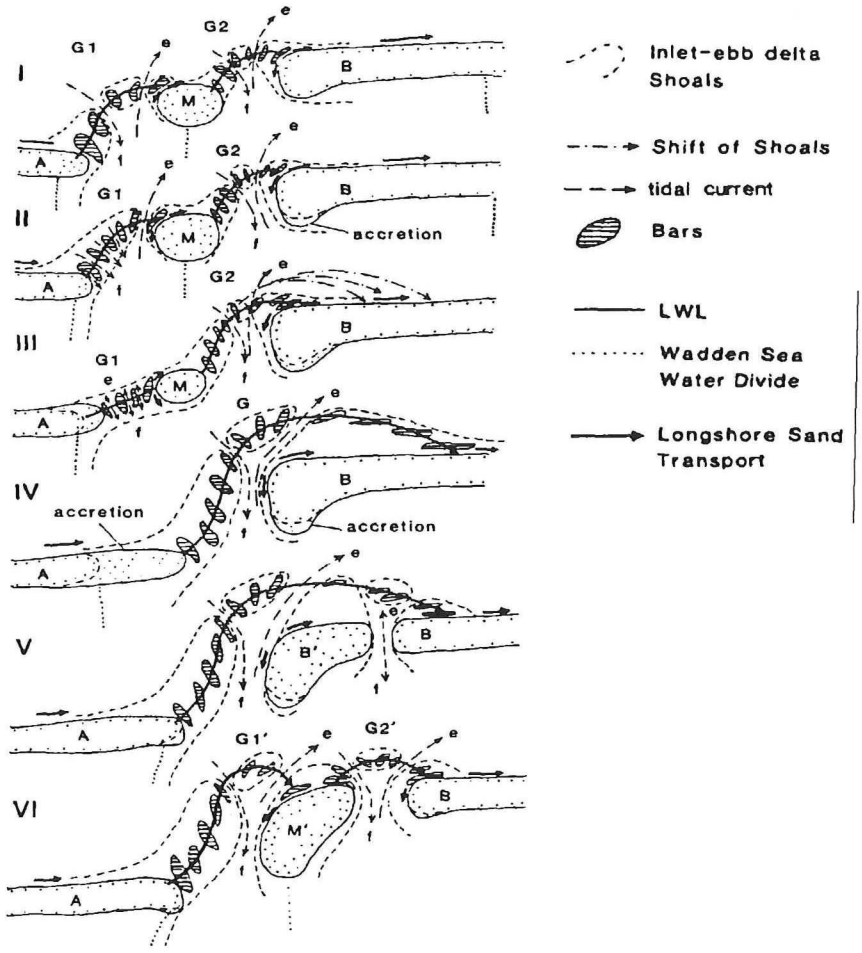

Figure 4 *Morphological development of the tidal inlet (after Luck, 1977).*

All supplies, carried out between 1951 and 1989 show high initial losses. These are expected to be mainly the result of a disturbance from the equilibrium profile and the associated cross shore transport (Kunz and Stephan, 1992). The structural erosion is predominantly affected by gradients in longshore transport (Van de Graaff et al, 1992).

Investigation of the effects of storm surges shows that even those beaches with the highest erosion rates recover from the erosion due to the storm surges (Homeier, 1976). This recovery takes only several weeks. The storm surges don't have significant impact on the mid-term trend of erosion. Beach erosion during storm surges leads to accumulation of sand at the inshore, which is partly transported back due to cross shore transport in the following calmer period.

2.2 Wave climate and wave induced currents

High energy wave conditions occur for winds from west to northeast, generating landward waves in the southern North Sea. The predominantly western and northwestern directions of wind, sea and swell result in a system of longshore currents having a northeasterly direction at the northwestern beach and a southeasterly direction in the vicinity of the Norderneyer Seegat (Niemeyer, 1986a).

The area where this energy-concentration of waves due to refraction, takes place is called the area of divergence. Here the longshore currents change in direction. The wave action at the structures on the southwestern and southern shores is small, because the shores are oriented parallel to the main direction of the wavecrests due to refraction, guided by the deep channel of the tidal inlet.

The ebb delta overlaps the island's shore seaward of the repeatedly nourished beaches. Waves propagating onshore from sea into this area have to pass the shoals of the ebb delta. The delta forces higher and steeper waves to break. The wave heights on the island's inshore are on average twice as high as in the tidal inlet, where the shoals, that are situated more seawardly, have a larger areal extension and are closer to each other (Niemeyer,1986a).

Though the wave lengths in both regions are nearly of the same scale, this effect leads to much larger differences in wave energy. The average wave energy flux on the island's inshore has a value of 30% of the one in the offshore area and in the tidal inlet this value is only 8% of the offshore value (Niemeyer,1986a).

Due to breaking of waves also a shift in energy takes place towards higher frequencies, combined with a transformation of the energy spectra from high concentrations in a single peak to multi-peak spectra (Niemeyer, 1986a). The annual averaged offshore significant wave height is about 0.7-1.0 m. The significant wave height with a yearly exceedance frequency of 1/50 per year on the seaward shoreface (on the outer delta)

is 6.7 m (Niemeyer, 1986c).

Because the velocities are significantly higher, wave induced currents affect the sediment transport on the beach more than the tidal currents. Even for moderate waves, there is a certain percentage of wave-induced currents exceeding the levels of 0.6 m/s and even 1.5 m/s. This percentage increases significantly in the case of storm surges. The highest velocities occur in undertows; longshore currents have lower velocities (Niemeyer, 1992).

During a storm surge there is a broad surf zone with breaking waves which occur as white rollers. The onshore directed mass flux of these rollers must be compensated by a relative large seaward current velocity below the level of the wavestroughs. The combination of the strong currents and the high suspension rates due to the high turbulence, causes the enormous scour (Niemeyer, 1990). This becomes especially visible in front of revetments after storm surges. At the shoreface (the deeper part of the inshore) of the North West beach, where the turbulence and currents are much lower, sedimentation of the eroded material takes place.

During calmer periods an onshore directed bed load transport occurs due to the high non-linearity of steep shoaling non-breaking waves. The capacity is much lower than the erosion during storm surges and the recovery process has therefore a relatively long duration.

The effectiveness of groins depends primarily on the relative reduction of the total water column due to the groin elevation above the beach and not on the water depth above the groin crest (Niemeyer, 1990). This implies that the deposition of material on the shoreface is more effective than on the beach itself. A replenishment at the beach reduces the effectiveness of the groins. When the sand is placed high at the beach, it covers the groins. This leads to large initial losses due to longshore transport on the beach.

Nourishment on the shoreface leads to lower cross shore transports due to the disturbance of the equilibrium profile. Because the nourishment usually takes place in the late spring or summer, a shift of material is expected from the shoreface to the beach, building up there a deposit for the erosion due to autumn and winter events with strong sea conditions including storm surges.

The main advantage of this process is that it takes a certain period of time to build up the deposit and within this period the nourished material will be mainly in a position where it is less sensitive to erosion by longshore currents.
The reduction of the effectiveness of the groins with a nourishment on the beach results in the fact that the nourished material is exposed from the beginning to the eroding capacity of even the relative small waves.
A shoreface nourishment might therefore be a successful solution to increase the effectiveness of nourishments (Niemeyer, 1990).

2.3 Tide and tide induced currents

The tidal range in the German Bight is mesotidal with a mean tidal range in the area of Norderney of 2.40 m with variations due to spring and neap tide of 0.7 m. The water level is expressed in meter, with respect to NN (see page vii). From measurements in the period 1982-1986 the following is computed : (Lassen und Siefert, 1991)

- the mean low water level (MLWL) equals NN-1.26 m.
- the mean high water level (MHWL) equals NN+1.14 m.
- the mean water level (MWL) equals NN-0.031 m.

The tide is lunar semi-diurnal with a mean period of 12 hour and 25 minutes. The highest measured storm set-up was approximately 3 m above MHWL. According to the German standard classification, the averaged yearly exceedance frequencies of storm surge peaks above MHWL are (Niemeyer, 1986c) :

- 10 for 0.93 m
- 0.5 for 1.95 m
- 0.05 for 2.86 m

The water level gradients due to ebb and flood cause high current velocities in the several channels. Through these channels water flows to and from the Wadden Sea behind the islands. Between the island of Juist and Norderney there are two channels, separated by several shoals. The deeper easterly channel, i.e., the Norderneyer Seegat, is dominated by the ebb current.

The mean velocities are for both ebb and flood currents about 0.7 m/s with maximum velocities of the order of 1.2 m/s, reaching extreme values of 1.4 m/s for flood and 2 m/s for ebb currents during storm surges. Ebb durations of more than 21 hours have been observed for storms from southwest to west (Koch and Niemeyer, 1978).

The tidal currents on the beach, between the groins, are weak, with mean velocities of about 0.10 m/s. Based on measurements covering 21 tidal cycles, a range of maximum velocities of 0.03 to 0.30 m/s for flood and 0.05 to 0.40 m/s for ebb have been estimated. At the inshore of the inlet, velocities are considerably higher, with maximum values of 0.44 to 0.56 m/s for flood and 0.49 to 0.69 m/s for ebb currents (Niemeyer, 1986b).

During the tidal phases with water levels in the range of nearly MHWL and higher, the differences between the current velocities on the channel's slope and in the groin fields along the inlet, are very small. The beach groins in the area of the inlet have no considerable influence on tidal currents (Niemeyer, 1986b).

In the groin fields on the northwestern shore and in the area of divergence, the tidal current velocities are remarkably smaller than those closer to the deep inlet channel. The tidal currents in this area depend directly on those on its inshore, which are much weaker than those in the tidal inlet channel. The low velocities of tidal currents on the

beaches with the largest erosion rates show that the tidal currents will create nearly no erosion on their own, but only as a result of superposition of wave and surf action (Niemeyer, 1986b).

2.4 Nourishments

To stop further migration of the tidal channel groins were built (ZbI and ZbII), which were extended to a depth of 18 m in the tidal channel (Figure 2). Due to these groins and the other groins, revetments and seawalls, the situation of the western part of Norderney is fixed.

The beaches suffer from structural erosion which endangers the stability of the protection structures. In 1951/52 the first nourishment was carried out to let the beaches recover. Many nourishments have followed since then (Table 1). The mean value of the volume which has been supplied since 1951 until 1989 is approximately 85.000 cubic meter per year.

year	length (km)	groinfields	volume (m3)	d50 (mm)
1951/52	6.0	O-V1	1.250.000	0.10-0.13
1967	2.0	E-K1	240.000	0.15-0.30
1976	1.1	E-E1	500.000	0.18-0.30
1982	1.5	D-H1	470.000	0.17-0.25
1984	1.7	C-J1	410.000	0.16-0.20
1989	1.8	D-J1	447.000	0.15-0.20
1992	2.0	D-K1	500.000	0.22
Dry fill				
1983	0.6	J1-N1	64.000	
1990	0.5	J1-N1	45.000	

Table 1 *Site and amount of the various supplies.*

A groinfield is the area between two adjacent groins.

Until 1989 nourishments were carried out mainly in the area above MLW. The sand deposits on the beaches were so high that these even covered the groins. In this situation the groins have no blocking effect on the longshore transport. The largest part of the initial losses in the first summer, are due to the gradients in the longshore transport in the first months after nourishment.

To decrease these losses in 1992 the supply was carried out differently. The nourishment was carried out as a stockpile in each groinfield (Figure 5). By just extending the pipes during nourishment in cross shore direction sand bodies were created with the shape of a groin. No distribution of sand was needed, because of the natural forces which transformed the body within weeks.

After a few weeks the groin shape of the nourishment had already disappeared in the area above NN-1 m. After the summer of 1992 the distribution of sand of the nourishment in the groinfields was already the same as in case of a traditional beach nourishment, but with a further extension in offshore direction.

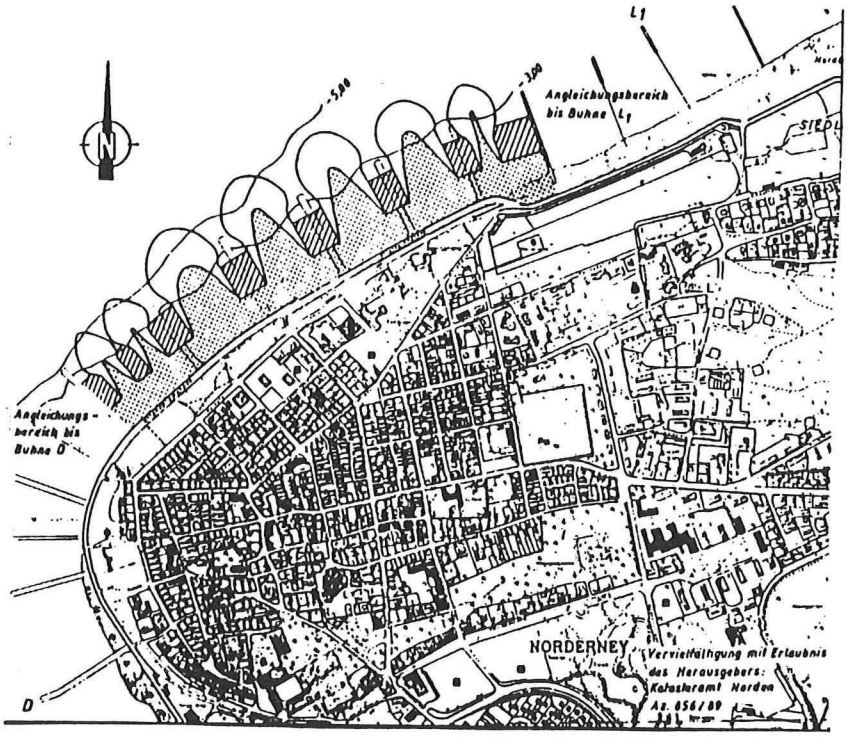

Figure 5 *Placing of the combined nourishment.*

3 Analysis of volume computations

3.1 Introduction

Since the first beach nourishments at Norderney the beach profiles are measured regularly to determine the development of the beaches in time. These profile data have been used to compute the volumes of sand in each groinfield, i.e., the area between two adjacent groins. Computations have been carried out by the FSK (Page vii) for all groinfields.
FSK made the results of these computations available for this study. The data consists of files containing the volume data per groinfield.

The computed volume data has been used for three reasons:
- to investigate the development of the volumes of sand in the nourished beaches and the adjacent beaches.
- to compare the development of combined nourishment (beach and inshore) with only beach nourishment.
- to elaborate the data to values in order to compare with the results of the computations with the line model.

In this chapter the results of the analysis are presented. In §3.2 the method of profile measurements is shortly described.

Apart from the volume data of the combined nourishment of 1992, also the data of the beach nourishment of 1989 has been analyzed. Background of this choice will be given in §3.3.

More detailed objectives of the analysis, description of the data and considerations in respect of the way of analyzing and presenting the data are given in §3.4. In the original form the volume data was not suitable for analyzing. Therefore, the data has been elaborated to more suitable values. This is explained in §3.4.3.

The graphs, which resulted from the elaborations of the original volume data, are partly shown in §3.5. The remaining graphs are shown in Appendix C.

Analyzing the graphs, depicting the volume data, leads to several observations which are presented in §3.6.

The recommendations, which follow from the study of the graphs, in respect to the application of the line modelling technique are presented in §3.7.

3.2 Method of profile measurements

The profile measurements on the inshore are carried out from a survey vessel with a small draught of about 0.4 m. It navigates along defined lanes. From the promenade the position of a reflector on the ship has been traced with the aid of a theodolite. From the angle and distance the position has been determined. At the same time the depth has been measured with an echo sounder. From these values the bottom topography has been computed.

3.3 Background of selection of data

The success of a supply should be related to the scheduled life time of the fill and to which extent the sand stays there where it is needed to reach its goal. This seems obvious, but too often the success is related to the visible effects. In chapter 2.1 it is already mentioned that the main goal of the supplies at Norderney is to secure the groins and seawalls. The supplies have to be regarded as a maintenance measure.

To determine the success of a supply by profile measurements, it is important to determine the maximum depth level of the area, which is supposed to be important for reaching the goal of the supply. The decrease of the sand volume above this level then could be considered as "loss". In practice often the MLW-level has been used, because the depth contours above this level are easily to measure, with a minimum of costs and technical needs.

The shape of the shoreface is also of importance for the beach itself due to both its interactions with hydrodynamics and particularly waves and the cross shore sediment transport in on- and offshore direction. This area has the function of storage area of sand resulting from offshore directed cross shore transport during storm tides. During calm weather conditions this sand will be partly transported back to the area above the MLW-level by cross shore transport. The other part will disappear as a result of a gradient in resulting longshore transport.

The area which is expected to be of most importance for the security of the groins and seawall during storm tides, is considered to be limited by the NN-5m depth contour (Thilo and Kurzack, 1952). However most of the measurements since 1952 are merely to the MLW-level, because of lack of resources.

The supply of 1989 is the first one for which the profiles have been measured extensively over all levels down to the depth of NN-5m for several years. In the period May 1989, just before the nourishment, until May 1992, just before the next nourishment, totally 10 measurements were carried out down to this NN-5m level. The measurements took place within the framework of the research project 'Interaction between coastal constructions and marine environment' of the KFKI.

3.4 The way of analyzing the volume data

3.4.1 Objectives

The main objective of analyzing the results of the volume computations is to get an impression of the aspects involving the development of the supplies along the coast of Norderney.

Several questions should be answered:
- Where and how much has been nourished?
- In what way does the supply reshape itself in cross shore direction?
- Which are the differences in development of the profiles along the coast?
- Is it possible to trace the losses of sand?

To achieve the answers on the questions the original data had to be elaborated. Firstly, in §3.4.2 the original data will be discussed, whereafter the elaboration will be presented in §3.4.3.

3.4.2 Original volume data

The original data consists of files with computed volumes above a certain level at a specific time per groinfield. As example a part of such a file is given in Appendix D.

The volumes are calculated for different depth intervals. The volumes are bounded by horizontal levels and by a vertical plane (the seawall). The levels which have used are:
NN-5m, NN-4m,
NN-3m, NN-2m,
NN-1.5m, NN-1m
and NN+0m

Many times the volumes are computed only down to NN-1.5m, because at these moments only the beach has been measured. This has already been explained in §3.3.

3.4.3 Elaboration of volume data

During the elaboration of the data it had to be determined in which form the data would possibly give the answers on the questions mentioned in §3.4.1. Two main types of graphs have been chosen to represent the original data:
1 development in time of all volumes in a certain groinfield.
2 development in longshore directions of a certain volume for all groinfields.

For type 1 the best way of showing information is by graphs which give the development in time of the total volume between two depth levels in a specific

groinfield.
For type 2, as the groins are not equidistant, reducing the volumes to volumes per linear metre gives the clearest display of the development in time of the volumes in longshore direction. Presented can be either "volumes above a certain level" or "volumes between two adjacent levels".

In the scope of the present investigation, data has been visualized in the following graphs (Appendix C):

For the nourishment executed in 1989:

- For each groinfield between groin D and R1 (see Figure 2, page 2) the development in time of the volumes (m^3) between all adjacent levels (Appendix C, Figure 1 to Figure 19).

- For each level the development in time of volumes (m^3/m') above this level for all groinfields between groin D and groin R1 (Appendix C, Figure 20 to Figure 29). Figure 6 (page 15) shows an example.
- For each level the development in time of volumes (m^3/m') between this level and the adjacent higher level for all groinfields between groin D and groin R1 (Appendix C, Figure 30 to Figure 37).

For the nourishment executed in 1992:

- For each groinfield between groin ZbI (called groin I in the graphs) and groin J1 the development in time of the volumes (m^3) between all adjacent levels (Appendix C, Figure 38 to Figure 44). Figure 7 on page 16 gives an example.

From the analysis of the graphs regarding the nourishment of 1989, it was concluded to concentrate on the area between groin ZbI and groin J1. This because of two reasons:
1 The profile measurement in the adjacent groinfields are mainly carried out down to NN-1.5m.
2 The sand on the inshore had been supplied between groin D and groin J1.

As a consequence, detailed graphs concerning the supply of 1992, showing the development in time of all volumes, were made only for groinfield A-D1 to groinfield H1-J1.

The graphs are analyzed in order to find the answers on the questions mentioned in §3.4.1. The graphs, presented in Appendix C, can be used to calibrate the line modelling technique with the data analysis.
Apart from the two types of graphs described above (of which Figure 6 and Figure 7 give an example), there is a third way of presentation, which puts the accent on the development of the volumes compared to the supplied volumes. Figure 8 to

Figure 10 give examples. It also shows the distribution over the depth in course of time. The bars represent the difference between the volume at that moment and the latest volume computed just before the supply was carried out.

3.5 Results

Figure 6 is an example of the graphs which show the development of the volumes in longshore direction.

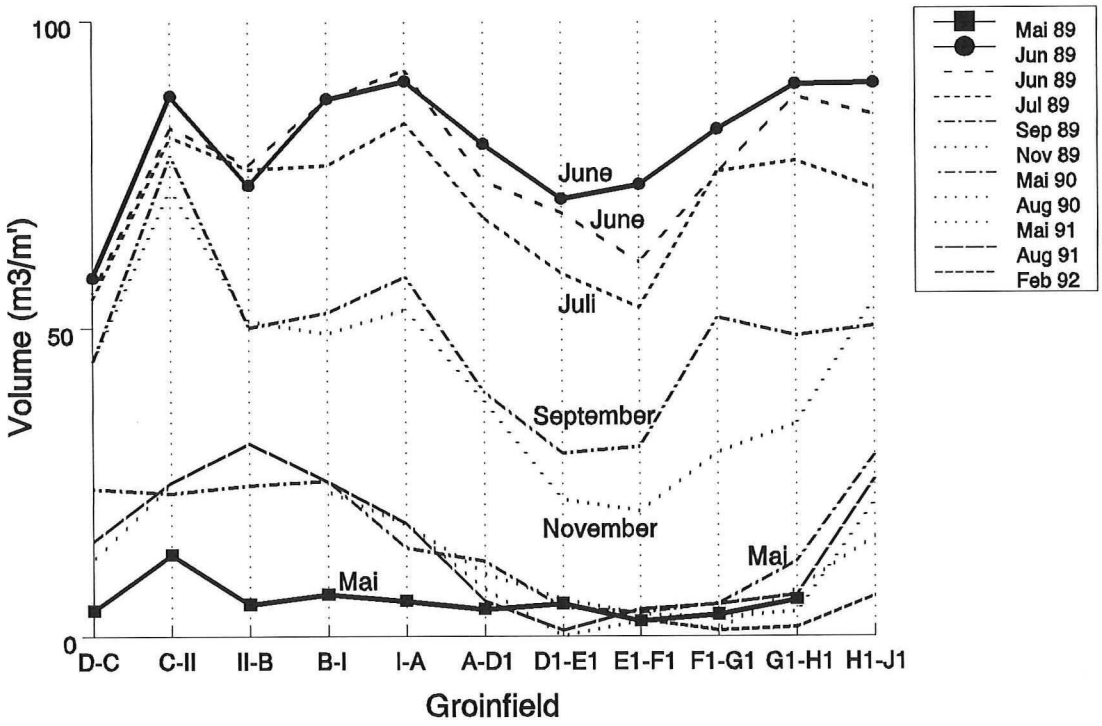

Figure 6 *Volumes above NN+0m, between May 1989 and Feb 1992.*

In Figure 6 the volumes per linear metre are shown. It clearly shows the large losses in all fields for the volumes above NN+0m. Especially the volumes of groinfield D1-E1 and E1-F1 decrease rapidly: 70% from June to November 1989. After the winter of 1990 the volumes between A and G1 are already the same as before the nourishment.

Figure 7 is an example of the graphs which show the development of the volumes, between depth intervals, in time per groinfield.

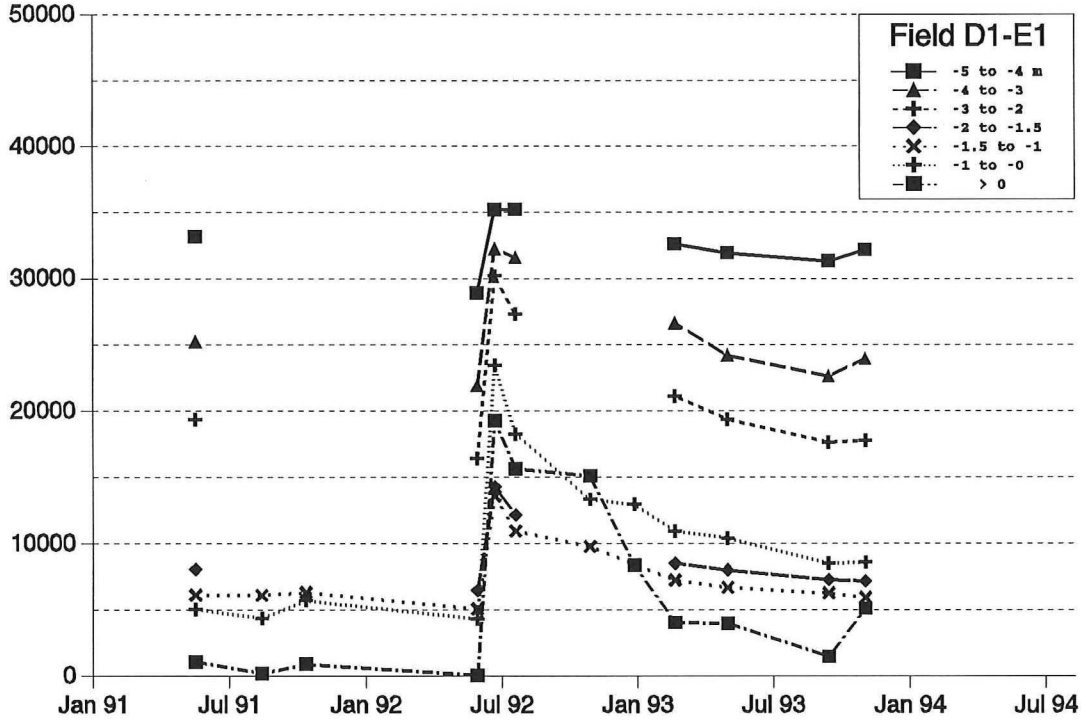

Figure 7 *Volumes between the levels for field D1-E1*

In Figure 7 the total volumes between the levels are shown. It clearly demonstrates the large and rapid decrease of the volumes of the highest levels in the first year. It also shows one of the difficulties of elaborating and analyzing the volume data: many times there are only volumes computed down to the level of NN-1.5m. Still, in comparison with the other supplies the supplies of 1989 and 1992 are relatively well observed.

In Figure 8 the development of the volumes after the supply of June 1989 is shown. In each plot the first bar of a groinfield indicates the difference between the volumes measured just before supply and just thereafter. The second shows the volumes of September 1989. Hence, the difference shows the erosion, c.q. accretion of the supply area in the first summer. The other two bars show the volumes measured in May 1990 and May 1991 respectively.

In Figure 9 the development of the volumes after the supply in June 1992 is shown.

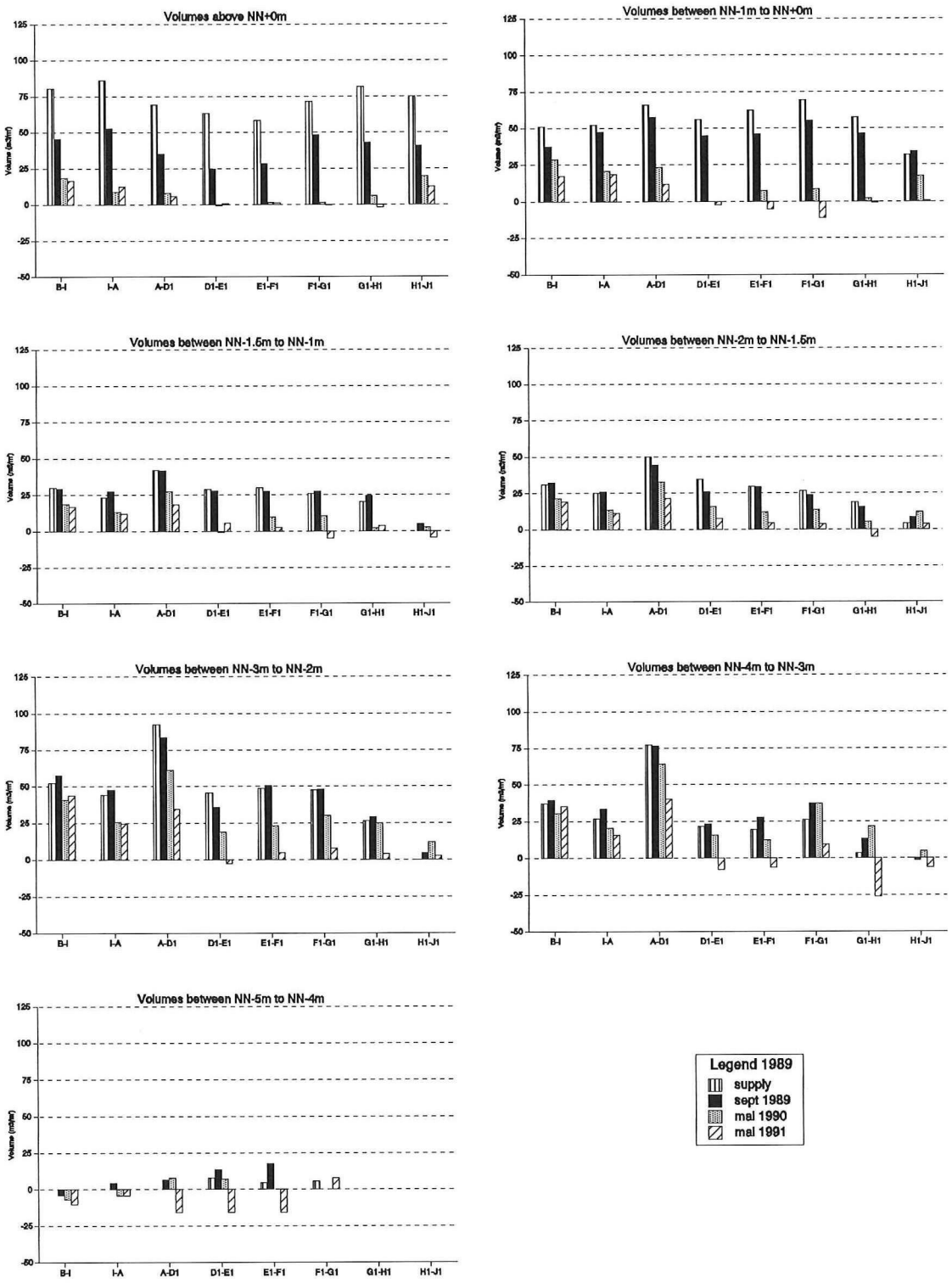

Figure 8 *The development of the supplied volumes in 1989.*

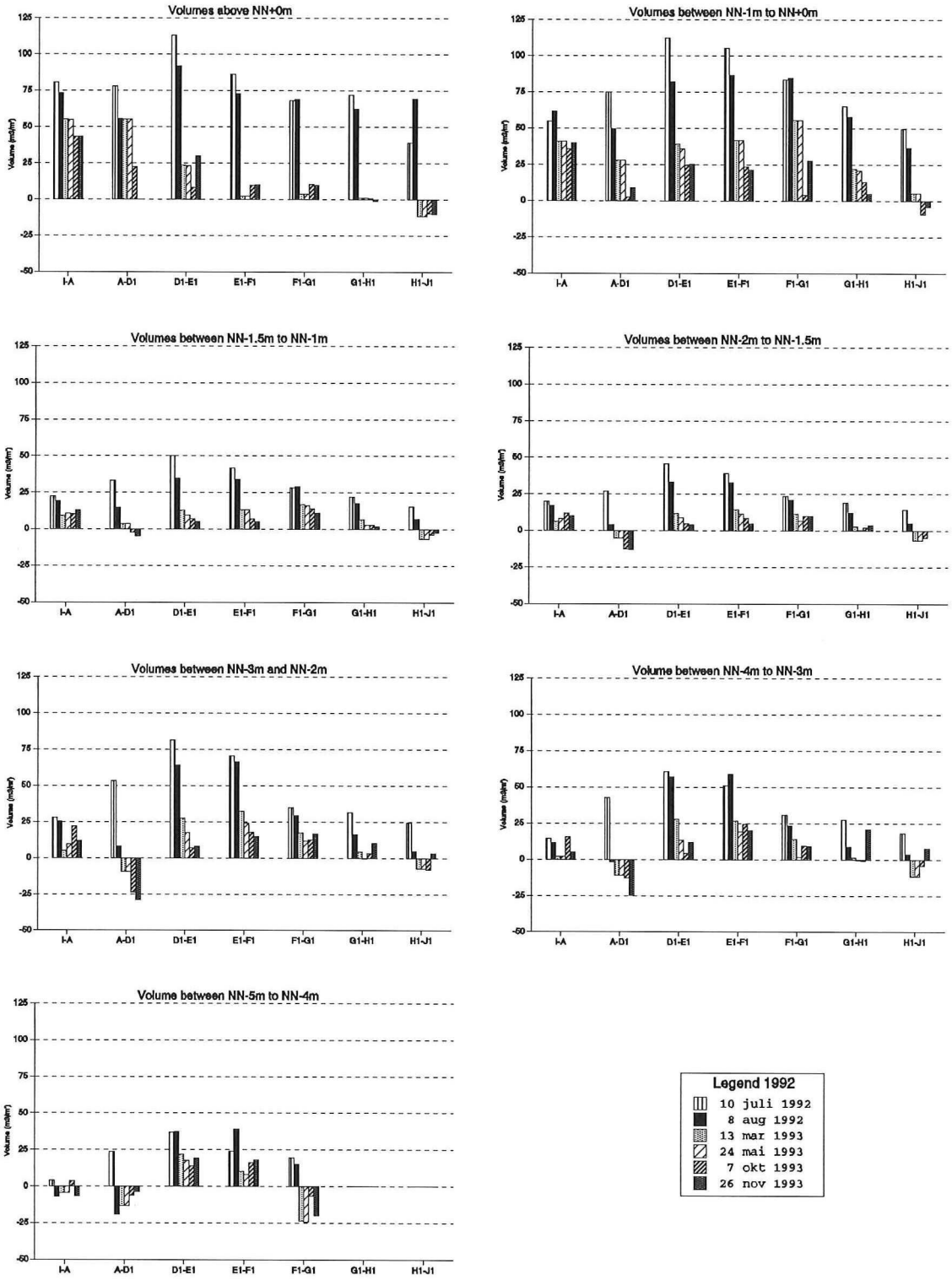

Figure 9 *Development of the supplied volumes of 1992.*

Figure 10 shows a comparison between the development of the total volume of both nourishments of 1989 and 1992. The losses in the first summer seem to be in the order of 5 to 20% of the total supplied volume. Figure 8 and Figure 9 show that these losses largely take place in the zone above NN-1m. There the losses amount to 70% as already mentioned.

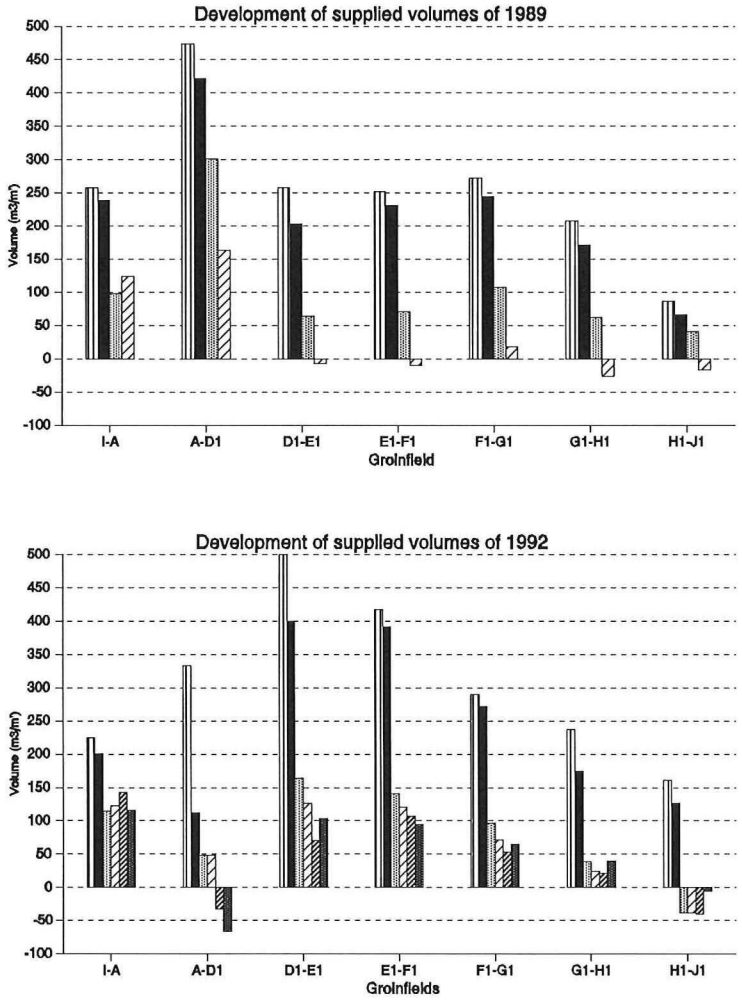

Figure 10 *Comparison of the development of the supplied volumes in 1989 and 1992. Legends in Figure 8 and Figure 9.*

In Table 2 a comparison is made between the placing of the supply in 1989 and 1992 for three fields.

In the zone from NN-5m to NN-3m the amount of supply in 1992 is 1.5 to 3 times as much in 1992 as in 1989. The volumes in the upper area are much larger in 1992 when compared to 1989. In both cases the volume placed below NN-1m is about 50%.

	zone	1989		1992	
D1-E1	h > NN-1m	135	50%	225	45%
	NN-1m > h > NN-3m	110	40%	175	35%
	NN-3m > h > NN-5m	30	10%	100	20%
	total	275		500	
E1-F1	h > NN-1m	125	50%	190	45%
	NN-1m > h > NN-3m	110	40%	150	35%
	NN-3m > h > NN-5m	25	10%	75	20%
	total	260		415	
F1-G1	h > NN-1m	140	50%	150	55%
	NN-1m > h > NN-3m	100	40%	85	30%
	NN-3m > h > NN-5m	30	10%	45	15%
	total	270		280	

Table 2 *Comparison of placing of nourishment over the profile for three fields for 1989 and 1992 (Volumes in m3/m).*

3.6 Some observations following from the volume data analysis

Behaviour of coast after beach nourishment in 1989:

1 All volumes of all groinfields westerly from groin A stabilize at a higher level than before the nourishment. After one year these profiles stabilize and remain stable (Appendix C, Figure 20 to Figure 37).

2 Until September 1989 the losses of the nourished volumes above NN+0 m are 30% to 60% between groin A and J1 (Figure 8).

3 Field D1-E1 and E1-F1 show little accretion in summer 1989 in the area NN-5m to NN-4m. This accretion is only up to 25% of the losses from the two highest zones (Figure 8). The rest is transported in longshore direction due to gradients in longshore transport or is transported to the areas still lower than NN -5m.

4 In the summer of 1989 no effect of the supply could be determined in the upper part (above NN-1.5m) of the profiles in the groinfields easterly of groin J1 (Appendix C, Figure 12 to Figure 20 and Figure 30 to Figure 33). No volume data was available to investigate if the volumes in the lower zones easterly of groin J1 did change due to longshore transport.

5 The increase in volumes easterly from J1 were due to the dry nourishment in 1990 (Appendix C, Figure 30 to Figure 33).

6 After one winter the nourished volumes in the groinfields above NN-1m were almost vanished in the fields between groin D1 to H1. The longshore transport capacities are after this period only important for the distribution of the sand in a groinfield. This is because of the fact that the level of the beach is significantly lower than the crests of the groins. The blocking effect of the groins reaches then its maximum and the rate of longshore transport over the groins will be minimal. A resulting gradient in longshore transport will then only occur in case of cross shore transport to a lower zone and longshore transport underneath the groins.

Behaviour of coast after combined nourishment in 1992:

1 First the supplied sand body transformed rapidly to a distribution in the fields as if it was a uniformly distributed beach nourishment. After this period the development of the supply of 1992 has about the same nature as the beach nourishment of 1989.

2 The nearer the ebb channel to the groinfield the larger the losses in the lower part of the profile due to tidal currents (Figure 9 and Figure 10).

4 In 1992 also a large volume is nourished on the beach. This volume decreases very rapidly. Only a part can be traced in the lower part of the profiles. It will probably be sufficient to supply a much smaller volume to reach the goal of protection of the structures. Only for tourism it would be attractive to supply more sand on the beach than strictly necessary.

5 During the summer (until Aug 1989) the losses of the volume above NN+0m are 5% to 20% (Figure 9).

6 After one winter the volumes in the groinfields above NN-1m are almost vanished in the fields between groin D1 to groin H1 (Figure 9).

7 The absolute losses relatively to the total nourished volume in the summer are in the same order as in the summer of 1989 (Figure 10).

3.7 Main conclusions in consideration to the line modelling

From the results of the analyses of the volume data several conclusions have been drawn in respect to the application of the line modelling technique:

1 Groinfield A-D1 shows (Figure 9) directly after supply rather high losses below the level of NN-2m. This could be explained by the position of this groinfield near the channel. Tidal longshore currents beneath the groins in the lower zone might transport the supplied sand to the tidal channel.

2 Beach nourishment in 1989 as well as in 1992 has been carried out between groin D and groin J1 (see Figure 2). The inshore nourishment in 1992 has been carried out between groin A and groin J1. The line modelling technique should be applied on the northwest beach easterly of groin A, because the beaches on the western and southern of Norderney are strongly influenced by the strong tidal currents, which are difficult to implement in the line modelling technique.

3 The profile measurements easterly of groin J1 were only carried out above the level of NN-1.5m. Results of computations below this level cannot be compared with any computed volume data. Combined with conclusion 2, this leads to an area of investigation between groin A and groin J1.

4 In this area there is sufficient volume data to compare the results of the computations with the results of the line modelling technique.

5 The coastal profile will be divided into three zones:
a) NN-5m to NN-3m
b) NN-3m to NN-1m
c) NN-1m higher (NN+2m)
The mean depth contour of the lowest zone is located outside the groinfields. This means that the (tidal) longshore currents will have a large influence on the transport rates there. The middle zone lies between the groins, hence, the longshore transport is partly blocked. The volumes in the highest zones have the ability to decrease by longshore transport over the groins. Especially, direct after the supply, when the groins are covered by the sand, the wave driven longshore current has the possibility to transport the sand in longshore direction.

6 Concerning the development of the supplied volumes summer and winter period should be considered separately. Figure 8 and Figure 9 show high losses in the highest zone in the first summer and all over the profile in the winter.

4 Wave climate and tide

4.1 Introduction

In anticipation to the calculation (given in ch.5) of the longshore transport capacity along the northwest beach (between the ebb channel and the "landfall" of the swash bars) first the wave boundary conditions for this beach have to be determined. In chapter 5, transport capacities will be calculated, taking the complete wave climate into account. Wave shelter by the outer delta will appear to be very important for the result of those computations. This wave shelter depends on the water level.
Thus, focusing on waves and tide, as will be done in the present chapter, not only the deep water wave boundary conditions should be investigated, but also the relation between waves and water levels.
This relation is to a certain rate determined by the "wind effect", the relation between storm surge level and wind velocity; this wind velocity on the other hand determines the wave height.

In this chapter first (§4.2) the bottom schematization which has been used will be depicted. Then (§4.3) the deep water wave climate which has been implemented is described. Although for the wave boundary conditions the probability distribution of the combinations of wave height (Hmo) and wave period (Tmo) of Schiermonnikoog has been used, another relation between the wind effect and the wind velocity was expected at Norderney in comparison with Schiermonnikoog (one of the Dutch Wadden Islands), where the wave data was measured.
The theoretical relationship between the water level elevation due to wind and the wave height, to be implemented in the longshore transport model, is investigated in §4.4.
Empirical relations between wave height and water level elevation are investigated in §4.5, where in §4.6 a comparison between empirical and theoretical values is given.
After that the schematization of the vertical tide in the model will be given (§4.7).

4.2 Schematization

The wave climate on the inshore and the beaches between the tidal inlet and the landfall, is strongly influenced by the swash bars in the ebb delta (see also §2.2). These bars reduce the energy of the incoming waves and also influence the propagation direction of the waves by refraction.
The ebb delta is schematized as shown in Figure 11 and Figure 12. In Figure 11 the results of a refraction model computation, carried out by the FSK (Niemeyer, 1986a) is shown, which indicates the relevance of the chosen schematization.

The schematized delta is characterized by a continuous bar, while reality shows a series of swash bars. This bar circumcises the inlet and is divided into three parts, having different orientation. The top of the bar is assumed to be at NN-3m. The direction of the bar is also given in Figure 12. The area enclosed by the bar and the western

shoreline of Norderney (grey area) is assumed to be flat. It is assumed to be a plain at NN-5m. Also the area Westward of the bar (second gray area in fig.12) is assumed to be plane, at a level of NN-3m.

For checking this schematization, for two different cases (wave period T=4 sec; water level NN=0 m, resp. T=8 sec.; water level=NN+3m) and for five different directions of wave approach refraction rays have been computed for the schematization mentioned above.

Niemeyer (1986a) shows five results of much more sophisticated refraction computations of which Fig.11 gives an example. These results were compared with wave ray refraction computations with similar boundary conditions, using linear wave theory and the bottom schematization of fig.12. A similar reaction of the waves on the bathymetry of the delta was found as in Niemeyer's refraction computations.

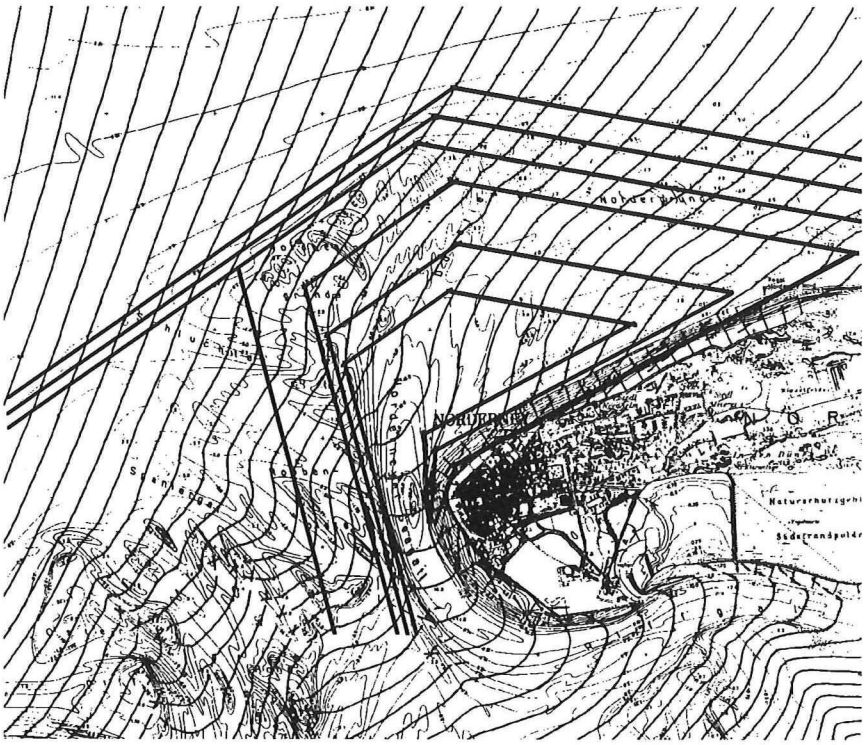

Figure 11 *Schematisation of the ebb delta of Norderney. The wave crest lines which are already drawn follow from another refraction computation (Niemeyer, 1986a).*

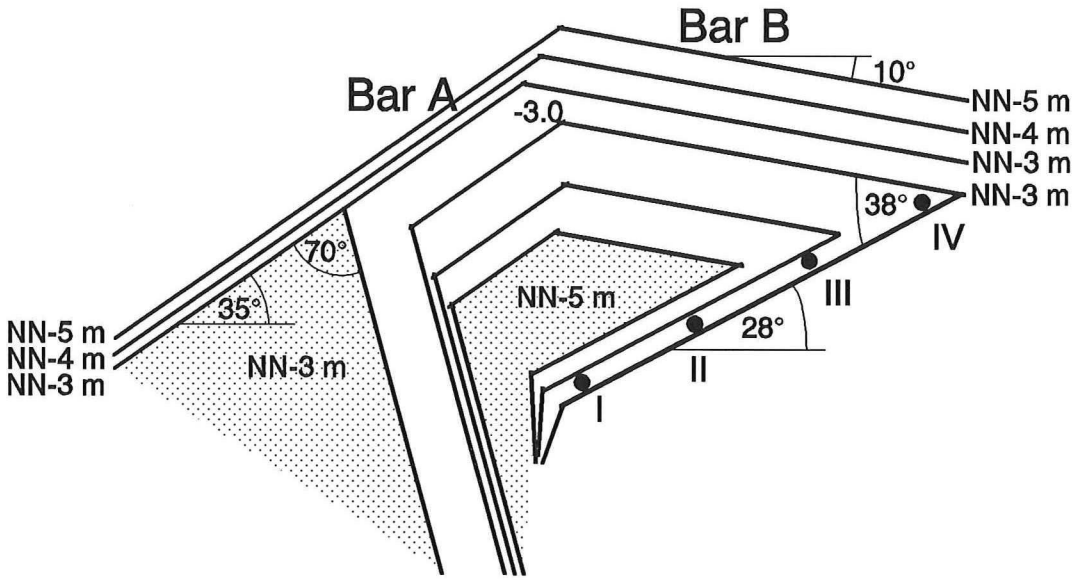

Figure 12 *Values of the schematisation of the ebb delta.*

4.3 Wave climate in deep water

For the deep water wave climate use has been made of the wave climate which has been measured during 12 years with a wave rider at deep water (NAP-19m) near Schiermonnikoog, a Dutch Wadden island (Roskam, 1988).

The data consists of two types of probability distributions:
- Probability of combinations of significant wave height (Hmo) and period (Tmo).
- Probability of combinations of Hmo and water level.

The data is presented in tables, with probability of occurrence in percentages (Appendix A1 and appendix A2).
The first type of distribution will be considered in the present §4.3, the second type is elaborated in §4.5.

For twelve direction sections of 30° these distributions have been determined. The measured values of Hmo are divided into classes with class width ΔHmo is 0.5 m. The class with maximum wave height is Hmo > 7.5 m.

The classes of wave period are from 0 s to > 9 s with ΔTmo of 2 s. The distributions of probability of occurrence of a combination of a class of Hmo and period per direction have been used in the following computations.

4.4 Wind effects; theoretical considerations

4.4.1 General

The second type of wave probability distributions in Schiermonnikoog (Appendix A2), mentioned in §4.3, is used for finding the relation between wind effect and wave characteristics at Norderney. This will be done in §4.5 (empirical relations); first, in the present section the theory will be considered, which will be applied in §4.5

Often high waves will be combined with a high surge level: both originate from large wind forces. It is important to implement this correlation in the computations: bars as sketched in Figure 11 and Figure 12 give less shelter than found by omitting the relation. For the relation between wave height, Hmo, and water level another relation than the one of Schiermonnikoog has been used, as described in the present section.

The water levels are the sum of a water level elevation due to tide and an elevation due to the wind effect. The mean tide at Norderney is well known, but the effect of the wind is less known. In the following, theoretical relations will be determined between Hmo and the water level elevation due to the wind effect.

In §4.4.2 using theoretical considerations it is investigated, whether the wind direction, giving maximum wind effect, and its magnitude will differ in Norderney from the ones

in Schiermonnikoog, where data is available. In §4.4.3 conclusions are drawn.

4.4.2 Existing relations for wind effects along the southern North Sea coast

The Koninklijke Nederlands Meteorologisch Instituut (KNMI, 1960) has determined a method of computing wind effects (elevation of the water level) the along the Dutch and the German coast from a wind field over the North Sea. For a detailed explanation of the method and principles, is referred to Weenink (1958) and Schalkwijk (1947). The results of the method and principles are relations between the setup and the wind for several places along the Dutch and German coast. These relations have the following form:

$$dh = (a * \cos\alpha + b * \sin\alpha) * C_1 * V^2 \qquad (1)$$

dh = water level elevation due to the wind effect
a,b = constants
C_1 = constant
V = wind velocity
α = direction of the wind in respect to North

The parameters a, b and C_1 have been determined empirically and are given in KNMI (1960). When the wind is assumed to be homogenous above a certain area, then the direction and the wind velocity determine the wind effect. The same wind results in another wind effect (dh) in another place along the coast. The wind effect is assumed to be proportional to the square of the wind velocity V. If the significant wave height is assumed to be proportional to the wind velocity, then the wind effect will be proportional to the square of the significant wave height.

Formula (1) can be rewritten as:

$$dh = \frac{b}{\cos\phi} * \sin(\alpha + \phi) * C_2 * Hmo^2 * f(\alpha) \qquad with \quad \phi = \arctan(\frac{a}{b}) \qquad (2)$$

where $f(\alpha)$ originates from the fact that the proportionality constant between wind velocity and wave height will depend on wind direction.

In this equation $(90°-\phi)$ is the direction with the largest wind effect, apart of the effect of $f(\alpha)$. If $\phi = -\alpha$ then the wave height from direction α will not result in setup. For simplicity, one might call ϕ a 'direction angle'.

The term $|b/\cos(\phi)|$ determines the magnitude of the wind effect for the wind direction $\alpha = 90-\phi$. To use the wave climate of Schiermonnikoog for the case of Norderney will therefore give a difference in direction angle and an amplitude difference. Although the constants a and b are determined for a number of sites in KNMI (1960), this is not the case for Schiermonnikoog and Norderney. For three places nearby the constants are known: Eierlandse Gat, Borkum and Cuxhaven (Table 3).

	a	b	ϕ	$b/\cos\phi$
Eierlandse Gat	0.32	-0.36	-41.6	0.48
Borkum	0.42	-0.51	-39.5	0.66
Cuxhaven	0.44	-0.75	-30.4	0.87

Table 3 *Values determining the wind effect according to KNMI.*

The five sites mentioned above are about in line (Figure 13). The two sites Schiermonnikoog and Norderney are situated between the other three. Therefore it is assumed that the values of ϕ and amplitudes of Schiermonnikoog and Norderney can be interpolated from the curve fit through the known values, given in table 3. The values of ϕ and $b/\cos(\phi)$ are shown in Figure 14.

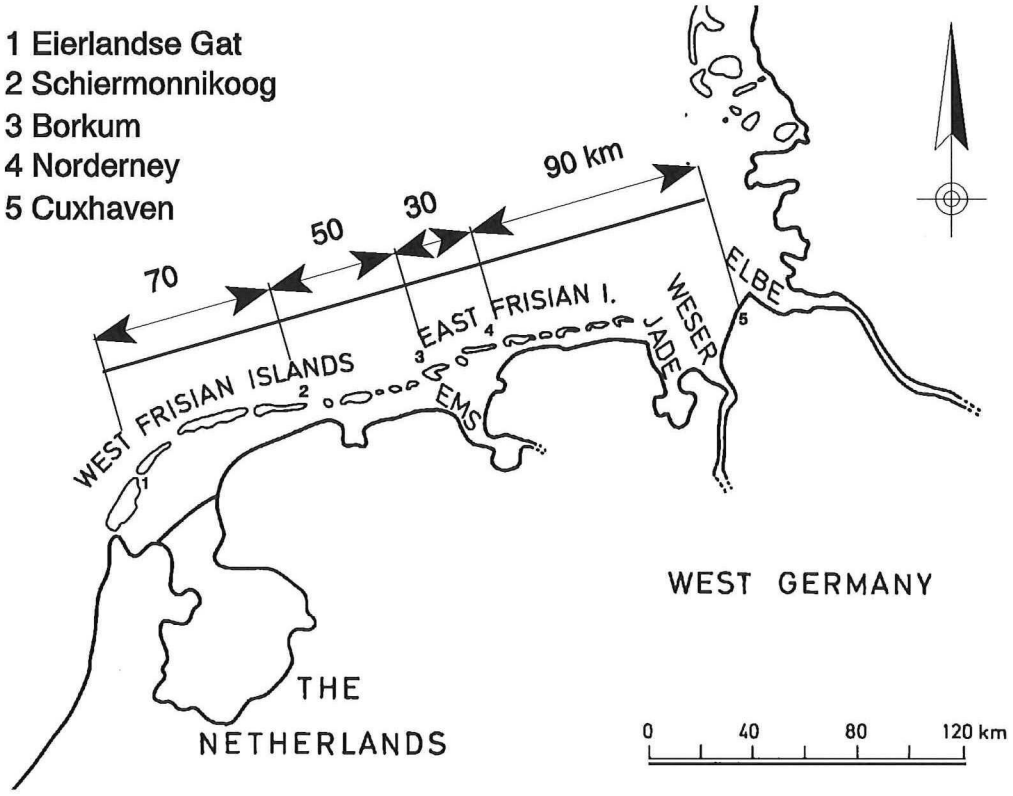

Figure 13 *Location of the five sites.*

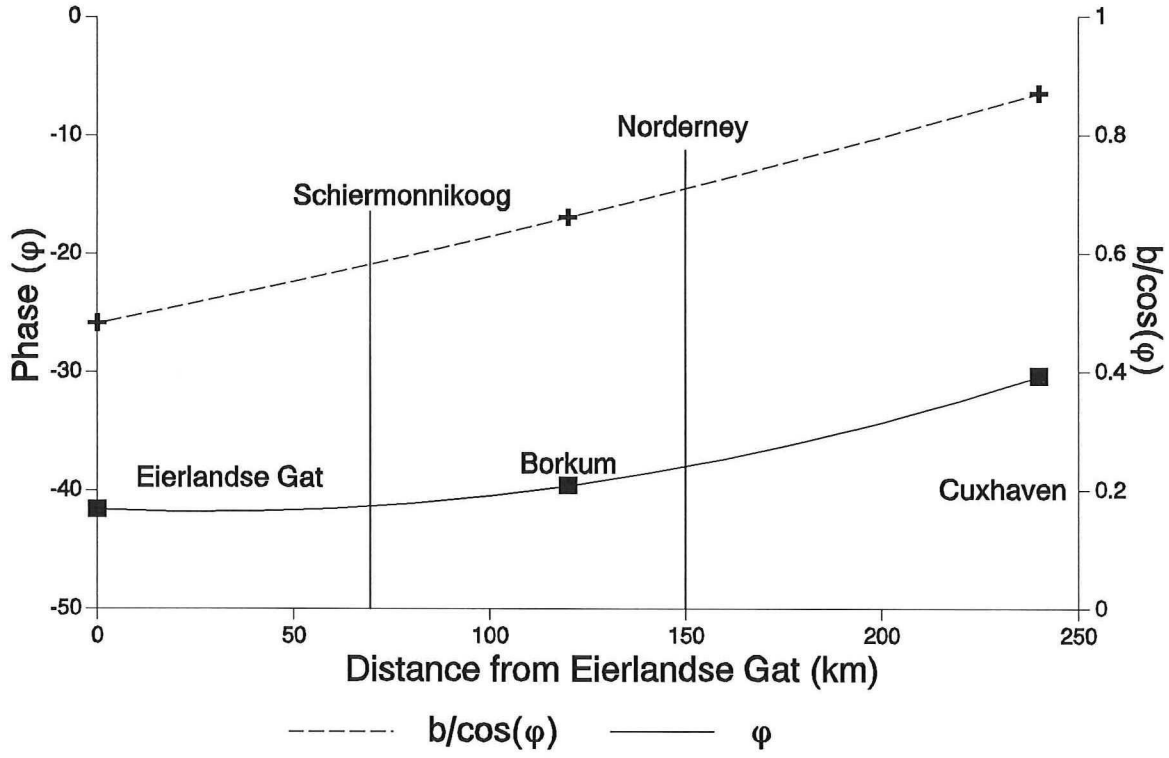

Figure 14 *Values of the amplitude and direction angle for the different sites.*

If the direction angle and amplitude are assumed to be a 2nd order function of the distance (x) to the Eierlandsche Gat (in km) the following values result:

$$\phi = 2.5*10^{-4}*x^2 - \frac{1}{75}*x - 41.6 \quad (3)$$

$$\frac{b}{\cos(\phi)} = 1.0*10^{-6}*x^2 + \frac{1}{730}*x + 0.482 \quad (4)$$

Schiermonnikoog:

$$x = 70 \qquad \phi = -41.3 \qquad \frac{b}{\cos\phi} = 0.583 \quad (5)$$

Norderney:

$$x = 150 \qquad \phi = -38.0 \qquad \frac{b}{\cos\phi} = 0.710 \quad (6)$$

Shift of direction angle between Schiermonnikoog and Norderney:

$$(-38.0 - 41.30) = 3.3° \quad (7)$$

Amplitude change between Schiermonnikoog and Norderney:

$$\frac{0.710}{0.583} = 1.22 \quad (8)$$

4.4.3 Conclusions in respect to the differences in water level elevation Schiermonnikoog and Norderney

The order of magnitude of change in ϕ seems to be small and is therefore neglected in the following computations.

Figure 14 gives a value for Norderney of a wind effect, being 22% higher in comparison with Schiermonnikoog. This value has been used in the computations.

4.5 Empirical relation between wave height and wind effect

Consider the table in Appendix A2: probability of combinations of wave height and water level at Schiermonnikoog. The table is valid for a certain class of wave directions. The mean water level can be determined for each wave height class. When many measurements have been made in a class, the influence of an individual tide measurement will decrease. The mean value of all water level measurements in 12 years is NAP-6 cm.

To determine the relation between the Hmo and the mean water level values a curve fit has been made of the shape:

$$dh = a + b * H^2 \tag{9}$$

where a,b are other constants than in §4.4.2. However, "b" in (9) is equivalent to dh/Hmo^2 in (2).

The number of registrations concerning each wave height class is known. These values are given in the same tables as the distributions (Appendix A). The mean water level is determined by all registrations per class. More registrations in a class therefore mean that the influence of an individual registration on the mean water level is smaller. The water level is also determined by the tide. If enough measurements are made in a class the influence of the tide will disappear.

In the higher wave height classes the number of registrations is lower. The influence of an individual registration is larger. Because the number of registrations is known, the value of the mean water level per wave class can be given a weight.

In Figure 15 (treating successive classes of wave direction) the mean water level is shown as a function of wave height. The solid lines in Figure 15 gives curve fitting results when the mean water values have all the same weight. The dotted line is a curve fitting in which each class of wave heights has a weight equal to the probability of occurrence P(Hmo).

The dotted line is less influenced by extreme higher values of the mean water level. In two cases this line lies higher than the dots. Therefore it is chosen to use the setup according to the solid lines.

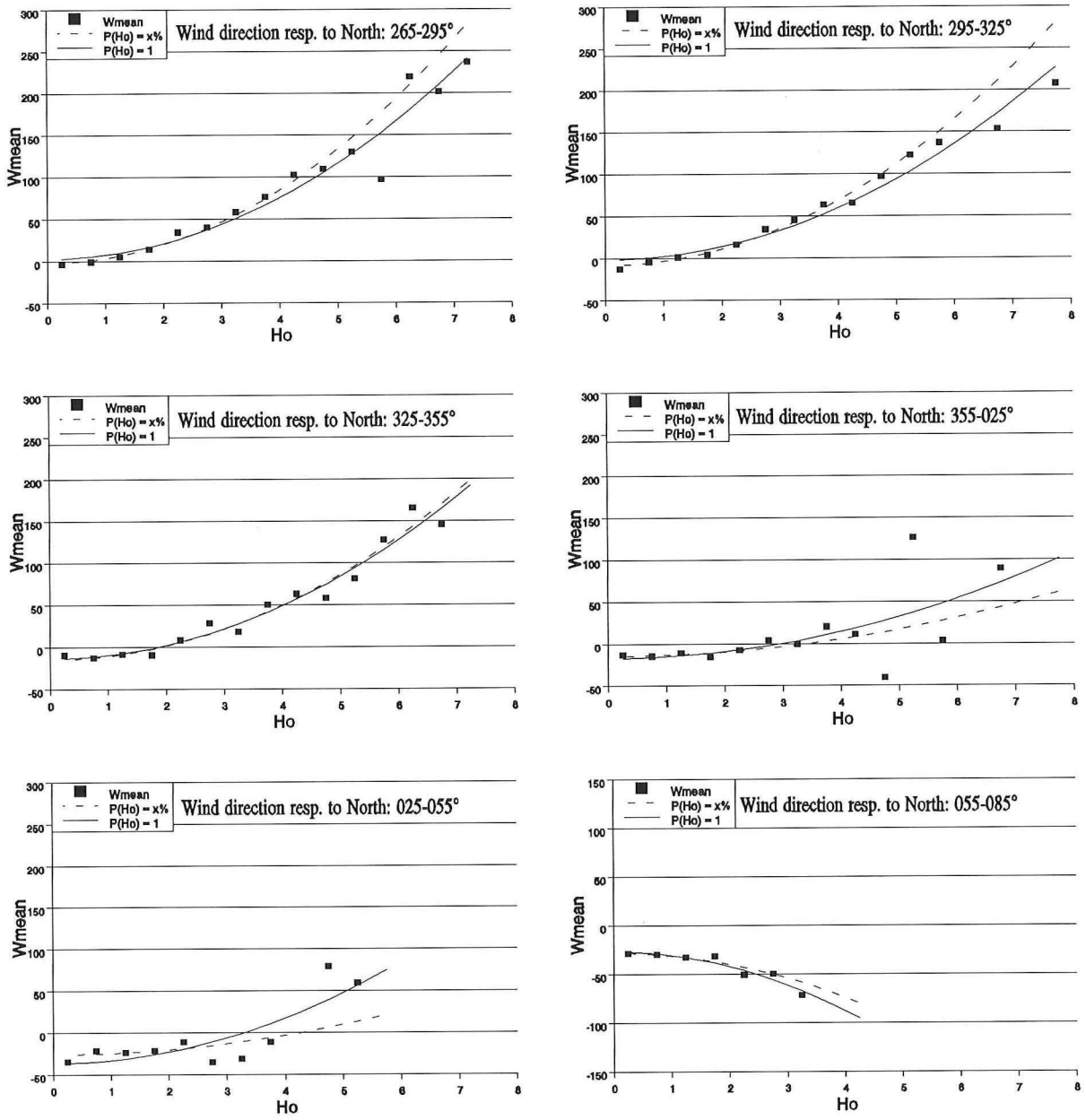

Figure 15 *Mean water level under condition of specific wave conditions.*

In Figure 15 the vertical scale denotes the water level, the horizontal scale the wave height. The parameter W_{mean} is the mean water level (in cm) in a wave class with respect to NAP. H_o is the significant wave height, equal to H_{mo} (m).

4.6 Comparison practical and theoretical values

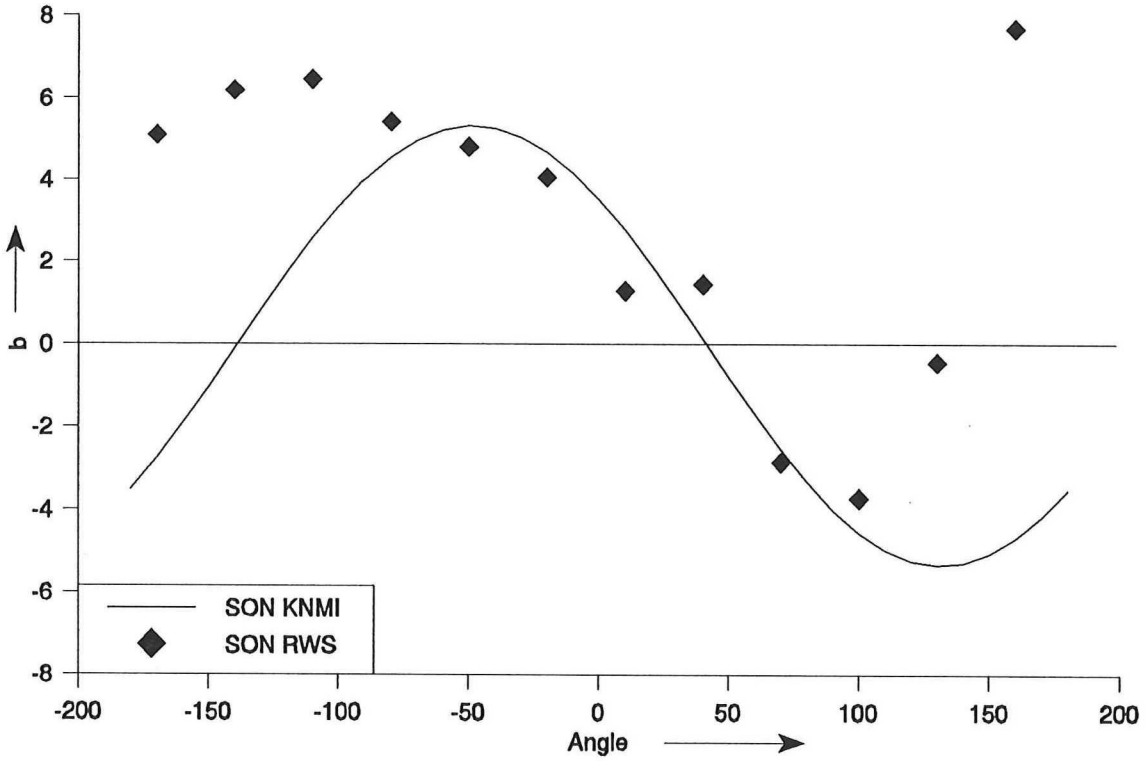

Figure 16 *Comparison of the relation between the wind direction and wind effect parameter according to the KNMI and the computed values from the data of SON.*

The b-values in equation (9) are depicted in Figure 16 as function of the (class of) wave direction. The plotted values are the results of the curve fit, as given in Figure 15 (drawn lines). All directions are used, applying the data of Schiermonnikoog.

Figure 16 shows indeed something like a sinus relation between the wind effect and direction in respect to North (angle = 0). Harmonic analysis of the b-values would have given some phase shift (to the left), compared with the theoretical curve derived in §4.4.2. This theoretical curve is depicted as a drawn line in Figure 16.

The difference between the sinus shape of the distribution and the actual values in Figure 16 is influenced by the function $f(\alpha)$. This relation between the wind velocity and wave height as function of wind direction, should be investigated more carefully. Another influence is the assumption that the wind direction is the same as the direction of wave approach.

4.7 Tide

Lassen and Siefert (1991) determined the shape and position of the mean tidal curve (Figure 17) for the period 1982 to 1986. They found a mean water level, MWL, of NN-3.1 cm.

To include the influence of the water level variation due to tide, in the sediment transport computations three water levels have been used for every wave height and wave period combination. For the computations three water levels have been used:

Reference MWL	Boundary values	Reference NN	Probability
MWL +1 m	NN+0.798m to NN+1.140m	NN+0.969m	22.6%
MWL	NN-0.802m to NN+0.829m	NN-0.031m	48.5%
MWL -1 m	NN-1.260m to NN-0.802m	NN-1.031m	25.9%

Table 4 *Probability of occurrence of three tidal ranges.*

The probability is the percentage of time the tidal level is between the boundary values, mentioned in Table 4. Inner boundary values are chosen as: reference value ± (top value - reference value).

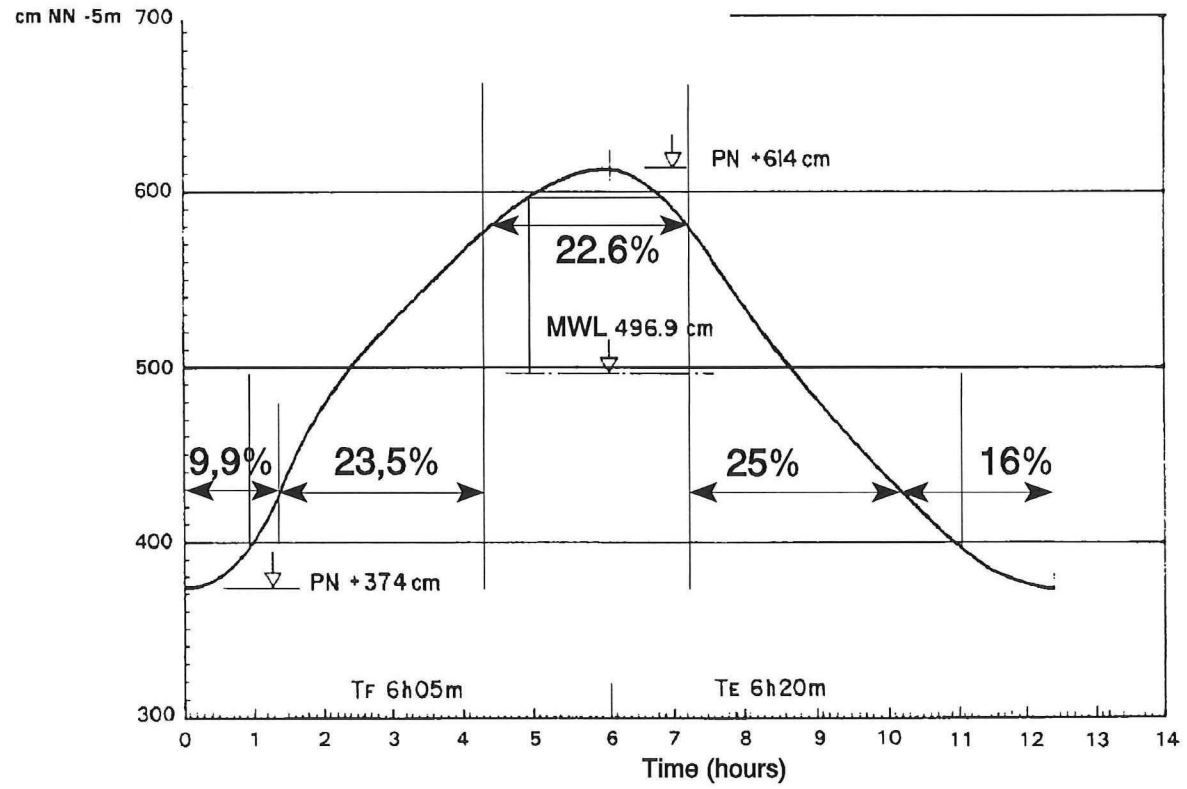

Figure 17 *Mean tide curve over the period 1982 till 1986*

4.8 Conclusions

The main conclusions which can be drawn are:

- The wind direction, which gives the highest setup due to wind, is about the same in Schiermonnikoog and Norderney.

- The setup due to wind is approximately 22% larger in the vicinity of Norderney than in the vicinity of Schiermonnikoog.

- The setup due to wind can be considered as proportional to the square of the wave height (Figure 15).

5 Longshore transport capacity

5.1 General

In this chapter sand transport computations are made, using the Svašek (1969) variation of the CERC formula. Furthermore, "coastal constants" are derived, which give a relationship between the longshore sediment transport and the coastal direction.

The principles of the way of transport computation are explained in §5.2.

In §5.3 is focused on the Norderney case. Adaptations in the way of computation necessary for this particular case are treated.

The refraction diagrams of Appendix E indicate that large waves first break on the seaward edge of the outer delta and next on the beach- and inshore area near the points I to IV (Figure 12). In both areas these breaking waves will cause wave-driven transport; only the transport in the coastal area (points I to IV) will be calculated in this report.

It is disclosed in §5.3 which transport can be calculated in a point at the beach for given offshore wave conditions; the effect of breaking on the outer delta is implemented.

Evidently, transport depends on wave conditions; in this chapter, the expectation of the yearly transport is calculated, by giving each transport statistically a "weight", depending on its probability of occurrence.

Effect of water level variation (§4.5 to §4.7) is taken into account.

It is shown in §5.4, in which way the formulae are implemented in the computer program, which has been used.

Results of the transport calculations are presented in §5.5. For finding the influence of the coastal direction on the coastal transport (the so-called coastal constant), calculations with another coastal direction than the present one have been carried out. §5.5.2 deals on this way of calculation of those coastal constants.

Finally, §5.6 gives a discussion on the transport mechanism as can be derived from §5.5.

5.2 Principles of transport computation

5.2.1 Assumptions

The transport computation, in this report, is based upon the CERC formula. The most important assumption of this CERC formula is:

> Longshore sand transport capacity is proportional to the component of the energy flux in longshore direction at the outer edge of the surf zone.

Furthermore:
- The formula is valid for beaches with sand with a mean diameter (D50) between 175 μm and 1000 μm.
- There is no transport capacity outside the breaker zone.

5.2.2 Transport formula according to CERC

From the assumption of a proportional relation between the longshore transport and the component of the energy flux one can determine:

$$S_x = A * H_{b,sig}^2 * n_b * c_b * \cos(\phi_b) * \sin(\phi_b) \qquad (10)$$

S_x = longshore sand transport (m^3/s)
$H_{b,sig}$ = significant wave height at the breaker line (m)
c_b = wave velocity at the breaker line (m/s)
n_b = ratio (group velocity / wave velocity) (-)
ϕ_b = angle of wave incidence at the breaker line (-)
A = proportionality constant (-)

The proportionality constant, A, depends on the other influences on the transport as for example the characteristics of the sand (mean diameter, density, etc.). For application of the constant in circumstances like the southern North Sea coast, the value mostly used for A is 0.040.

5.2.3 Refraction

A usual assumption of wave height calculation with refraction theory is: no energy loss before the waves break. The result is a constant value for the wave energy between two wave rays (outside the breaker zone):

$$E_o * n_o * c_o * b_o = E_b * n_b * c_b * b_b \quad (11)$$

E = wave energy per unit of wave crest width
n = ratio (c_{group} / c_{wave})
c = wave velocity
b = width between two wave rays

The subscripts 'o' and 'b' determine whether the wave is at deep water respectively at the breaker line.
Assuming depth contours parallel to the coastline, refraction theory gives:

$$\frac{b_o}{b_b} = \frac{\cos(\phi_o)}{\cos(\phi_b)} \quad (12)$$

In formula (10) the parameter $\sin(\phi_b)$ can be substituted using Snel's Law:

$$\frac{\sin(\phi_o)}{\sin(\phi_b)} = \frac{c_o}{c_b} \quad (13)$$

giving:

$$S_x = 0.040 * H_{b,sig}^2 * n_b * \frac{c_b^2}{c_o} * \sin(\phi_o) * \cos(\phi_b) \quad (14)$$

Assuming that the breaking takes place in relative shallow water gives:

$$c_b = \sqrt{g * h_b} \quad (15)$$

h_b = depth at breaker line
g = gravity acceleration

Substitute into (14) the ratio between wave height and depth at the breaker line as the breaker criterium:

$$\frac{H_{b,sig}}{h_b} = \gamma \quad (16)$$

This gives with (15):

$$S_x = 0.040 * (\gamma * h_b)^2 * n_b * \frac{\left(\sqrt{g * h_b}\right)^2}{c_o} * \sin(\phi_o) * \cos(\phi_b) \quad (17)$$

resulting in:

$$S_x = 0.040 * g * \gamma^2 * h_b^3 * n_b * \frac{\sin(\phi_o)}{c_o} * \cos(\phi_b) \quad (18)$$

This is the total longshore sand transport capacity in the breaker zone.

5.2.4 Distribution of sand transport capacity over the depth

For the distribution over the profile use is made of the Svašek variation (1969) of the CERC formula. The transport capacity, S_i, in the zone above a depth, h_i, is proportional to the ratio $((h_i/h_b)^3 * S_x)$. For the detailed derivation and background is referred to Bakker (1969) and Bakker et al (1972). In formula:

$$S_i = \frac{h_i^3}{h_b^3} * S_x \quad (19)$$

$$S_i = 0.040 * g * \gamma^2 * h_i^3 * n_b * \frac{\sin(\phi_o)}{c_o} * \cos(\phi_b) \quad (20)$$

h_i = depth at depth contour i.
S_i = transport capacity in the zone higher than depth h_i

The transport in the zone between the breaker line and the depth contour, h_i, is therefore:

$$S_0 = 0.040 * g * \gamma^2 * (h_b^3 - h_i^3) * n_b * \frac{\sin(\phi_o)}{c_o} * \cos(\phi_b) \quad (21)$$

This concept has been extended to more zones.

5.2.5 Computation of breaker depth and wave height

The wave energy per unit of surface is:

$$E = \frac{1}{8} * \rho * g * H_{rms}^2 \tag{22}$$

From (11) and (22) can be derived:

$$H_{b,rms}^2 = H_{o,rms}^2 * \frac{n_o * c_o * b_o}{n_b * c_b * b_b} \tag{23}$$

For deep water n_0 is ½.

For a relative small spectrum:

$$H_{sig}^2 = 2 * H_{rms}^2 \tag{24}$$

Substitution of (12), (15), (16) and (24) yields:

$$(\gamma * h_b)^2 = H_{o,sig}^2 * \left(\frac{\frac{1}{2} * c_o * \cos(\phi_o)}{n_b * \sqrt{g * h_b} * \cos(\phi_b)} \right) \tag{25}$$

And so:

$$h_b = \left(\frac{H_{o,sig}^2 * c_o * \cos(\phi_o)}{2 * \sqrt{g} * \gamma^2} \right)^{0.4} * \left(\frac{1}{(n_b * \cos(\phi_b)} \right)^{0.4} \tag{26}$$

The first factor on the right is constant. By first assuming $n_b \cos\phi_b = 1$, the breaker depth can be determined by iteration.

5.3 Application for the Norderney case

5.3.1 General

The principles, as mentioned in §5.2, are suitable for application at a coast with parallel depth contours like Terschelling (Bakker & Kersting, 1994). In case of Norderney two main complications occur (Figure 18):

- the seaward shoreface of the outer delta is not parallel with the inshore
- the existence of breaker bars.

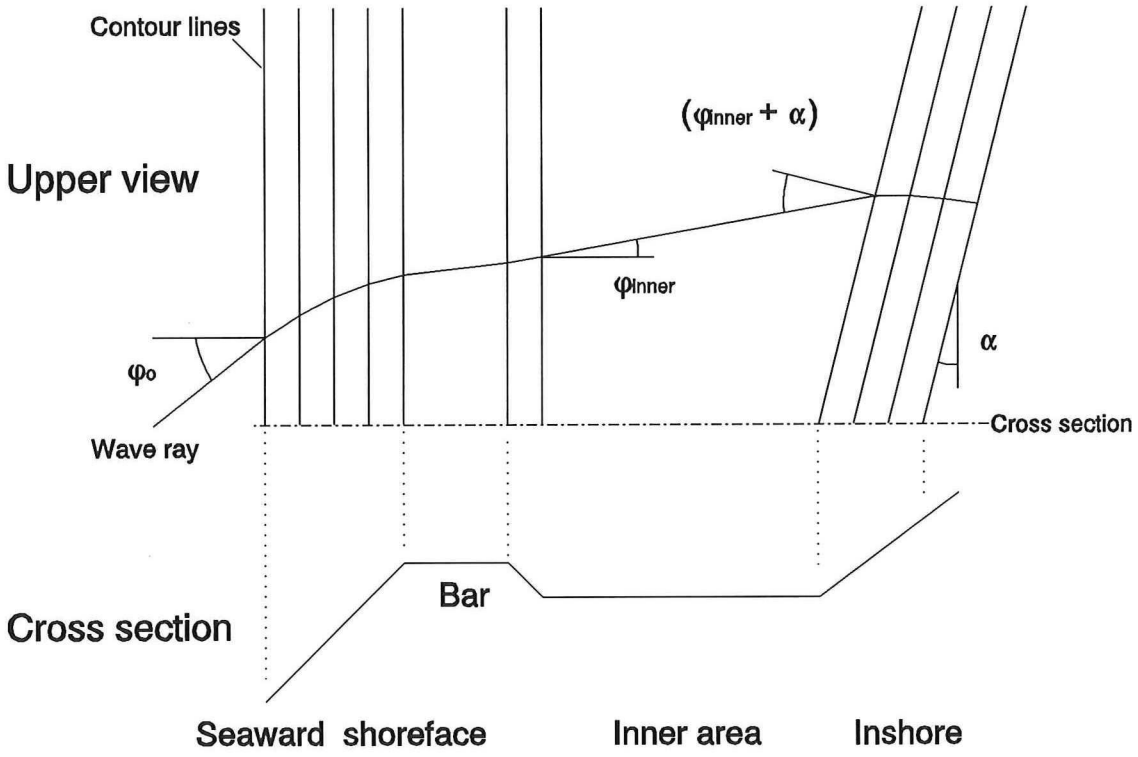

Figure 18 *Schematisation of bathymetry.*

The bathymetry is schematized as mentioned in §4.2 : the bars are schematized as one continuous bar with parallel depth contours at both sides of the bar (See also Figure 11 and Figure 12). The inner area is schematized as a plane area.

The existence of the plane inner area and a certain angle, α, between the depth contours of both the seaward shoreface and inshore, will cause a larger angle of approach of most of the waves at the inshore.

The existence of the bar will change the direction of the waves and cause energy dissipation of the larger waves.

5.3.2 Implementation of presence of outer delta in the formulae

The existence of the bar changes the formula (18) for the longshore transport capacity. The transport capacity cannot directly be expressed in the values angle of approach,φ_o, and celerity, c_o, at deep water. These values are replaced by the values, φ_{inner}, and c_{inner} at the place and depth where the wave enters the plane inner area. The latter values can be expressed in the values at deep water.

The wave angle at the breaker line can be expressed in φ_{inner} and c_{inner}:

$$\frac{\sin\phi_b}{\sin(\phi_{inner}+\alpha)} = \frac{c_b}{c_{inner}} \tag{27}$$

In the same way φ_{inner} and c_{inner} can be expressed in φ_o and c_o:

$$\frac{\sin\phi_o}{\sin\phi_{inner}} = \frac{c_o}{c_{inner}} \tag{28}$$

Subsequently formula (18) changes in:

$$S_x = 0.040 * g * \gamma^2 * h_b^3 * n_b * \frac{\sin(\phi_{inner}+\alpha)}{c_{inner}} * \cos(\phi_b) \tag{29}$$

with

$$\phi_{inner} = \arcsin\left(\sin\phi_o * \frac{c_{inner}}{c_o}\right) \tag{30}$$

The wave will get no change in direction while propagating over the plain. In case a wave breaks at the bar not all the energy will be dissipated on the bar. It is assumed that the wave energy, which passes the bar, is equal to the energy of a wave which comes from the same direction and with the same wave period as the original wave, however, having such a height, that it just passes the bar without breaking. The iteration method, mentioned at the end of §5.2.5 is used to compute backwards this $H_{o,sig}$.

5.4 Computations of longshore transport capacity

5.4.1 Input

To compute the transport distribution , according to the Svašek variation of the CERC formula, a program has been written in Turbo Pascal (Appendix B).

This program computes the distribution for each wave direction. For each direction the distribution of probability of occurrence of each wave height and wave period combination (H,T) is known (Appendix A1).

The program takes into account the water level variation as a result of both wind effect and tide.

The wind effect belonging to each direction is determined in §4.5. The probability of occurrence of the different tide levels is determined in §4.7.

For each computation the following parameters form the input of the program:

- phio the angle, ϕ_o, of wave approach at the coast.
- dhTide the water level due to tide relative to the mean water level.
- filename the name of the file in which the distribution of the probability of occurrence of each combination (H,T) is stored.

The angle between the depth contours of the seaward shoreface and of the inshore is assumed to be the angle between the bars and the inshore (Figure 12):

Bar A: 35 - 28 = 7 degrees
Bar B: 28 + 10 = 38 degrees

5.4.2 Structure of the program

The computation exists of three parts:

- The determination of the effect of the bar. It determines whether the wave breaks and the direction of the (resulting) wave entering the inner area.

- The determination of the angle of the wave and the depth at the moment of breaking of the wave at the inshore.

- The determination of the transport capacity distribution as a result of this combination (H,T). Finally the values will be multiplied by the probability of occurrence of the combination (H,T) and summarized to a total resulting transport capacity distribution.

The schematized structure of the program is as follows:

For every wave height do			
	For every wave period do		
		Determine water level.	
		Determine breaker depth in case of parallel contour lines.	
		If wave breaks at bar then do	
			Compute the wave height, which just passes the bar having the same wave period, wave direction and water level.
		Compute the angle, φ_{inner}, of the wave entering the plane area.	
		Compute the angle of incidence of the wave approaching the inshore.	
		Compute the breaker depth.	
		Compute the transport capacity distribution over the three zones.	
		Compute the resulting total transport capacity distribution using the probability of occurrence of this combination of wave height and wave period.	

Table 5 *Structure of the program for computation of longshore transport capacity.*

5.4.3 Cases

First the computations have been carried out for the situation, where the coastal direction (I=>IV), is assumed to make everywhere an angle of 28 degrees with the East-West axis (Figure 20). For all four points along the inshore coast of Norderney (Figure 12) the transport capacity distribution has been computed.
As well refraction over bar A as over bar B (Figure 12) is considered. If under certain conditions a certain point (I to IV) is attacked by breaking waves under various angles (as well by waves passing over bar A as well by waves passing over bar B) then the transports calculated for each of those refraction cases are added algebraically.

To determine the influence of the coastal direction, for point IV further computations have been made where the coastal direction of III-IV makes an angle of 5 degrees with the East-West axis (Figure 20).

In §5.5 the results of the longshore transport computations are presented. In (§5.5.1) the results, with a straight coast (schematization according to §4.2) are displayed ,where in §5.5.2 the results in case of another coastal direction in point IV are shown.

5.5 Results

5.5.1 Distribution of longshore transport capacity (coast assumed straight).

In Figure 19 the computed transports are visualized. However, in this case the coastline of Northwest Norderney is assumed to be straight. In §5.5.2 more realisticly has been taken into account, that the coast in point I and point IV has a different direction.

The profile is divided into three zones:

Zone	Depth contours	Transport capacity
Zone 1	> NN-1m	S_1
Zone 2	NN-3m to NN-1m	S_2
Zone 3	NN-5m to NN-3m	S_3

Table 6 *The division of the profile in three zones.*

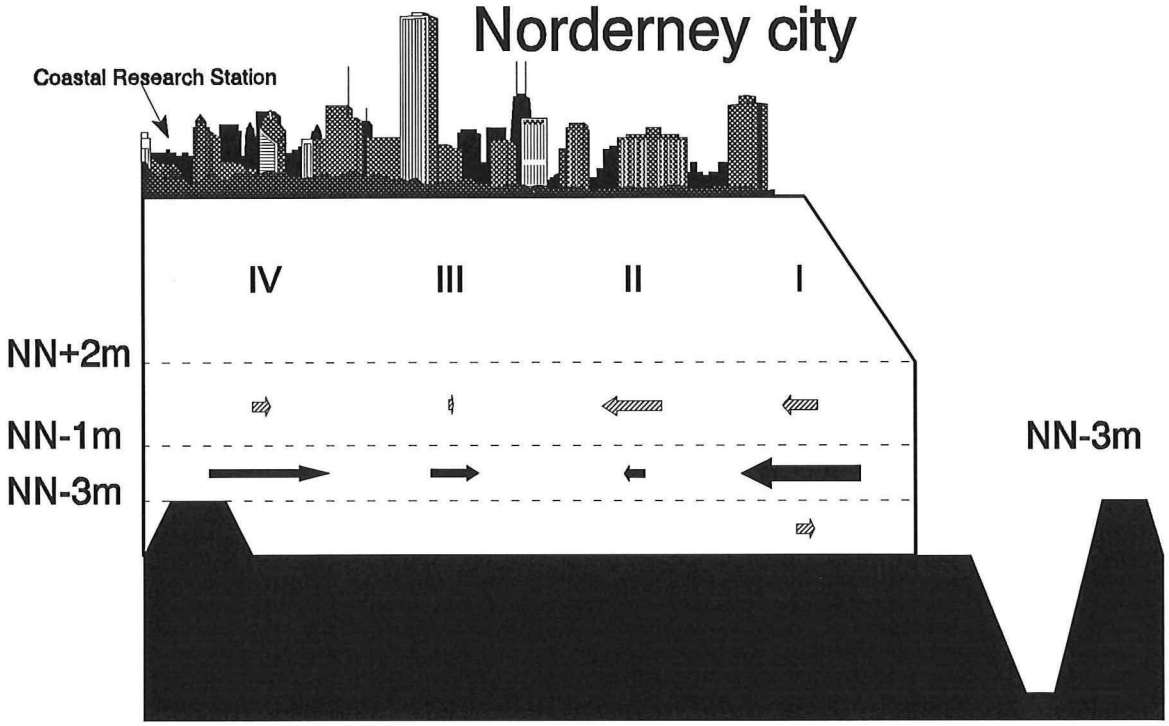

Figure 19 *Longshore transport capacities if the coast would be straight.*

The size (volumes) of the arrows correspond with the computed values of the longshore transport, presented in Table 7.

The computed values of transport capacities are given below:

Direction	Transport	I	II	III	IV
280	S1	-95.6	-95.6	-97.3	-98.8
	S2	-398.7	-398.7	-411.6	-430.6
	S3	0	0	0	0
310	S1	-43.9	-43.8	1.97	12.5
	S2	-235.9	-235.9	16.9	112.1
	S3	0	0	1.74	0
340	S1	6.36	31.1	35.9	42.4
	S2	7.19	180	209	251.5
	S3	30.5	0.37	0.03	0
010	S1	33	33	34.7	36.8
	S2	143	143	161.3	186
	S3	0	0	0	0
040	S1	30.4	31.9	33.5	33.5
	S2	72.3	84.0	104.1	104.1
	S3	0	0	0	0
Total	ΣS1	-70	-96.3	8.8	26.4
	ΣS2	-412	-34.6	79.9	223.2
	ΣS3	30.5	0.37	1.8	0

Table 7 *The transport capacities in 10^3 m^3/year in case of a straight coast.*

The wave direction at deep water, mentioned in Table 7, is the mean value of a section of 30 degrees. For example: the direction 270 (westerly direction) represents the mean value of the section 255 to 285 degrees.

A positive transport capacity is directed towards the ebb-channel.

Figure 19 shows that the transport direction changes along the coast. Near the ebb channel a large longshore transport in eastern direction is computed. In point IV the direction of the longshore transport capacity is westerly.

This would result in accretion of the entire northwest coastline of Norderney though in reality erosion takes place. In reality, however, the difference in coastal direction between point I and point IV is about 23° (Figure 20).

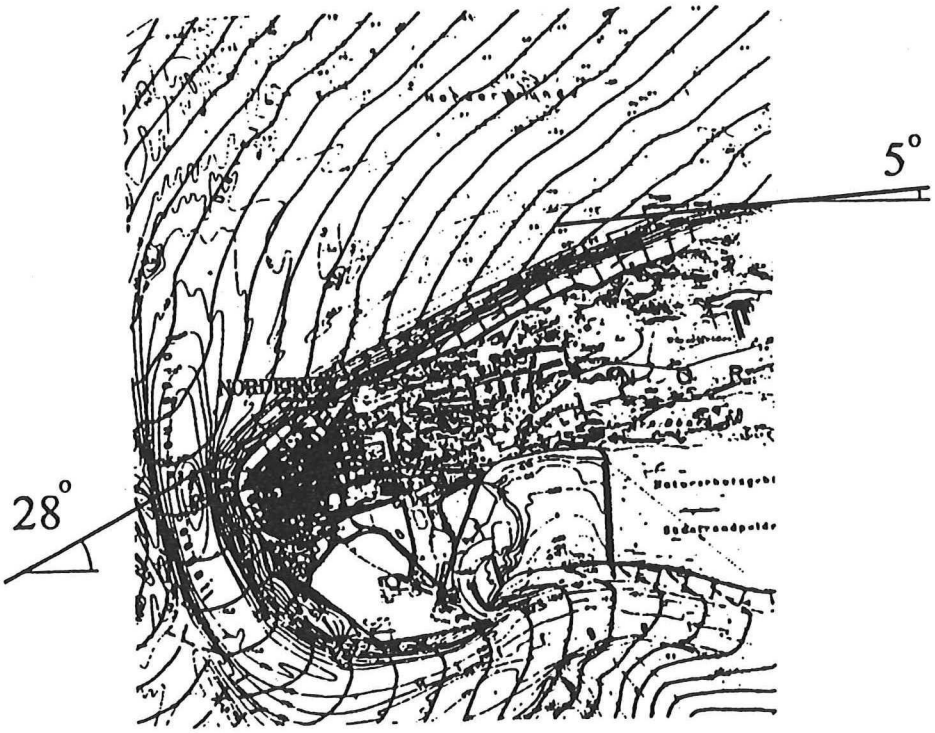

Figure 20 *Coastal curvature.*

In §5.5.2 the influence of the coastal direction is investigated.

5.5.2 The influence of the coastal direction

The computed values of transport capacities at point IV for two different angles of the shoreline are presented in Table 8.

Direction		IV old	IV new
280	S1	-98.8	-106.3
	S2	-430.6	-446
	S3	0	0
310	S1	12.5	-48.4
	S2	112.1	-168.8
	S3	0	0
340	S1	42.4	-8.7
	S2	251.5	-22.1
	S3	0	0
10	S1	36.8	18.2
	S2	186	97.2
	S3	0	0
40	S1	33.5	35.4
	S2	104.1	108.8
	S3	0	0
Total	ΣS1	26.4	-109.8
	ΣS2	223.1	-430.9
	ΣS3	0	0

Table 8 *The transport capacities in 10^3 m^3/year in point IV for different coastal directions.*

In this table "IV old" stands for the computed values in case of a straight coast and "IV new" for the values in case the coastal direction differs 23° with the coastal direction in point I.

The change in coastal direction results in a large transport in eastern direction in the same order as the longshore transport computed in point I. A small erosion would occur according to these results.

From the results in Table 8 the coastal constants (concerning the longshore transport) in point IV can be computed by dividing the difference in transport by the change in coastal direction:

$$s_i = \frac{\Sigma S_{i,IVold} - \Sigma S_{i,IVnew}}{\varphi_{old} - \varphi_{new}} \qquad (31)$$

where

s_i = coastal constant in zone i
ΣS_i = total resulting transport in zone i (see Table 8)
φ = angle of coast with East-West direction (see Figure 20)

$$s_1 = \frac{26.4 + 109.8}{28 - 5} * \frac{180}{\pi} * 10^3 = 0.34 * 10^6 \ m^3/year/rad \qquad (32)$$

$$s_2 = \frac{223.1 + 430.9}{28 - 5} * \frac{180}{\pi} * 10^3 = 1.63 * 10^6 \ m^3/year/rad \qquad (33)$$

The transport capacity in zone 2 is much higher then the capacity in zone 1. The groins however reduce this capacity strongly. Bakker and Joustra (1970) have investigated the influence of groins on the transport capacity and found a reduction factor of 4. Assuming that only the transport capacity in zone 2 is reduced by the groins, the real transport of both zone 1 and zone 2 are of the same magnitude according to the computations.

As an example of an application of the constants, given in eqs (32) and (33), one could calculate the direction in point IV, which theoretically would result in a stable beach, c.q. inshore between point I and point IV.

In the present situation an erosion of the beach is found of ($\Sigma S1_{IV,new}$ - $\Sigma S1_{I,old}$) = (109.8 -70) = $39.8*10^3$ m^3/yr. The numbers "109.8" and "70" originate from Table 8 and Table 7 respectively.

A turning of the beach over an angle 39.8/340 rad = 6.7 degrees could compensate this erosion. Here "340" denotes the coastal constant s_1, expressed in thousands of m^3/year. In the same way, turning of the inshore over an angle of (430.9-412)/1630 rad=2.1 degrees could compensate for the erosion of the inshore.

5.6 Discussion concerning the transport mechanism

1. From the computations and the literature study the following picture concerning the sand transport near the west-end of Norderney can be made.
Because of the refraction pattern on the strongly convex outer delta, the beach behind this delta needs to have a certain (convex) curvature in order to be stable. This contrarily to a coast with parallel contour lines, where a straight coast is stable.
From the calculations of §5.5 is found, that a difference in coastal direction of 17 to 21 degrees (23 - (2 to 6) degrees) between point I and point IV, would give a stable coast.

2. However, the convexity of the present beach is somewhat larger (ca 23 degrees) than a beach in equilibrium should have, which might partly explain the present erosion.

3. The present computations only deal with longshore transport. A second probable cause of erosion is downwards cross shore transport, which could move sand to the inshore, where it could be eroded away by the resulting current in flood direction, towards the ebb channel.
Current measurements at levels lower than the groin fields are not available to check this hypothesis. However, a morphological investigation as in chapter 6 might give some indications.

4 Tidal currents are able to augment or reduce these capacities. At Norderney from measurements was concluded that no significant tide induced transports take place in the groin fields (see §2.3).

5 Structures like groins will reduce the capacities. The largest capacities are computed for the zone NN-3m to NN-1m, where the groins have relatively the largest blocking effect.
Bakker & Joustra (1970), comparing coastal erosion along the dutch coast before and after the construction of groins, indicate, that groins might reduce coastal transport with a factor 4. This would reduce the value of S_2 (in case of erosion) in the same way.

6 The effect of focusing of wave rays on the longshore transport has been neglected. Although differences in direction of incoming waves on the area I-IV, caused by differences in refraction on bar A and bar B (fig.12) are taken into account, concentration of wave energy by focusing, resulting in higher wave heights and higher transport has been neglected. One may make the following remarks:
   - it changes the internal distribution of the sand transport over the area, but the input of sand on one side and the output of sand on the other side will not change considerably. Conclusions remain the same.

- the effect will be blurred because of the dispersion on the many small bars, found in reality instead of the prismatical bar in the mathematical model.

- The results concerning the sand transport and coastal constants along the North West coast of Norderney give an order of magnitude of the actual values. However, the values do not explain the details of the coastal behaviour between point I and IV (Figure 12). The values are rather sensitive for changes in the applied schematization. Refinement of the schematisation is therefore recommended by, for example, the implementation of the curvation of the coast between point I and IV. Also the influence of the tidal inlet the "Norderneyer Seegat" has to be regarded.

6 Application of the line modelling technique

6.1 General

The analysis of the volume computations leads to the conclusion to apply the line modelling technique on the North West beach of Norderney (§3.7, ad 4). Only in this area sufficient data is available.

This chapter deals with the application of the line modelling technique and its results.

In §6.2 the schematization of the North West beach of Norderney is described. The way of determination of the coastal constants is described in §6.3. In §6.4 the results of the computations are presented. Conclusions, based upon ch.5 and 6 are drawn in ch. 76.4.

6.2 Situation description of the study area

The supply of 1992 consisted of beach nourishment between groin D and groin H1, combined with inshore nourishment at the North West beach of Norderney (Figure 5). This is about the area between groin ZbI, near the tidal channel, and groin H1 (Figure 21). In the latter area a large part of the supplied sand is dumped below the level of NN-1.5m down to a depth of NN-5m.

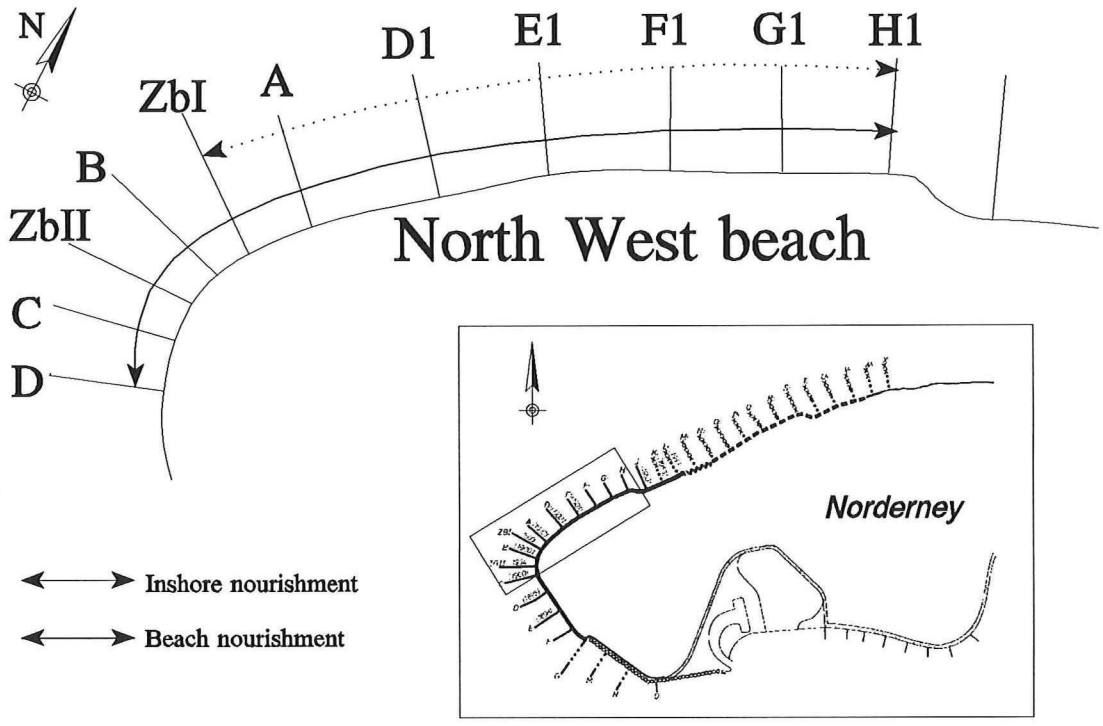

Figure 21 *The study area, on which the line modelling technique has been applied.*

In the area more south of groin ZbI the influence of the tidal channel is of great importance on the beaches. The beaches at that site are very steep. An inshore nourishment would lead to large losses into the tidal channel by the tidal current and cross shore transport.

The groinfield ZbI-A is much smaller than the groinfields eastward of groin A. This field is also more influenced by the tidal current. The effect of the groins ZbI and A is therefore different from the effect of the groins in the other groinfields. The area to schematize for application of the line modelling technique is therefore chosen between groin A and groin H1.

For each groinfield the volumes per linear meter (m3/m') per zone have been computed from the original volume data (Appendix D). The mean distance of the contour lines in a groinfield to a reference line (the seawall), has been computed by dividing the volumes per zone by the height of this zone.

To clarify the effect of the nourishment the changes of the volumes are computed with reference to the situation directly before supply (May 1992). The results will therefore show the change of the supplied volumes of sand, compared to the reference situation.

The area has been schematized as shown in Figure 22. The area is bounded by groin A and H1 and exists of five groinfields with a total length of almost 0.9 km. In these five fields the sand volumes are known.

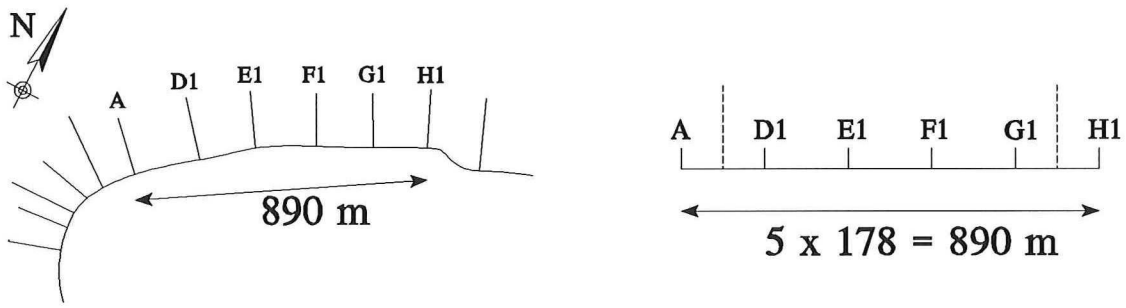

Figure 22 *Schematisation of the study area.*

The boundary conditions of the area are presented by the volumes in groinfields A-D1 and G1-H1. As initial values for all fields, the "volumes" (N.B.: elaborated as mentioned above; in the following the word "volumes" will be used in this sense) directly after supply are used.

Mind, that the stretch A-H_1 is schematized by a straight line, where in fact it is curved (N.B. curvature plays a role in coastal erosion). The philosophy is, that coastal processes are schematized by linear equations and therefore can be superimposed.

Thus only the rate of change, compare to the situation without supply is investigated, i.e. the volumes changes caused by the supply.

It is assumed that, at the considered time scale of ca 2 years, the effect of the deformation of the supply completely dominates the autonomous erosion of the area. The latter effect is therefore neglected in the following considerations.

6.3 Transport constants

6.3.1 Longshore transport constants

Erosion in an area is determined by a gradient in longshore sediment transport.
The volume decrease in that area is equal to the difference (S2-S1) in longshore transport on both sides of this area (Figure 23).

Figure 23 *Wave induced longshore sediment transport.*

As mentioned in Bakker & Kersting (1994) the change in wave induced longshore transport is assumed to be proportional to the change of coastal direction compared to a reference axis. This axis (roughly parallel to the coastal direction) is called the x-axis.

From the volume data the decrease of sand volumes in this area is computed between the measurements. Dividing this by the duration of the period between the measurements gives a rate of decrease, to be compared with a difference S_2-S_1, in transport in this period.

Consider Figure 24 (a plan view) and define:

AD1 The middle of groinfield A-D1.
Δx_i Distance between (for instance) AD1 and D1E1, where "AD1" and D1E1 stand for the transects in the centre of respectively groinfield A-D1 and groinfield D1-E1 (Figure 22).
y_i Distance of mean contour line to the reference axis in groinfield A-D1 i.e. volume in a zone divided by the height of this zone.
φ_1 The angle the coastline makes with the x-axis at the site of groin D1.
φ_2 The angle the coastline makes with the x-axis at the site of groin G1.

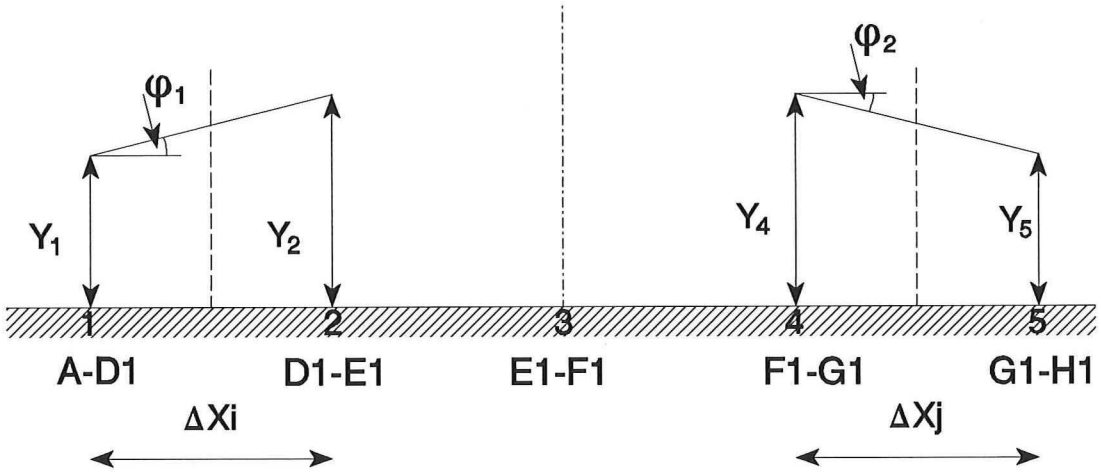

Figure 24 *Schematization to compute the longshore transport constants.*

The difference in coastline angle, φ_2-φ_1, is determined by computing the angles at the borders (Figure 24).

The difference, φ_2-φ_1, is computed at the moments of the measurements. The volume decrease, the change of ((y2+y3+y4) * Δx * zone height), is determined as a mean value between two of those successive moments. By taking the mean value of φ_2-φ_1 from two successive measurements, both values dS and dφ are computed at the same time.

This procedure has been carried out for all three zones (Table 6, page 46) and also for the total profile. The results are presented in Figure 25.

With linear regression linear relationships have been computed between Ds and dφ. The results are presented in Figure 25 as the solid lines.

The gradients of the lines give values for the longshore coastal constants:

$s_1 = 1.1 * 10^6$ m^3/year/rad
$s_2 = 0.9 * 10^6$ m^3/year/rad
$s_3 = 7.0 * 10^3$ m^3/year/rad
$s_{tot} = 2.0 * 10^6$ m^3/year/rad

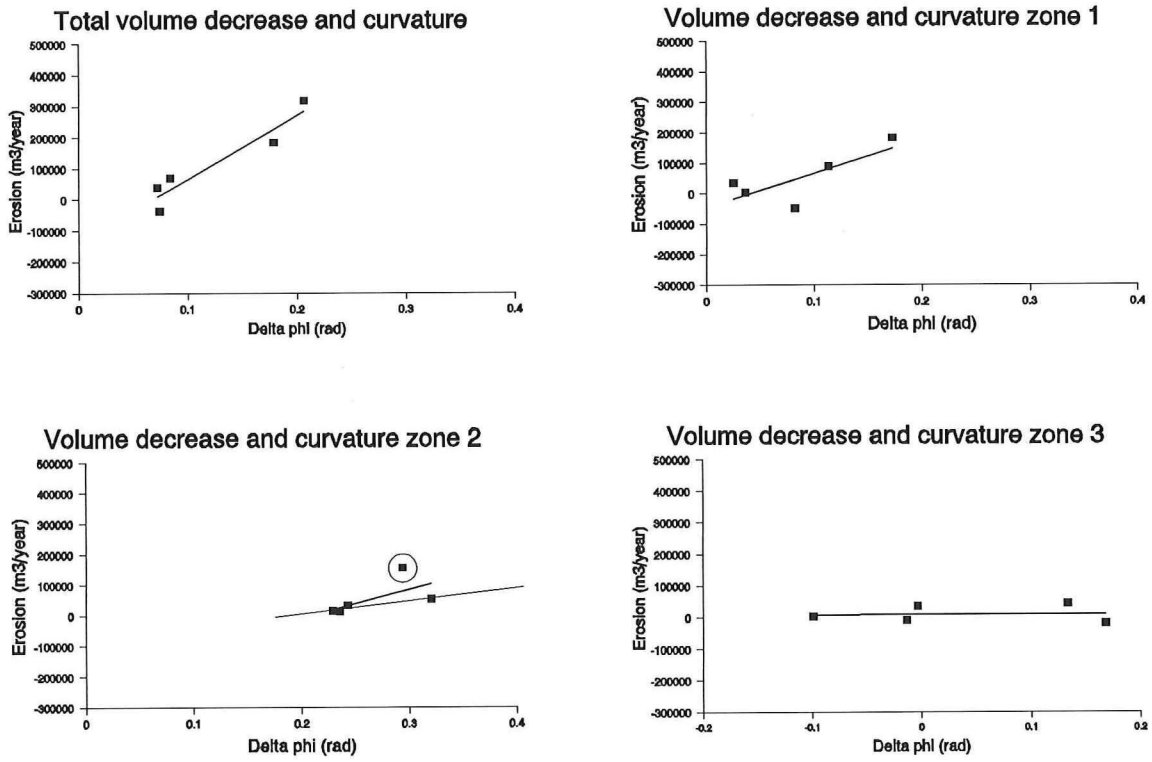

Figure 25 *The relation between erosion in the study area and the curvature. By linear regression a linear relation is computed between the volume decrease and curvature.*

In Figure 25 for s_2 the first observation (encircled), in the plot of zone 2, leads to rather high value for s_2. In the beginning, the supply covers the groins and then the groins do not affect the erosion. This differs from the situation later on. Therefore, the first observation is discarded, leading to:

$s_2 = 0.4 * 10^6$ m^3/year/rad

6.3.2 Cross shore transport constants

The cross shore transport constants in the line model determine the rate of reaction of the profile, on a disturbance with respect to the equilibrium profile.

In case of a supply the constants determine the velocity of diffusion of the sand until an equilibrium profile is reached.

These constants have to be determined by calibration. From earlier applications of the line modelling technique (Smit, Zwiers) and research about these constants (Swart), values in order of 2 m/year at a depth of approximately MWL-2m are found. This depends e.g. on the wave climate, the equilibrium profile, the tide and the grain size.

In case of Norderney a rough approximate calculation leads to the following values:

s_{y1} = 4 m/year at a depth of NN-1m

s_{y2} = 4 m/year at a depth of NN-3m

This calculation was based upon 2-line theory, in the (degenerated) case, that only cross shore transport occurs (straight contour lines). In that case, the coastal profile tends to an equilibrium profile and this equilibrium is reached in a negative-exponential way. The rate of decay under non-equilibrium conditions gives information on s_y.

The values are equal and seem rather high in comparison with the above mentioned values. Two reasons may justify the choice:

- In comparison with the circumstances in the cases, where the line method already has been used, the mean tidal range at Norderney is larger. This is a reason for considerable wave action over a large part of the profile, which results in a more equally distributed capacity of cross shore transport over the profile.
- In the study area the wave climate is relatively strong, which results in a larger cross shore transport capacity.

6.4 The way of computation and the results

Some elaborations are needed before measured volumes can be compared with line model computations. The model computations give values at regular time intervals. For this reason the measured volumes have been interpolated in the time in order to find values at regular time intervals, with a time step of 0.2 year. The results of these interpolations are shown in Figure 26.

Line model computations first were carried out with the constants given on page 57, where the small value of s_3 was replaced by zero.

However, the assumed value of s2 still appeared to be too high; it was adjusted., leading to:

$s_1 = 1.1 * 10^6$ m^3/year/rad
$s_2 = 0.2 * 10^6$ m^3/year/rad
$s_3 = 0.0 * 10^3$ m^3/year/rad

By using a value of 0.2 m^3/year/rad for s_2 the computed lines fit rather well with the interpolated values. This value is less than the value found in §6.3.1. This could lead to the conclusion that the groins have a favourable influence on maintaining the supplied sand on its place (see further ch.7).

In Figure 28 and Figure 29 a comparison is given of the interpolated measured volumes and the computed volumes. It can be noticed that the lowest zone shows a rather rapid erosion, which feature is not substantiated by the line model theory.

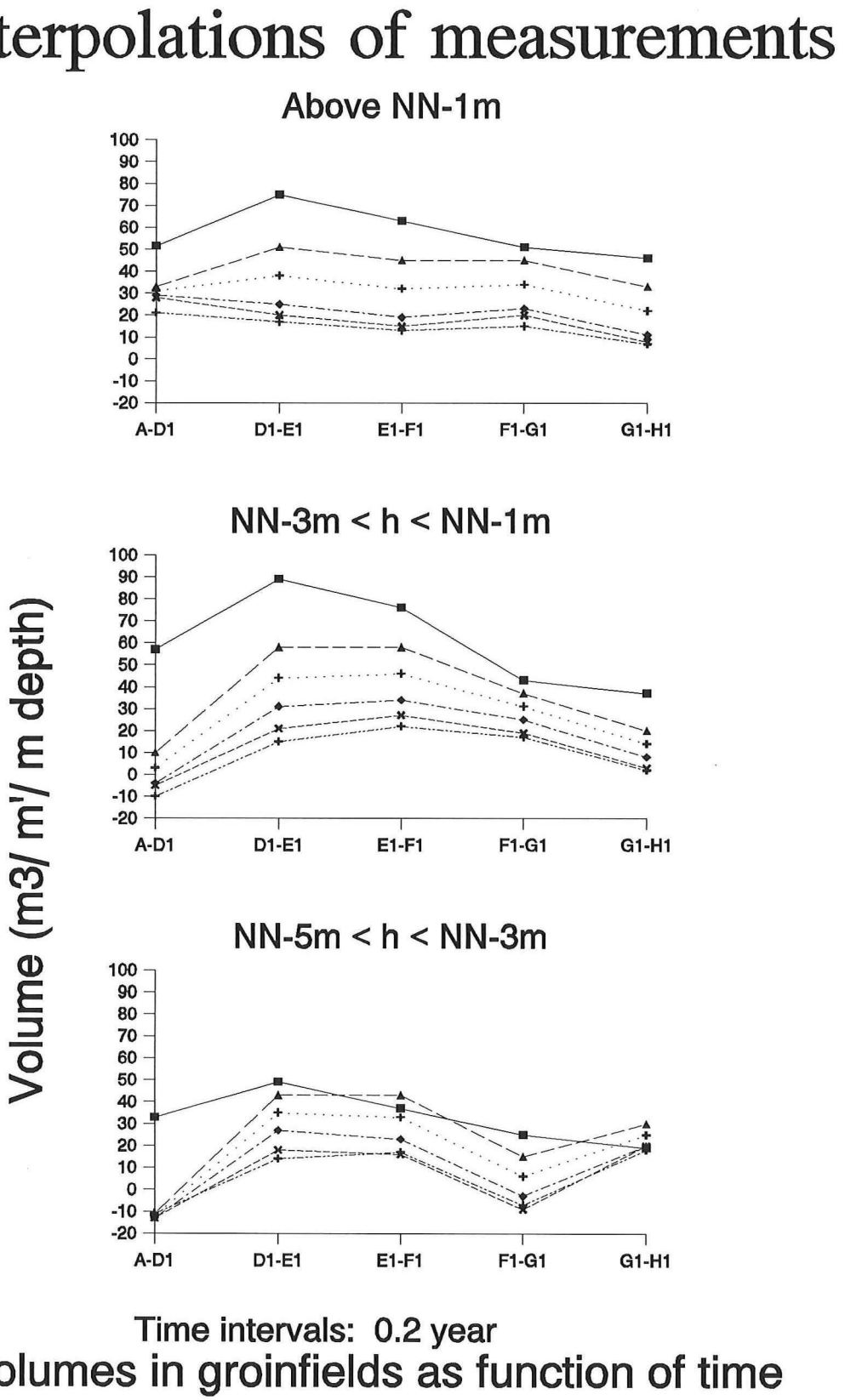

Figure 26 *Development of the volumes in the different zones in case of interpolation of the volume data, according to the measurements.*

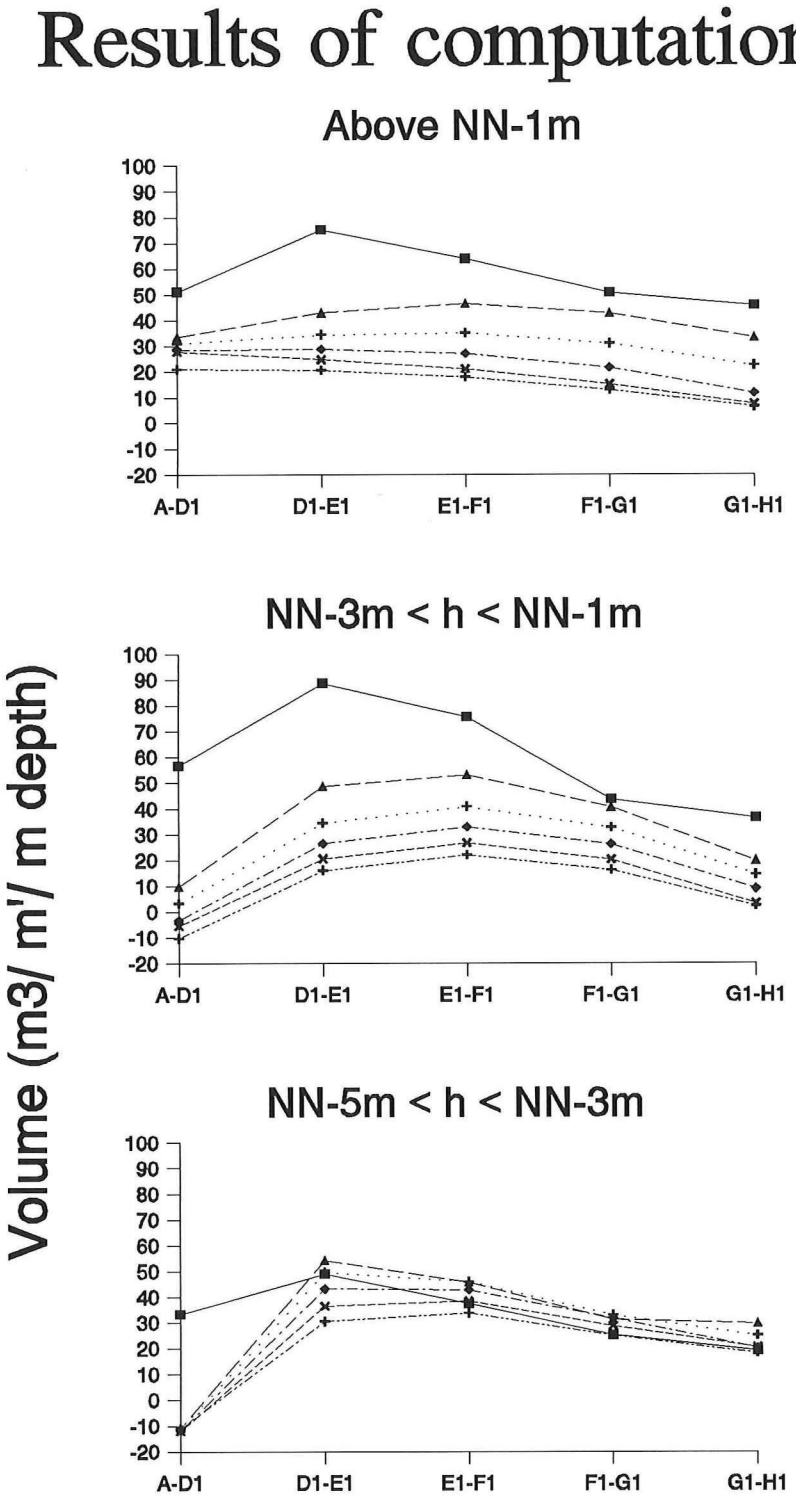

Figure 27 *Development of the volumes in the different zones, according to the computation with the line model.*

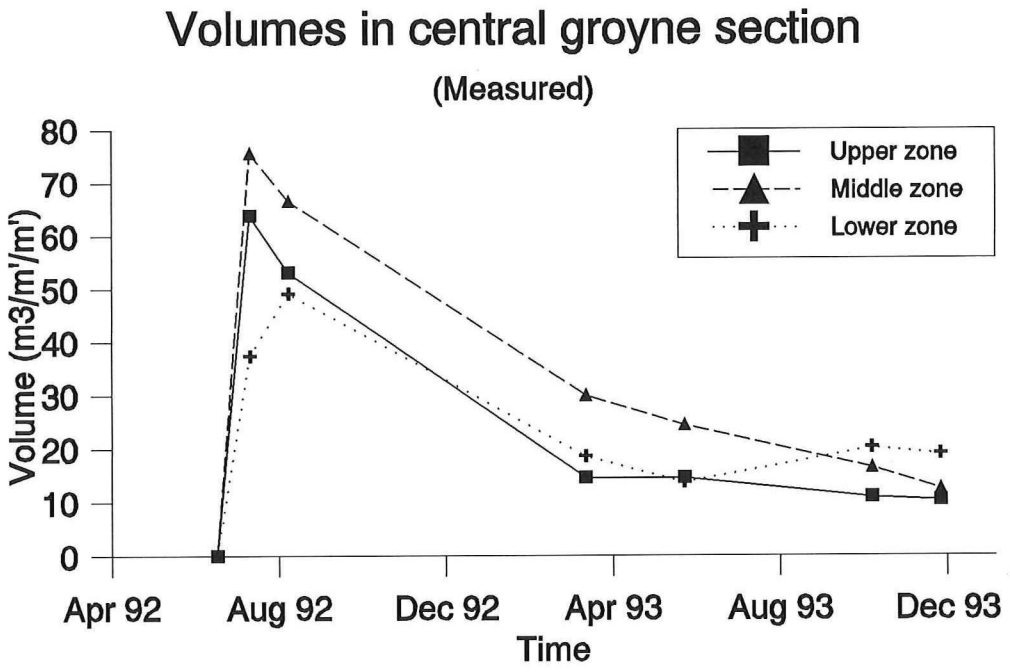

Figure 28 *Development of volumes in central groinfield E1-F1 according to the measurements.*

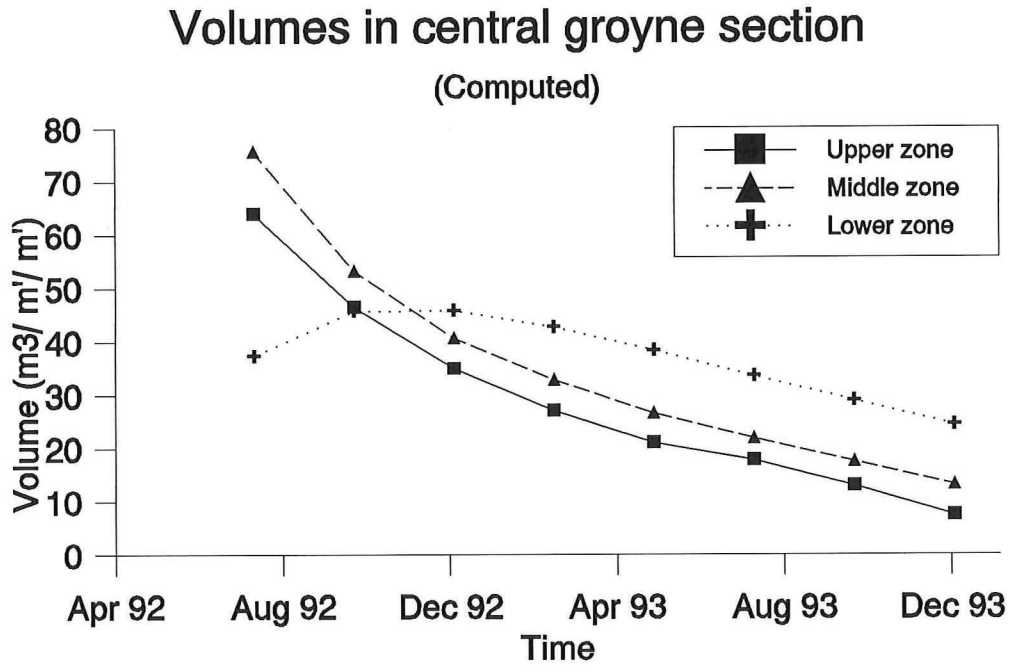

Figure 29 *Development of the volumes in the central groinfield E1-F1 according to the computations.*

7 General discussion and conclusions

7.1 Discussion on longshore coastal constants

The following compares the coastal constants, derived from transport formulae (§5.6) and from evaluation of topographic field data (ch. 6).

	Transport formulae		Field data
Groins taken into account	No	Yes	
s_1	0.34		1.1
s_2	1.63	0.41	0.2
s_3	0.0		0.0

Table 9 *Longshore coastal constants in 10^6 m^3/year/rad.*

In Table 9, a reduction factor of 4 for the coastal constant of the inshore has been applied, in order to take the groins into consideration (see Bakker & Joustra, 1970). The s_2-value found from the field data is small, compared to the one calculated from transport formulae, even if one takes the groins into account.
On the other hand, the s_1-value along the beach is much higher than expected. Taking into account the inaccuracy of the reduction factor 4, the total of s_1+s_2 is of the right order of magnitude.

7.2 Discussion on cross-shore coastal constants

The value of the cross-shore transport coefficient s_{y2} of 4 m/year at NN -3 m (comparable to NAP-3m) might be considered as very high, compared with values found elsewhere (Bakker et al.,1988). The highest value found up to now has been s_y=3 m/year at NAP-2m for Cadzand (CUR et al.,1986). As in Norderney, in Cadzand a tidal channel is in the coastal region. In the Norderney case, the wave attack is probably larger than at Cadzand.

7.3 General conclusion

Combination of line theory and evaluation of measurements gives a rather consistent picture of the transport mechanisms which occur at the North West coast of Norderney.

Coastal constants are derived, which give the possibility to make forecasts concerning coastal behaviour as influenced by future coastal protection, considering various alternatives. Knowledge of the coastal constants enables to compare quantitatively the investigated area with other coastal areas concerning influence of wave action etc.

The low value of the s_2, compared to the high s_1-value (as found in practice; ch. 6) gives numerical support to the German "Fingerspitzengefühl", that shoreface nourishment is feasible for Norderney (§2.2).

7.4 Future research

Up to now investigations on calculation of coastal constants are confined in two ways:

- With respect to the theoretical way (Chapter 5) only the large scale behaviour (difference in coastal behaviour between point I and IV) has been investigated. Detailed investigations on coastal direction and transport in the intermediate points are omitted up to now.
- With respect to the phenomenological way (Chapter 6) only the behaviour of the most western part is considered.

In the future, more detailed computations would be useful.

It is useful to compare in the future calculated sand transports and sandtransport gradients with results from other computations.

For instance: the results of the refraction computations could be compared with the results of HISWA-computations.

Sand transport measurements in the deeper zone (NN-3m to NN-5m) would be useful in order to get a better understanding of the erosion in that area.

Extension of the area of investigation in eastward direction would be useful.

The same holds for an in-depth investigation of the interaction between the whole outer delta and the Western side of Norderney.

8 References

Arbeitsgruppe Norderney des Küstenausschusses Nord- und Ostsee.
Gutachtliche Stellungsnahme zu den Untersuchungen über die Ursachen der Abbruchserscheinungen am West- und Nordweststrand der Insel Norderney sowie zu den zum Schutz der Insel vorgeschlagenen seebautechnischen Maßnahmen.
Die Küste, Heide.
1952.

Bakker, W.T.
Berekening van het langstransport door golven met de methode van evenwijdige dieptelijnen.
Rijkswaterstaat, Dir. Waterhuishouding en waterbeweging.
Studierapport WWK 69-7. (in Dutch)
1969.

Bakker, W.T.; Joustra, D.Sj.
The history of the Dutch coast in the last century.
Proceedings of the 12th ICCE, Washington, 1970.

Bakker, W.T.; ten Hoopen, H.G.H.; Grieve, G.R.H.
Berekening van het zandtransport volgens de methode Svašek bij een strand en een vooroever die een hoek met elkaar maken. (in Dutch)
Rijkswaterstaat, Dir.Waterhuishouding en Waterbeweging.
Studierapport WWK 71-18.
Juni 1972.

Bakker, W.T. ; Delver, G.
Coastal changes, caused by a shallow water sanddam in front of the Delfland coast.
Delft University of Technology; Coastal Engineering Group.
Sept. 1986.

Bakker, W.T. ; van de Kerk, C.P.T. ; de Vroeg, J.H.
Determination of coastal constants in mathematical line-models.
Second European Workshop on Coastal Zones, Loutraki.
1988.

Bakker, W.T.
Gidsstudie naar het gedrag van een vooroeversuppletie op het eiland Terschelling. (in Dutch)
Rijkswaterstaat, Dienst Getijdewateren, internal report.
Okt. 1992.

Bakker, W.T.; Kersting N.F.
Pilot study concerning the behaviour of coastal supply on the Dutch Wadden Island of Terschelling.
Delft University of Technology; Coastal Engineering Group.
April 1994.

CUR; Rijkswaterstaat; Waterloopkundig Laboratorium.
Manual on Artificial Beach Nourishment.
1988.

Dijkman, M.J.; Bakker, W.T.; de Vroeg, J.H.
Prediction of coastline evolution for specific parts of the Holland coast.
The Dutch coast; Report of a session on the 22nd ICCE, Delft.
1990.

Graaff, J. van de ; Niemeyer, H.D. ; Overeem, J. van.
Beach Nourishment, Philosophy and Coastal Protection Policy.
Coastal Eng., vol. 16, No. 1.
1991.

Hayes, M.O.
Barrier island morphology as a function of tidal and wave regime.
In: Leatherman: Barrier islands, Academic Press. New York.
1979.

Homeier, H.
Historisches Kartenwerk 1:50000 der Niedersächsischen Küste.
Forschungsstelle Küste Nordeney, Germany. (in German)
1962.

Homeier, H.
Supplement 1. Historical map 1:50000
No. 5 of the lower Saxonian coast. (in German)
Forschungsstelle Küste Nordeney, Germany
1964.

Homeier, H.
Die Auswirkungen schwerer Sturmtiden auf die Ostfriesische Inselstrände und Randdünen. (in German)
Forschungsstelle Küste Norderney, Germany.
1976.

K.N.M.I.
Meteoorologische en Oceanografische aspecten van stormvloeden op de Nederlandse kust. (in Dutch)
Bijdrage tot het rapport van de Delta commissie.
1960

Koch, M. ; Niemeyer, H.D.
Sturmtiden-Strommessungen im Bereichs des Norderneyer Seegats. (in German)
Forschungsstelle Küste Norderney, Germany.
1978.

Kunz, H. ; Stephan, H.J.
Morphologische Untersuchungen zu Wechselwirkungen zwischen Küstenbauwerken und mariner Umwelt. (in German)
Forschungsstelle Küste Norderney, Germany.
Sept. 1992.

Lassen, N. ; Siefert, W.
Mittlere Tidewasserstände in der Südöstlichen Nordsee - säkularer Trend und Verhältnisse um 1980. (in German)
Forschungsstelle Küste Norderney, Germany.
1991.

Luck, G
Inlet changes of the East Frisian island.
Proceedings 15th Int. Conf. Coastal Eng. Honolulu, ASCE, New York
1977.

Niemeyer, H.D.
Ausbreitung und Dämpfung des Seegangs im See- und Wattengebied von Norderney. (in German)
Forschungsstelle Küste Norderney, Germany.
1986a.

Niemeyer, H.D.
Tidestrommessungen in Buhnenfeldern. (in German)
Forschungsstelle Küste Norderney, Germany.
1986b.

Niemeyer, H.D.
Zur Klassifikation und Häufigkeit von Sturmtiden. (in German)
Forschungsstelle Küste Norderney, Germany.
1986c.

Niemeyer, H.D.
Morphodynamics tidal inlets.
Course "Coastal Morphology".
Delft University of Technology; Proceedings Comett Course.
April 1990a.

Niemeyer, H.D.
Field Measurements and Analysis of Wave Induced Nearshore Currents.
Proceedings 22nd ICCE, Delft.
1990b.

Niemeyer, H.D. ; Kaiser, R ; den Adel, H.
Anwendung des mathematischen Seegangsmodells HISWA auf Wattenmeer-bereiche. (in German)
Forschungsstelle Küste Norderney, Germany.
1992a

Niemeyer, H.D.
Naturuntersuchungen hydrodynamisch-morphologischer Wechselwirkungen an erodierenden Stränden. (in German)
Forschungsstelle Küste Norderney, Germany.
1992b

Pelnard Considère, R.
Essai de theory de l'evolution de formes de rivages en plages de sable et de galets. (in French)
Quatrième Journees de l'Hydraulique, Paris
Les Energies de la Mer, Question III.
June 1954.

Roskam, A.P.
Golfklimaten langs de Nederlandse kust. (in Dutch)
Rijkswaterstaat, Dienst Getijdewateren (RIKZ).
1988.

Schalkwijk
A contribution of the study of storm surges on the Dutch coast.
K.N.M.I. Med. en Verh., Serie B, deel I, No. 7.
1947.

Smit, E.S.P.
De rol van sedimentdwarstransport in de ontwikkeling van de Hollandse kust vanaf het begin van de grote kustuitbouw (ca 5000 jaar geleden).
Notitie in het kader van het project Kustgenese.(in Dutch)
April 1987.

Stephan, H.J.
Fünf Strandaufüllungen vor Norderney; Ergebnisse morphologischer Untersuchungen; (in German)
Bericht Forschungsstelle Küste, Norderney.
1988.

Svašek, J.N.
Invloed van brekende golven op de stabiliteit van zandige kusten. (in Dutch)
Rijkswaterstaat, Deltadienst, Waterloopkundige Afdeling, Nota W 68.083.
1968.

Svašek, J.N. ; Bijker, E.W.
Two methods for determination of morphological changes induced by coastal structures.
XXIInd Int. Nav. Congress Paris, section II, item 4.
1969.

Thilo, R. ; Kurzak, G.
Die Ursachen der Abbrucherscheinungen am West- und Nordwest-Strand der Insel Norderney; (in German)
Die Küste, Heide.
1952.

Velden, E.T.J.M. van der
Coastal Engineering.
Delft University of Technology; Coastal Engineering Group.
Dec. 1990.

Weenink, M.P.H.
A Theory and method of calculation of wind effect on sealevels in a partly enclosed sea, with special application to the southern coast of the North Sea.
K.N.M.I. Med. en Verh. No. 73
1958.

Appendix A1 Example of table with wave height and wave period of one wave direction sector as has been used to determine the longshore constants.

STATION : SCHIERMONNIKOOG-NOORD (SON)

PERIOD : FROM 21-11-1979 TILL 31-12-1991
3-HOURS INTERVAL MEASUREMENTS SERIES

WIND DIRECTION SECTOR : 205 - 235

WAVE HEIGHT Hmo IN CLASSES OF 50 CM (VERTICAL)
WAVE PERIOD Tmo IN CLASSES OF 2.0 SEC (HORIZONTAL)

FREQUENCIES IN PROCENTS

NUMBER OF VALUES IN THIS SECTOR = 3723.

	<1.0	1.0-2.9	3.4.9	5.-6.9	7.-8.9	>=9.0	ALL	Tmean	CUM.
0-49	0	1.397	11.362	0.833	0	0	13.591	3.71	100
50-99	0	0.269	31.91	4.244	0.107	0	36.53	4.08	86.409
100-149	0	0	23.127	5.963	0	0	29.089	4.53	49.879
150-199	0	0	8.783	5.855	0.054	0	14.692	4.94	20.79
200-249	0	0	1.155	3.492	0.081	0.027	4.754	5.37	6.097
250-299	0	0	0	0.86	0.107	0	0.967	5.95	1.343
300-349	0	0	0	0.188	0.081	0	0.269	6.32	0.376
350-399	0	0	0	0.054	0.027	0	0.081	6.7	0.107
400-449	0	0	0	0	0.027	0	0.027	7.9	0.027
450-499	0	0	0	0	0	0	0	0	0
500-549	0	0	0	0	0	0	0	0	0
550-599	0	0	0	0	0	0	0	0	0
600-649	0	0	0	0	0	0	0	0	0
650-699	0	0	0	0	0	0	0	0	0
700-749	0	0	0	0	0	0	0	0	0
>750	0	0	0	0	0	0	0	0	0
ALL	0	1.665	76.336	21.488	0.483	0.027	100	4.38	100
Hmean	0	38.9	95.5	149.3	233.1	235	106.8		

Appendix A2 Example of table with wave height and water level of one wave direction sector, as has been used to determine the longshore constants.

STATION : SCHIERMONNIKOOG-NOORD (SON)

PERIOD : FROM 21-11-1979 TILL 31-12-1991
3-HOURS INTERVAL MEASUREMENTS SERIES

WIND DIRECTION SEKTOR : 205 - 235

WAVE HEIGHT Hmo IN CLASSES OF 50 CM (VERTICAL)
WATER LEVEL IN CLASSES OF 50 CM (HORIZONTAL)

FREQUENCIES IN PROCENTS

NUMBER OF VALUES IN THIS SECTOR = 3723.

	<-100	-100 -50	-50 -1	0 +49	+50 +99	>= +100	ALL	WL mean	CUM.
0-49	2.901	1.853	1.612	2.498	4.136	0.591	13.59	-8	100
50-99	6.608	5.748	4.996	6.473	10.556	2.149	36.53	-5	86.409
100-149	4.19	5.238	4.136	5.345	7.843	2.337	29.09	-1	49.879
150-199	1.504	2.337	2.444	2.417	4.163	1.826	14.69	11	20.79
200-249	0.161	0.645	0.886	1.128	1.155	0.779	4.75	26	6.097
250-299	0	0.188	0.215	0.215	0.134	0.215	0.97	27	1.343
300-349	0	0	0.054	0	0.081	0.134	0.269	89	0.376
350-399	0	0	0.027	0.027	0	0.027	0.081	32	0.107
400-449	0	0	0	0	0.027	0	0.027	87	0.027
450-499	0	0	0	0	0	0	0	0	0
500-549	0	0	0	0	0	0	0	0	0
550-599	0	0	0	0	0	0	0	0	0
600-649	0	0	0	0	0	0	0	0	0
650-699	0	0	0	0	0	0	0	0	0
700-749	0	0	0	0	0	0	0	0	0
>750	0	0	0	0	0	0	0	0	
ALL	15.364	16.009	14.37	18.104	28.096	8.058	100	0	100
Hmean	90.9	108	114.1	106.7	104.1	132	106.8		

Appendix B CERC.PAS

```
{$IFDEF CPU87} {$N+} {$ELSE} {$N-} {$ENDIF}

PROGRAM CERC (INPUT,OUTPUTFILE);                {For three lines and a bar}

USES CRT, DOS, GRAPH;

CONST  pathin  = 'c:\nordney\data\splits\' ;          { inputdata       }
       pathout = 'c:\nordney\prog\cerc\' ;            { outputfiledata  }
       gamma   =  0.6   ;                             { breakersindex   }
       g       =  9.81  ; { (m/s²) }                  { gravityconstant }
       cerc    =  0.040 ;                             { cerc constant   }
       year    = 31557600 ; {year in seconds}

       setupfactor = 1.22;
       days : array [0..6] of String[9] = ('Sunday','Monday','Tuesday',
            'Wednesday','Thursday','Friday', 'Saturday');


LABEL  FINISH;

TYPE Datamatrix = ARRAY [1..16, 1..6] OF REAL;
     Constants  = ARRAY [1..6] OF REAL;

VAR chance                : REAL    ; { probability of occurrence          }
    C_inner               : REAL    ; { wave celerity in  area             }
    Co, Cbr               : REAL    ; { wave celerity                      }
    CosPhi_inner          : REAL    ; { cosiness wave angle in  area       }
    delta, alpha          : REAL    ; { angle between inshore and beach    }
    dh                    : REAL    ; { water level change due to wind & tide }
    dhTide                : REAL    ; { water level change due to tide     }
    dhWave                : REAl    ; { water level change due to waves    }
    h2, h1, h0            : REAL    ; { depth's at the lines               }
    Ho_sig                : REAL    ; { significant wave height            }
    Ho_rms                : REAL    ; { rootmeansquare wave height         }
    Ho_tempsig            : REAL    ; { temporary Ho_sig                   }
    hbr                   : REAL    ; { breaker depth                      }
    h_bar                 : REAL    ; { depth of bar                       }
    Hosig_bar             : REAL    ; { the wave height just passing the bar}
    h_insh                : REAL    ; { depth of inshore                   }
    Hb                    : REAL    ; { sign breakerwave height            }
    Phio                  : REAL    ; { angle of approach                  }
    Phibr                 : REAL    ; { angle at breakerpoint              }
    Phi_inner             : REAL    ; { wave angle in  area                }
    number, exponent      : REAL    ;
    Phi                   : REAL    ; { variable angle                     }
    dS1, dS2, dS3         : REAL    ; { total transport at the lines       }
    S1CERC                : REAL    ; { effective transport in zone 1      }
    S2CERC                : REAL    ; { effective transport in zone 2      }
    S3CERC                : REAL    ; { effective transport in zone 3      }
    dS1CERC               : REAL    ; { transport in zone 1 by CERC        }
    dS2CERC               : REAL    ; { transport in zone 2 by CERC        }
    dS3CERC               : REAL    ; { transport in zone 3 by CERC        }
    dSbarCERC             : REAL    ; { transport at the bar               }
    SbarCERC              : REAL    ; { effective transport at the bar     }
    Tmo                   : REAL    ; { wave period at deep water          }
    x                     : REAL    ; { variable                           }
    nb                    : REAL    ; { nameless factor                    }
    dummy                 : REAL    ;
    S1T1H,S2T1H,S3T1H     : REAL    ; { transport from one H, one T        }
    S1_1H,S2_1H,S3_1H     : REAL    ; { transport from one H, all T        }
    S1_1Hbar              : REAL    ;
    S1T1Hbar              : REAL    ;
    SUMpHT_1H             : REAL    ;
    SUMpHT                : REAL    ;
    inputfile,outputfile: TEXT      ;
    dirfilename           : STRING  ;
    filename, answer      : STRING  ;
```

```
    i,j,k                : INTEGER ;
    parameter            : INTEGER ;
    Notbreaker           : BOOLEAN ; { breakercase                    }
    y, m, d, dow         : Word    ;
    h, min, s, hund      : Word    ;
    probability          : Constants  ;
    setupconst           : Constants  ;
    pHT                  : Datamatrix ;


FUNCTION Power ( number:REAL; exponent:REAL) : REAL;
BEGIN
  x:=1;
  IF number<=0 THEN BEGIN number:=abs(number); x:=-1; END;
  Power := x * exp (exponent*ln(number));
END;  { Power }

FUNCTION ArcCos( Phi: REAL) : REAL;
BEGIN
  ArcCos := ArcTan (sqrt (1-sqr (Phi)) /Phi);
END;  { ArcCos }

FUNCTION Tanh (x : REAL) : REAL;
VAR e2x : REAL;
BEGIN
  e2x  :=  exp(2*x);
  Tanh := (e2x-1)/(e2x+1);
END;  { Tanh }

FUNCTION Sinh (x : REAL) : REAL;
VAR ex : REAL;
BEGIN
  ex   :=  exp(x);
  Sinh := (ex-(1/ex))/2 ;
END;  { Sinh }

FUNCTION CosPhi (C, Co, Phio :REAL) : REAL;
VAR var1, var2  : REAL;
BEGIN
  var1   := (C * sin(phio)) / Co;          {sin(phi)/c  ==  sin(phio) /co }
  var2   := 1 - sqr(var1);                 {cos²(phi)   ==  1 - sin²(phi) }
{test:}  IF VAR2 <= 0 THEN
         BEGIN
           WRITELN('error in line 119');READLN;
           VAR2:=0.000001;
         END;
  CosPhi := sqrt(var2);                    {cos(phi)    == √(1 - sin²(phi)}
END;  { CosPhi }
```

```
FUNCTION Celerity ( h, Tmo : REAL) : REAL;
VAR xn, a, Lo, f, fx : REAL;
    i : integer;
BEGIN
  Co := (g*Tmo)/(2*pi);
  Lo := Tmo*co;
  a  := 2*pi*h/Lo;
  x  := 0;
  xn := 1;
  i  := 1;
  WHILE ABS(xn-x) > 0.00001 do
  BEGIN
    x  := xn;
    f  := x - Tanh((a/x));
    fx := 1 + (a/sqr(x))*(1-sqr(Tanh((a/x))));
    xn := x - (f/fx);
    i  := i+1;
  END;
  Celerity := Co * xn;
END;  { Celerity }

FUNCTION n (hbr, c, Tmo: REAL) : REAL;
VAR kh2 : REAL;
BEGIN
  kh2 := (4 * pi * hbr)/(c * Tmo);
  n  := 0.5 * (1 + (kh2 / Sinh(kh2)) );
END;  { n }


PROCEDURE makematrices(VAR pHT : datamatrix);
VAR i,j    : INTEGER;
    dummy  : REAL;
BEGIN
  FOR i:=1 TO 16 DO
  BEGIN
    FOR j:=1 TO 6 DO
    BEGIN
      READ(inputfile,dummy);
      pHT[i,j]:= dummy;
      WRITE(pHT[i,j]:9:4);
    END;
    READLN(inputfile);
    WRITELN;
  END;
  READLN;
END;  { makematrices }


PROCEDURE initialisation (filename                                  : STRING;
                          VAR h2, h1, h0, h_bar, h_inner, alpha     : REAL;
                          VAR setupconst,probability                : Constants;
                          VAR k                                     : INTEGER;
                          VAR Notbreaker                            : BOOLEAN);
BEGIN

  h2      := 1;
  h1      := 3;
  h0      := 20;
  h_bar   := 1.5;
  h_inner:= 5;

  k:=6;
```

```
  IF filename = '265_295' THEN k:=1 ELSE
  IF filename = '295_325' THEN k:=2 ELSE
  IF filename = '325_355' THEN k:=3 ELSE
  IF filename = '355_025' THEN k:=4 ELSE
  IF filename = '025_055' THEN k:=5 ;

  notbreaker:=true;      { Wave is not(!) breaking at the bar !!}

  setupconst[1]:= 4.54;   probability[1]:= 0.10514;          {265_295}
  setupconst[2]:= 3.80;   probability[2]:= 0.08900;          {295_325}
  setupconst[3]:= 3.91;   probability[3]:= 0.07637;          {325_355}
  setupconst[4]:= 1.98;   probability[4]:= 0.05832;          {355_025}
  setupconst[5]:= 3.13;   probability[5]:= 0.05791;          {025_055}
  setupconst[6]:= 0;      probability[6]:= 1;
END;  { initialisation }


PROCEDURE OvertoppingHsig(h_bar, dh, Phio, Tmo  : REAL; VAR Hosig_bar : REAL);
VAR Hobar_const, Hosig     : REAL;
    var1, var2, var3       : REAL;
    CosPhibr, cosfrac      : REAL;
    CosPhio                : REAL;
    i, imax                : INTEGER;
BEGIN
  var1      := Power((h_bar+dh),2.5);
  var2      := sqr(gamma);
  var3      := sqrt(g);
  Co        := (g*Tmo)/(2*pi) ;
  CosPhio   := cos(Phio);
  Hobar_const := Power(( var1 * 2 * var2 * var3)/(Co * CosPhio)), 0.5);
  Hosig     := Hobar_const;

  imax      := 10;
  FOR i:= 1 TO imax DO
  BEGIN
    Cbr       := Celerity((h_bar+dh),Tmo);
    CosPhibr  := CosPhi(Cbr, Co, Phio);
    Phibr     := ArcCos(CosPhibr);
    nb        := n ((h_bar+dh), Cbr, Tmo);
    cosfrac   := Power((nb*CosPhibr), 0.5);
    Hosig     := Hobar_const * cosfrac;
  END;
  Hosig_bar   := Hosig;
END;  { OvertoppingHsig }


PROCEDURE breakerdepth(Ho_rms, Phio, Tmo  : REAL; var hbr, Phibr, Co, nb : real);
VAR temphbr, hbrconst      : REAL;
    var1, var2, var3       : REAL;
    CosPhibr, cosfrac      : REAL;
    CosPhio                : REAL;
    i, imax                : INTEGER;
BEGIN
  hbr       := 0;
  var1      := sqr(Ho_rms);
  var2      := sqr(gamma);          {hbr will be computed with the rms}
  var3      := sqrt(g);
  Co        := (g*Tmo)/(2*pi) ;
  CosPhio   := cos(Phio);
  hbrconst  := Power((( 2 * var1 * Co * CosPhio) / (2 * var2 * var3)), 0.4);
  hbr       := hbrconst;
```

```
  imax      := 10;
  FOR i:= 1 TO imax DO
  BEGIN
    Cbr       := Celerity(hbr,Tmo);
    CosPhibr  := CosPhi(Cbr, Co, Phio);
    Phibr     := ArcCos(CosPhibr);
    nb        := n (hbr, Cbr, Tmo);
    cosfrac   := Power((nb*CosPhibr),-0.4);
    hbr       := hbrconst * cosfrac;
  END;
END;  { breakersdepth }


PROCEDURE breakerdepthalfa(Ho_tempsig, Phio, Tmo, alpha            : REAL;
                           VAR hbr, Phibr, Co, nb                  : REAL;
                           VAR CosPhi_inner, Phi_inner, C_inner    : REAL);
VAR temphbr, hbrconst      : REAL;
    var1, var2, var3       : REAL;
    cosfrac, CosPhibr      : REAL;
    hbrold                 : REAL;  {temporary parameter}
    i, imax                : INTEGER;
    negativ                : SHORTINT;
BEGIN
  negativ   := +1;
  var1      := sqr(Ho_tempsig);      {hbr will be computed with the sig}
  var2      := sqr(gamma);
  var3      := sqrt(g);
  Co        := (g*Tmo)/(2*pi) ;
  hbrconst  := Power((( var1 * Co * cos(Phio)) / (2 * var2 * var3) ), 0.4);
  hbr       := hbrconst;
  imax      := 50;            {maximal 50 iterations}
  hbrold    := hbr;

  C_inner      := Celerity((h_+dh), Tmo);
  CosPhi_inner := CosPhi(C_inner, Co, Phio);
  phi_inner    := ArcCos(CosPhi_inner);

  IF (Phi_inner + alpha) < 0 THEN
  BEGIN             {if  (Phi_inner + alpha) < 0  the Phibr will also be }
    negativ := -1; {negatief but Cosphi(..,..,..) computes a positive  }
  END;              {value for Phibr. That's why is should be made negativ }
                    {at the end of this procedure. It has no effect on hbr }
  FOR i:= 1 TO imax DO
  BEGIN
    hbrold   := hbr;
    Cbr      := Celerity(hbr,Tmo);
    CosPhibr := CosPhi(Cbr, C_inner, (Phi_inner+alpha));
    Phibr    := ArcCos(CosPhibr);
    nb       := n (hbr, Cbr, Tmo);
    IF ((phi_inner+alpha)*180/pi) > 90 THEN
    BEGIN
      hbr := 0 ;
      i:= imax ;  WRITELN('(phi_inner+alpha)*180/pi) > 90, line 297');
    END ELSE
    BEGIN
      cosfrac := Power((cos(Phi_inner+alpha)) / (nb*(cos(Phi_inner)*cos(Phibr))),
      0.4);
      hbr     := hbrconst * cosfrac ;
      IF ((abs(hbrold-hbr))/hbr) > 0.001 THEN hbrold := hbr ELSE i:=imax;
    END;
  END;
  Phibr := Phibr * negativ;
END;  { breakersdepthalfa }
```

```
PROCEDURE Setup (Ho_sig       : REAL     ;
                 setupconst   : Constants;
                 k            : INTEGER  ;
                 VAR dhWave   : REAL    );
BEGIN
  dhWave := 0.01 * setupfactor * setupconst[k] * SQR(Ho_sig);
END;  { Setup }


PROCEDURE CERCTransportBars(Tmo, nb, Cbr, hbr, Phio, Co, Phibr   : REAL;
                            VAR dSbarCERC                        : REAL);
VAR var1, var2, var3, dSbarCERC2 : REAL;
BEGIN
  var1 := sqr(gamma);
  var2 := Power((h_bar+dh),3);
  var3 := Power(hbr, 3);
  dSbarCERC2 := 3600000 * Power((hbr * 0.6),2.5) * sin(2*Phibr) / year;
  dSbarCERC  := cerc * (var3-var2)*nb*var1*g*sin(Phio) *cos(Phibr) /Co;
END;  { CERCTransportBars }


PROCEDURE CERCTransport(Tmo, nb, Cbr, hbr, Phio, Co, Phibr, alpha : REAL;
                        CosPhi_inner, Phi_inner, C_inner          : REAL;
                        VAR dS1CERC,dS2CERC,dS3CERC               : REAL);
VAR var1, var2, var3, var4, dS1, dS1CERC2 : REAL;
BEGIN                   { If a negativ value is chosen for alpha then the  }
  dS1CERC:=0;           { transports are positive to the left, which occurs}
  dS2CERC:=0;           { when (Phi_inner + alpha) > 0                      }
  dS3CERC:=0;
  BEGIN                      { hbr < (h2+dh),  breaking in the highest zone}
    var1 := sqr(gamma);
    var2 := Power(hbr, 3);
    dS1CERC2 := 3600000 * Power((hbr * 0.6),2.5) * sin(2*Phibr) / year;
    dS1CERC  := cerc * var2*nb*var1*g*sin(Phi_inner+alpha) *cos(Phibr) /C_inner;
  END;

  IF hbr > (h2+dh) THEN         { hbr < (h2+dh),  breaking in the second zone}
  BEGIN
    var1 := sqr(gamma);
    var2 := Power((h2+dh),3);
    var3 := Power(hbr, 3);
    dS1CERC  := cerc * var2 *nb*var1*g*sin(Phi_inner+alpha) *cos(Phibr) /C_inner;
    dS2CERC  := cerc * (var3-var2) *nb*var1*g*sin(Phi_inner+alpha) *cos(Phibr)
      /C_inner;
  END;

  IF hbr > (h1+dh) THEN         { hbr < (h2+dh),  breaking in the lowest zone}
  BEGIN
    var1 := sqr(gamma);
    var2 := Power((h2+dh),3);
    var3 := Power((h1+dh),3);
    var4 := Power(hbr, 3);
    dS1CERC  := cerc * var2 *nb*var1*g*sin(Phi_inner+alpha) *cos(Phibr) /C_inner;
    dS2CERC  := cerc * (var3-var2) *nb*var1*g*sin(Phi_inner+alpha) *cos(Phibr)
      /C_inner;
    dS3CERC  := cerc * (var4-var3) *nb*var1*g*sin(Phi_inner+alpha) *cos(Phibr)
      /C_inner;
  END;
  WRITE  ('      dS1CERC = ', dS1CERC:6:5);
  WRITE  ('      dS2CERC = ', dS2CERC:6:5);
  WRITELN('      dS3CERC = ', dS3CERC:6:5);
  WRITELN('  all dSxCERC = ', (dS1CERC + dS2CERC + dS3CERC):6:5);
END;  { CERCTransport }
```

```
PROCEDURE  WriteOutputFile(SUMpTH,S1CERC,S2CERC,S3CERC          : REAL;
                           SbarCERC                             : REAL;
                           alpha,phio,h0,h1,h2                  : REAL;
                           filename                             : STRING;
                           dh, hbr, Phibr, year                 : REAL);
BEGIN
  WRITELN(outputfile);  GetDate(y,m,d,dow); GetTime(h,min,s,hund);
  WRITE(outputfile,'Time is : ',h:0,':',min:0,':',s:0,'                    ');
  WRITELN(outputfile,'          Tmo =',Tmo:4:1,'      Ho_rms = ',Ho_rms:4:1);
  WRITELN(outputfile,'S1CERC = ',((S1CERC*probability[k])/1000):6:3,
                                                        ' * 10^3 m3/year');
  WRITELN(outputfile,'S2CERC = ',((S2CERC*probability[k])/1000):6:3,
                                                        ' * 10^3 m3/year');
  WRITELN(outputfile,'S3CERC = ',((S3CERC*probability[k])/1000):6:3,
                                                        ' * 10^3 m3/year');
  WRITELN(outputfile);
  WRITELN(outputfile,'StotCERC   = ',(((S1CERC+S2CERC+S3CERC)
                                   *probability[k])/year):10:6,' * m3/sec');
  WRITELN(outputfile,'SbarCERC   = ',(((SbarCERC)*probability[k])/year):10:6,
                                                            ' * m3/sec');
  WRITELN(outputfile,'Total transport is : ',(((S1CERC+SbarCERC+S2CERC+S3CERC)
                                   *probability[k])/year):10:6,' * m3/sec');
  WRITELN(outputfile);
  WRITELN(outputfile,'   hbr = ',hbr:4:2,'        Phibr = ',(Phibr*180/pi):4:2);
  WRITELN(outputfile,'    dh = ',dh:4:2);
  WRITELN(outputfile,'  alpha = ',(alpha*180/pi):5:3,'°       Phio  =  ',
                                (phio*180/pi):5:1,'   ', filename:15,'.dat');
  READLN;
  WRITELN(outputfile,'  gamma   = ', gamma:3:2  );
  WRITE  (outputfile,'  h2      = ', h2:3:1     );
  WRITELN(outputfile,'  dhTide  = ', dhTide:5:3    ,' cm' );
  WRITELN(outputfile,'  h1      = ', h1:3:1     );
  WRITELN(outputfile,'  h0      = ', h0:3:1     );
  WRITELN(outputfile,'  h_bar   = ', h_bar:3:1  );
  WRITELN(outputfile,'  h_inner = ', h_inner:3:1 );
  WRITELN(outputfile,'  probability[k] = ',probability[k]:6:5);
  WRITELN(outputfile,'  setupconst[k]  = ',setupconst[k]:6:5);
  CLRSCR;
  FOR i:=1 TO 10 DO WRITELN;
  WRITELN('                                *****   READY   *****        ');
  READLN;
END;  { WriteOutputFile }


{*************************************************************************}
{*************************                 ***********************}
{*************************   Mainprogram   ***********************}
{*************************                 ***********************}
{*************************************************************************}

BEGIN
  CLRSCR;
  WRITE('Which filename?           : ');
  READLN(filename);
  dirfilename := pathin + filename + '.dat';
  ASSIGN(inputfile,dirfilename);
  RESET(inputfile);

  initialisation(filename,h2,h1,h0,h_bar,h_inner,alpha,setupconst,probability,k,
      Notbreaker);

  dirfilename:= pathout + 'CERCUIT.PAS';
  WRITELN(dirfilename:40);
  ASSIGN(outputfile,dirfilename);
  APPEND(outputfile);
  CLRSCR;
  WRITELN;

  WRITE('Which Tide?  : ');
```

```
  READLN(dummy);      dhTide:= dummy/100;
  WRITE('Which alpha?  : ');
  READLN(dummy);      alpha:= dummy * pi/180;
  WRITE('Which angle of approach?  : ');
  READLN(dummy);      phio:= dummy * pi/180;

  MakeMatrices(pHT);

  S1CERC     :=0;
  S2CERC     :=0;
  S3CERC     :=0;
  SbarCERC   :=0;

  S1_1H:=0;  S2_1H:=0;  S3_1H:=0;


  FOR i:=1 TO 16 DO
  BEGIN

    Ho_sig := -0.25 + (i*0.50)        ;
    Ho_rms :=  sqrt(0.5 * sqr(Ho_sig));

    S1T1H     :=0;     S1_1H     :=0;
    S2T1H     :=0;     S2_1H     :=0;
    S3T1H     :=0;     S3_1H     :=0;        { transportrates for one H   }
    S1T1Hbar :=0;      S1_1Hbar :=0;

    SUMpHT_1H := 0;          {probability of occurrence of a H  }

    FOR j:=2 TO 6 DO
    BEGIN
      dS1CERC    :=0;
      dS2CERC    :=0;
      dS3CERC    :=0;
      dSbarCERC :=0;

      Ho_tempsig := Ho_sig;
      Tmo := (j*2) - 2 ;

      SETUP(Ho_sig, setupconst, k, dhWave);
      dh  := dhTide + dhWave;

{*****************************************************************************}
{*****************************  test:   **********************************}
    {       h2       := 1;
            h1       := 2;                {F7 pag 166}
    {       h0       := 20;
            h_bar    := 3;
            h_inner := 5;
                          { pay attension:  gamma_rms = 0.8 }
    {       k       := 6;    { no setup, probability = 1, see initial settings}

    {       dh      := 0;
            Tmo     := 7;
            Ho_rms  := 2;
            Ho_sig  := sqrt(2 * sqr(Ho_rms));
            Ho_tempsig := Ho_sig;
    {       phio    := (phio + j*5)* pi/180;       }
    {       pHT[i,j]:=100/(16*5);             {all wave heights and periods}
{*****************************  test close  ******************************}
{*****************************************************************************}
```

```
    Breakerdepth(Ho_rms, Phio, Tmo, hbr, Phibr, Co, nb );

    IF hbr > (h_bar+dh) THEN
    BEGIN                          {computing transport on outer delta bars S1}
      CERCTransportbars( Tmo, nb, Cbr, hbr, Phio, Co, Phibr, dSbarCERC);
      OvertoppingHsig(h_bar, dh, Phio, Tmo, Hosig_bar);
      Ho_tempsig :=  Hosig_bar * 0.999;
      Notbreaker :=  false;      {the wave breaks}
    END;

    Breakerdepthalfa( Ho_tempsig, Phio, Tmo, alpha, hbr, Phibr, Co, nb,
                      CosPhi_inner, Phi_inner, C_inner                 );


    CERCTransport( Tmo, nb, Cbr, hbr, Phio, Co, Phibr, alpha, CosPhi_inner,
                      Phi_inner, C_inner, dS1CERC, dS2CERC, dS3CERC  );


    IF Phibr>(1/2)*pi THEN BEGIN dS1CERC:=0; dS2CERC:=0; dS3CERC:=0;
    WRITELN('Phibr>(1/2)*pi'); READLN; END;

       {transports dSx from one h, one T and one dh}


    S1T1H    := S1T1H    + (dS1CERC   *  pHT[i,j] * 0.01)  ;
    S2T1H    := S2T1H    + (dS2CERC   *  pHT[i,j] * 0.01)  ;
    S3T1H    := S3T1H    + (dS3CERC   *  pHT[i,j] * 0.01)  ;
    S1T1Hbar := S1T1Hbar + (dSbarCERC *  pHT[i,j] * 0.01)  ;

    SUMpHT_1H := SUMpHT_1H + pHT[i,j];


  END; {j} {transports SxH1T from one H, one T }

  S1_1H    := S1T1H    * year;
  S2_1H    := S2T1H    * year;
  S3_1H    := S3T1H    * year;
  S1_1Hbar := S1T1Hbar * year;

  S1CERC   := S1CERC   + S1_1H;
  S2CERC   := S2CERC   + S2_1H;
  S3CERC   := S3CERC   + S3_1H;
  SbarCERC := SbarCERC + S1_1Hbar;

  SUMpHT := SUMpHT + SUMpHT_1H;

  WRITELN(outputfile, ' Ho_sig = ',Ho_sig:4:2,'  dh = ':13,dh:4:2,
                                                ' SUMpHT_1H = ',SUMpHT_1H:5:3);
  WRITELN(outputfile,'S1_1H = ':10,(S1_1H*probability[k])/1000:6:3,
                                                        ' *10^3 m3/jaar');
  IF S2_1H <> 0 THEN
  BEGIN
    WRITE(outputfile,'S2_1H = ':10,(S2_1H*probability[k])/1000:6:3,
                                                        ' *10^3 m3/jaar');
    IF S3_1H <> 0 THEN
    BEGIN
      WRITELN(outputfile,'S3_1H = ':10,(S3_1H*probability[k])/1000:6:3,
                                                        ' *10^3 m3/jaar');
    END
    ELSE WRITELN(outputfile);
  END
  ELSE WRITELN(outputfile);

END;  {i}  {**** transports Sx from all H and all T ****}


WRITELN(SUMpHT:4:1);

FINISH :
```

```
  WriteOutputFile(SUMpHT,S1CERC,S2CERC,S3CERC,SbarCERC,alpha,phio,h0,h1,h2,
                  filename,dh,hbr,Phibr,year);

  WRITELN(outputfile,'=======================================================');
  CLOSE(outputfile);
END.
```

Appendix C Figures with results of volume computations

All groins at Norderney are numbered. There are two different types of numbering: with figures and with characters. For completeness all groins at the west side of Norderney are listed in the following . In this also the width (in m) of each groinfield is listed.
This width has been used to obtain the volumes per linear meter.

number	groins	width	number	groins	width	number	groins	width
1	J-I		11	I-A	80	21	M1-N1	170
2	I-H	235	12	A-D1	185	22	N1-O1	160
3	H-G	220	13	D1-E1	170	23	O1-P1	160
4	G-F	190	14	E1-F1	170	24	P1-Q1	150
5	F-E	195	15	F1-G1	150	25	Q1-R1	170
6	E-D	200	16	G1-H1	150	26	R1-S1	165
7	D-C	190	17	H1-J1	155	27	S1-T1	165
8	C-II	80	18	J1-K1	155	28	T1-U1	170
9	II-B	85	19	K1-L1	140	29	U1-V1	180
10	B-I	85	20	L1-M1	170	30	V1-W1	180

The width is given in meter. The position of the groins are shown in Figure 2 in chapter 1.

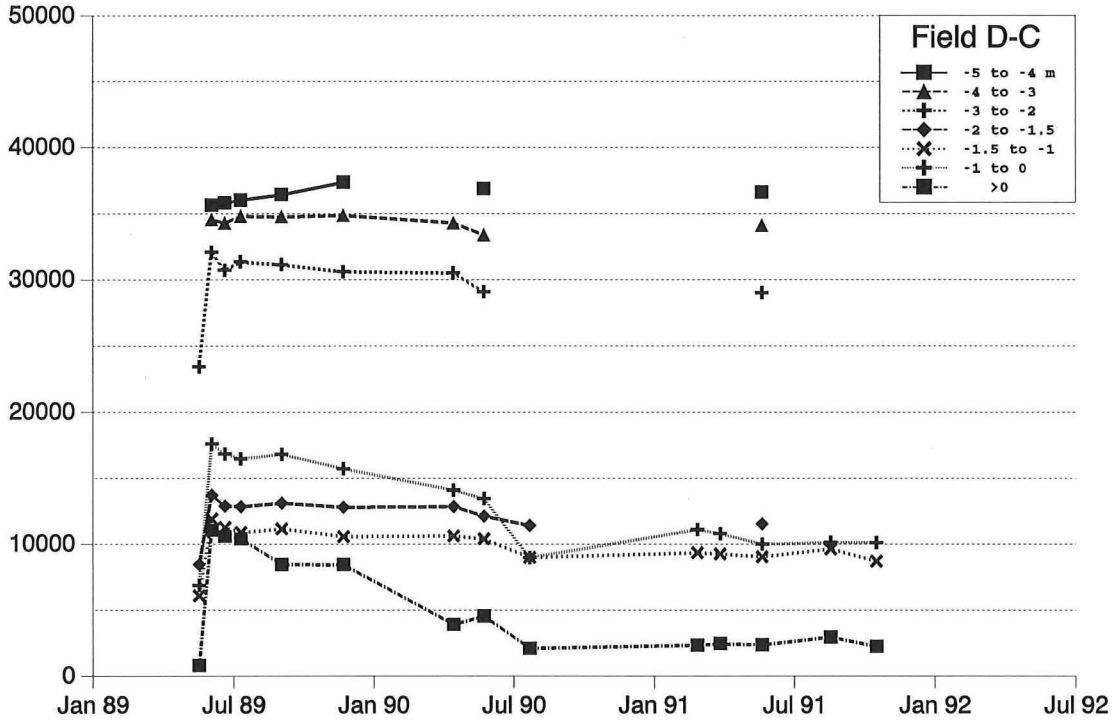

Figure 1 *Volumes between the levels for field D-C.*

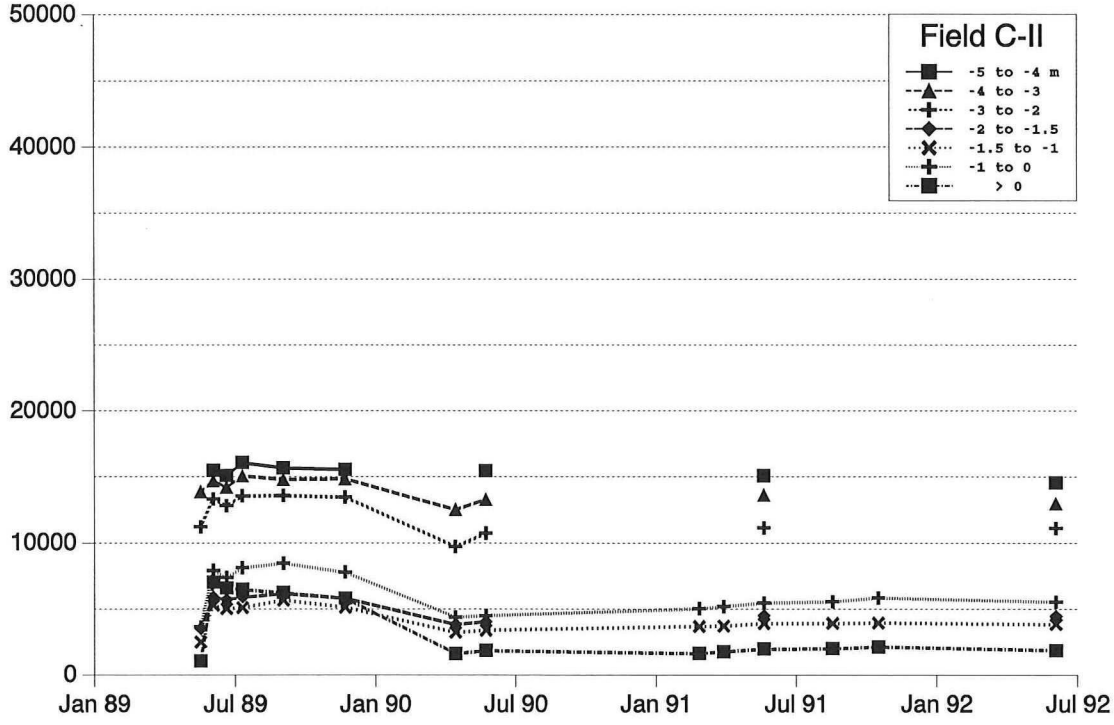

Figure 2 *Volumes between the levels for field C-ZbII.*

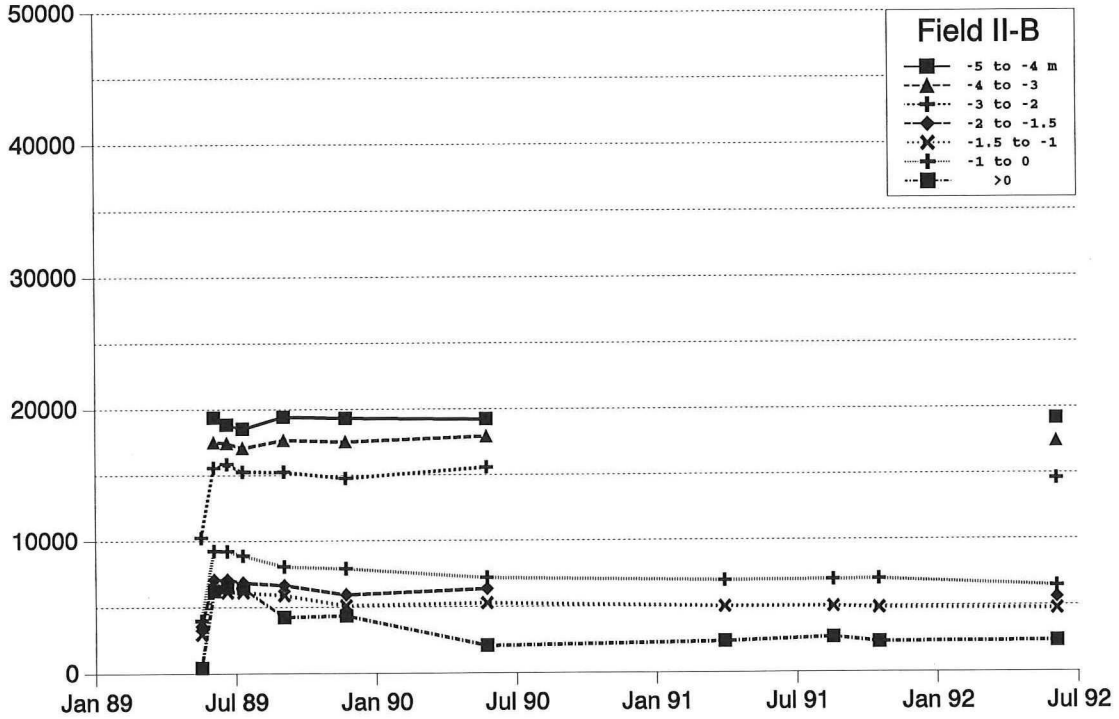

Figure 3 *Volumes between the levels for field ZbII-B.*

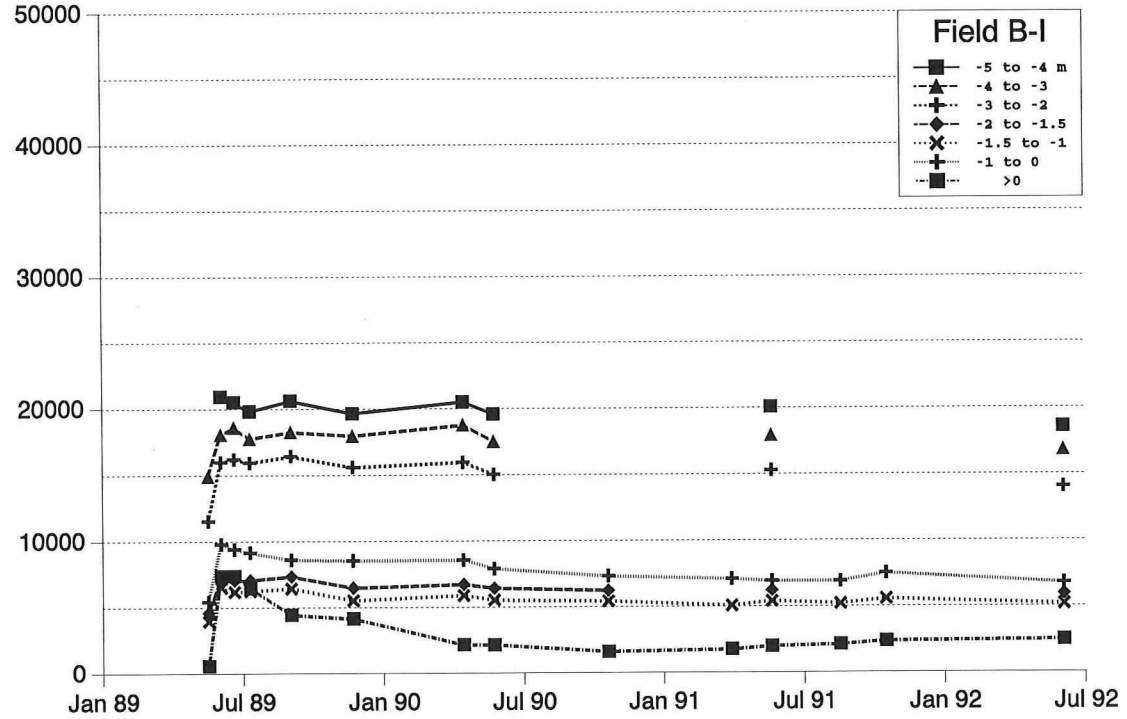

Figure 4 *Volumes between the levels for field B-ZbI.*

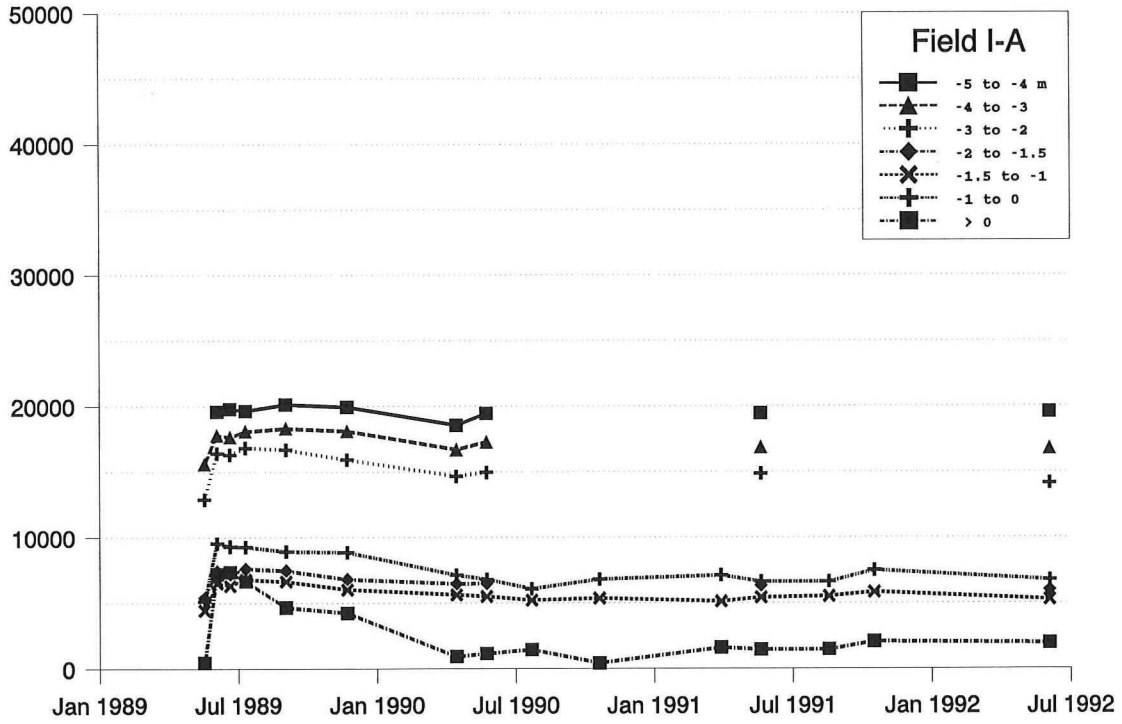

Figure 5 *Volumes between the levels for field ZbI-A.*

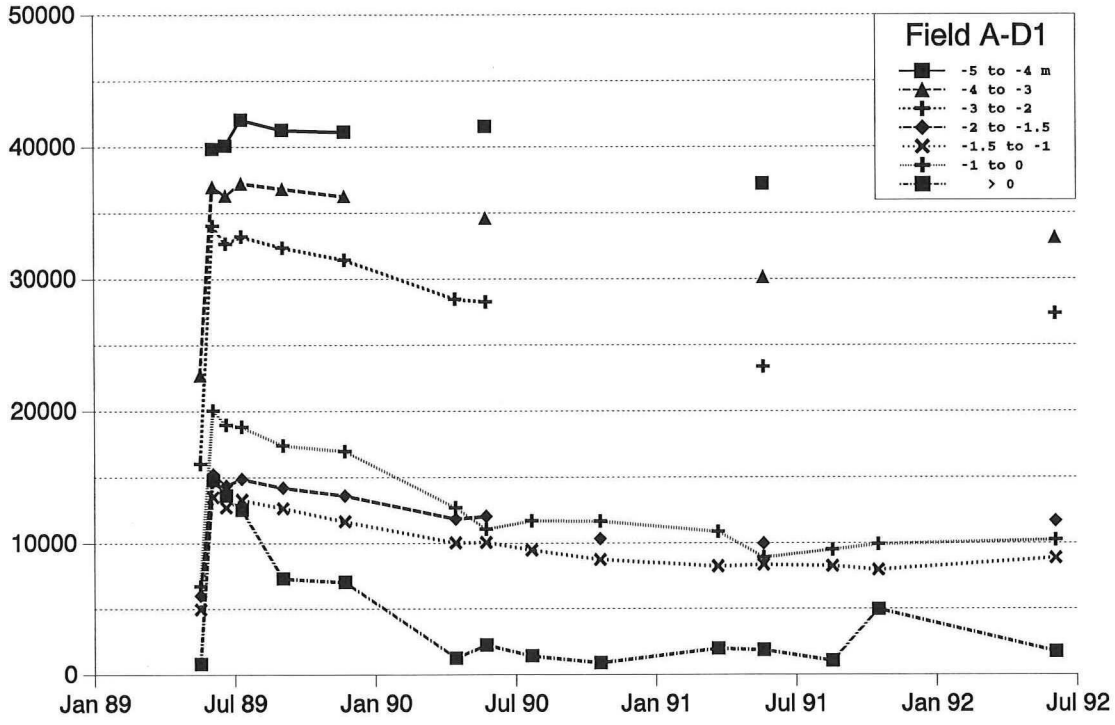

Figure 6 *Volumes between the levels for field A-D1.*

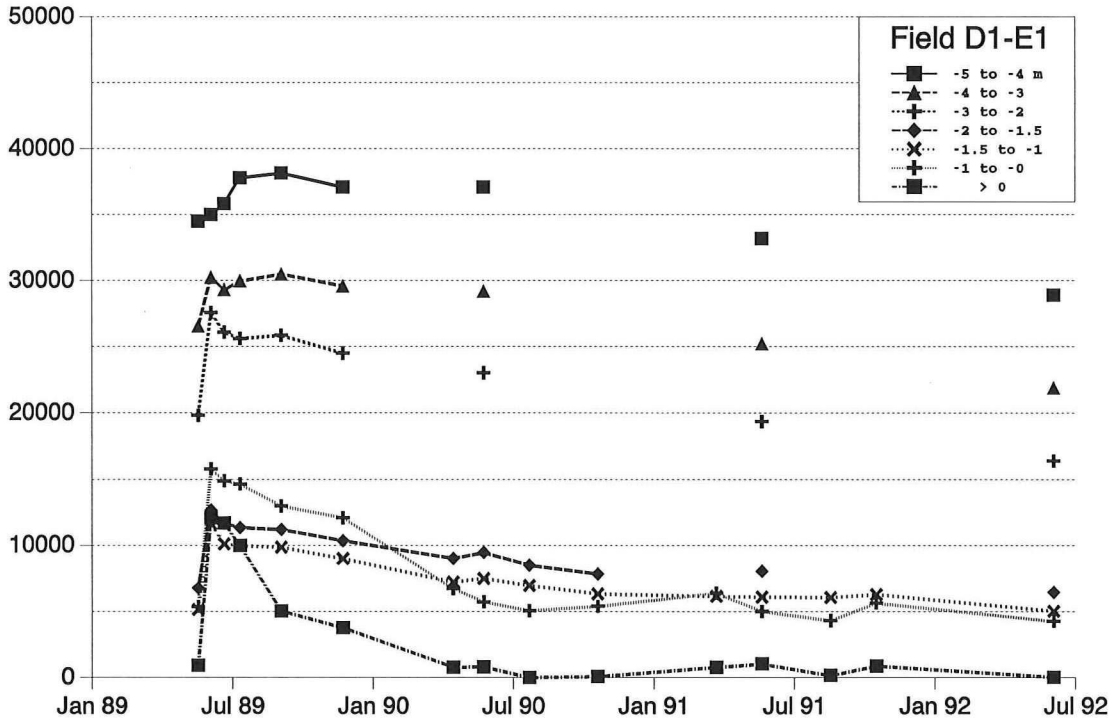

Figure 7 *Volumes between the levels for field D1-E1.*

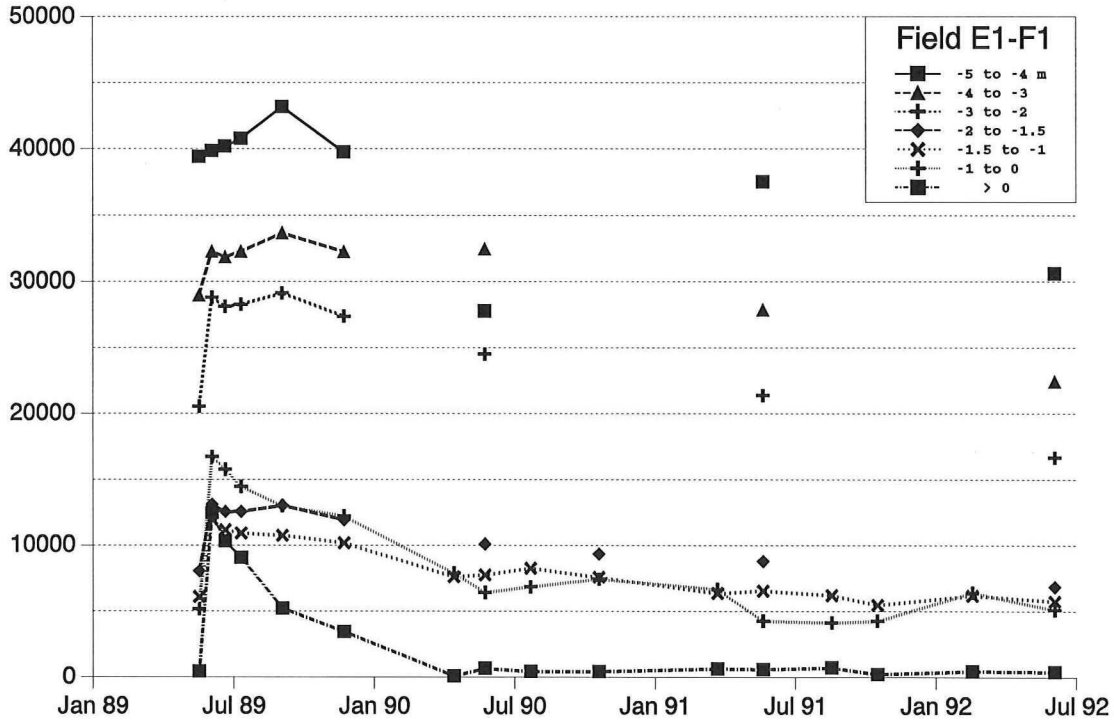

Figure 8 *Volumes between the levels for field E1-F1.*

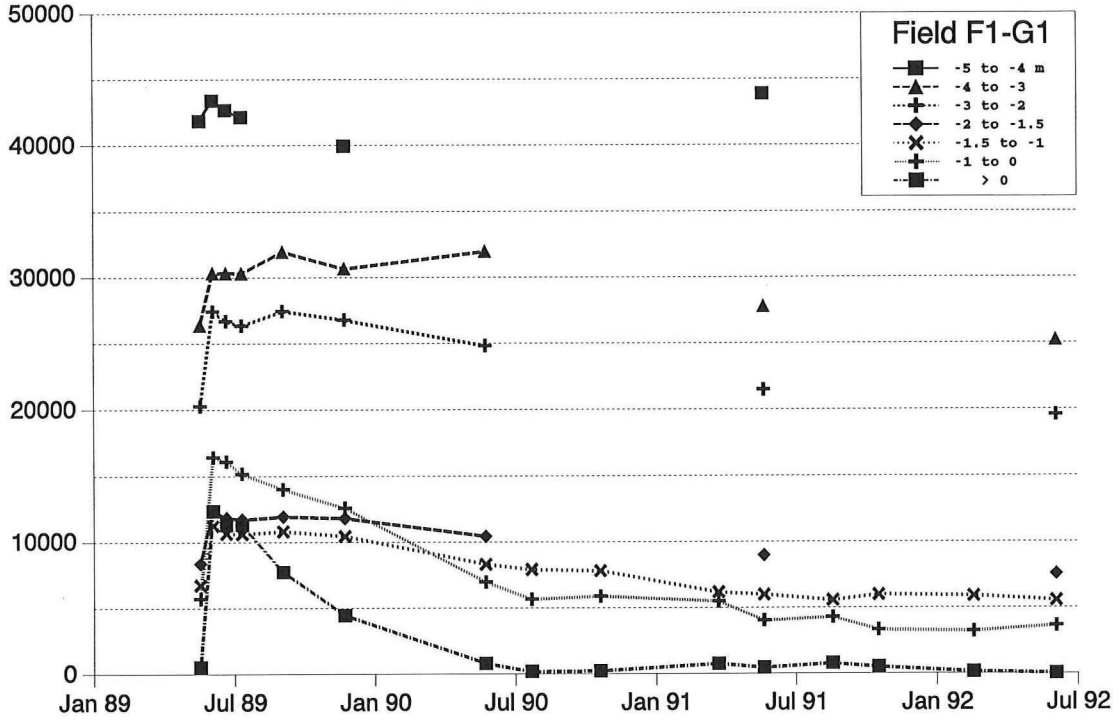

Figure 9 *Volumes between the levels for field F1-G1.*

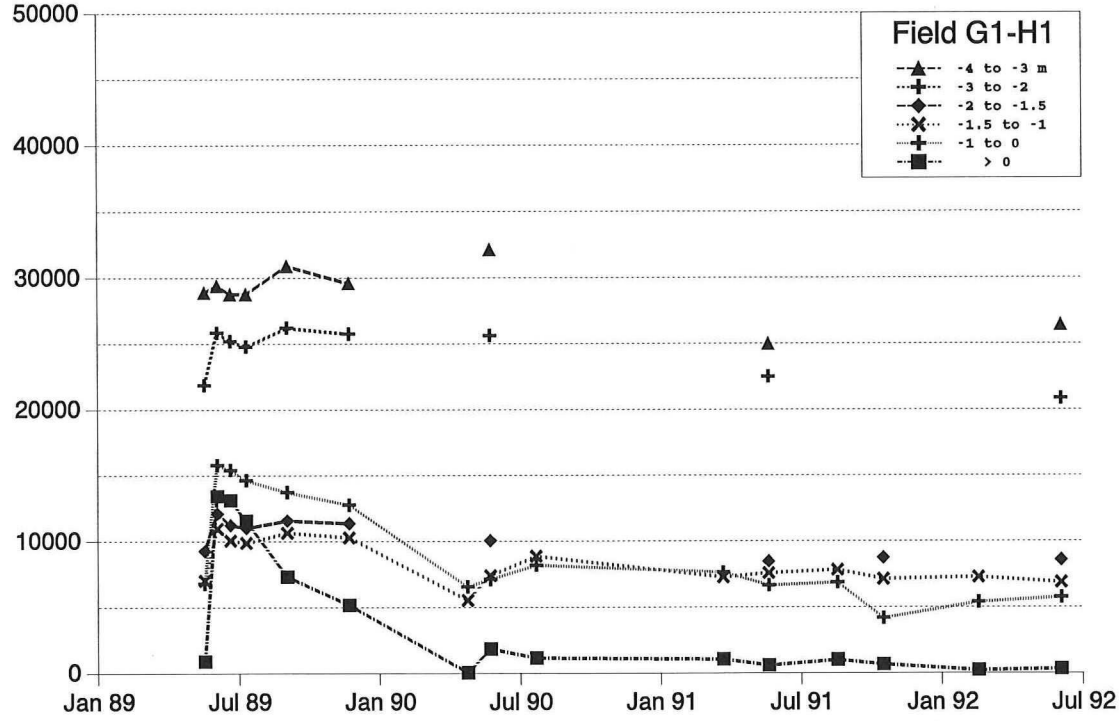

Figure 10 *Volumes between the levels for field G1-H1.*

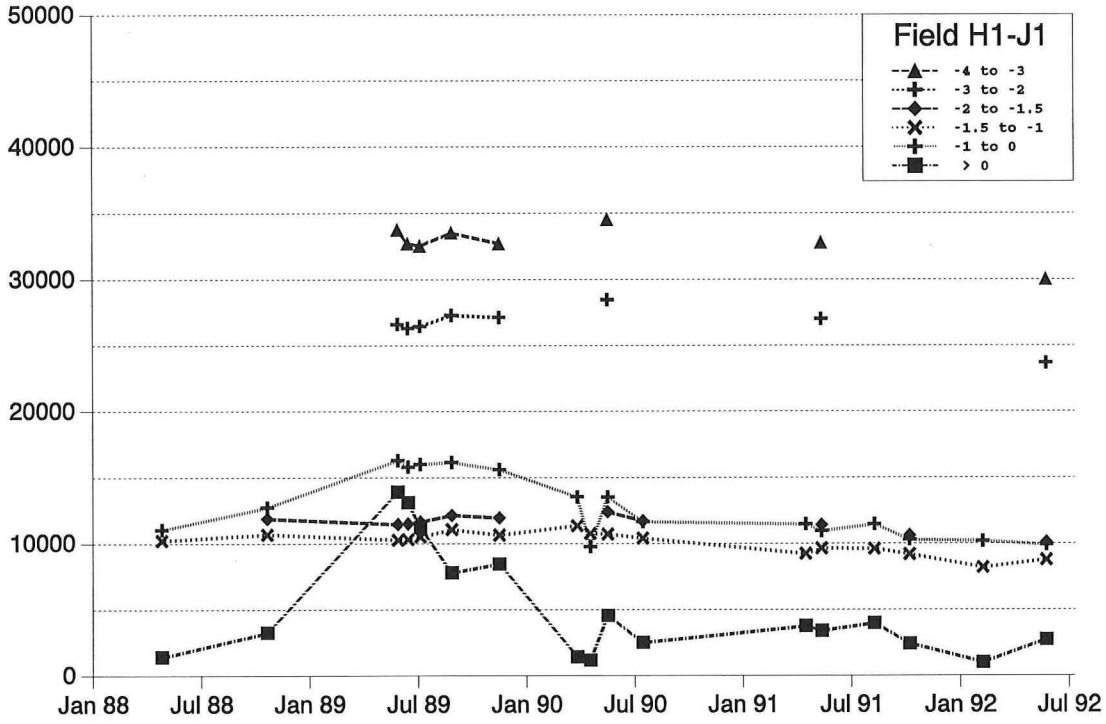

Figure 11 *Volumes between the levels for field H1-J1.*

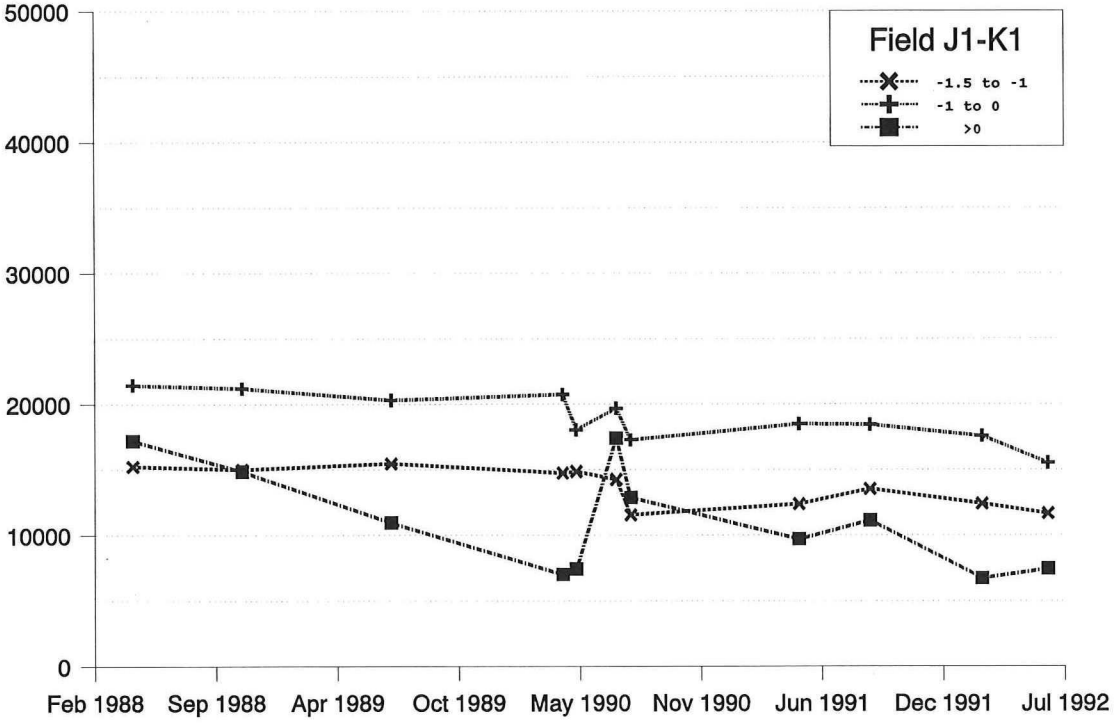

Figure 12 *Volumes between the levels for field J1-K1.*

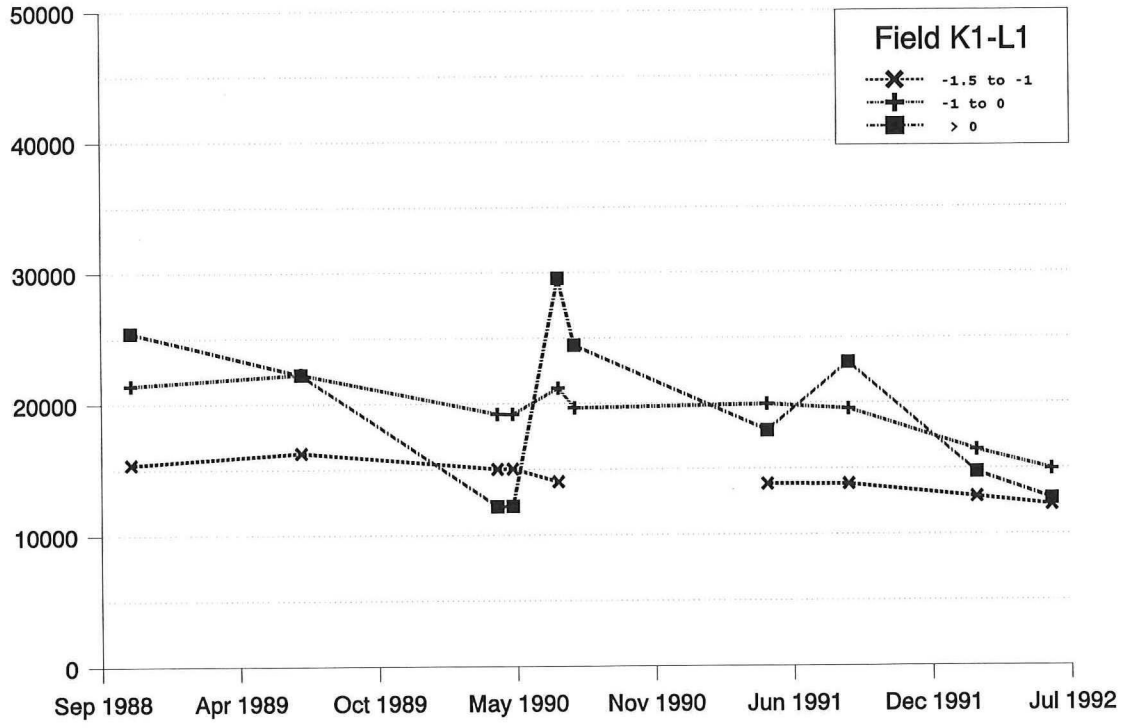

Figure 13 *Volumes between the levels for field K1-L1.*

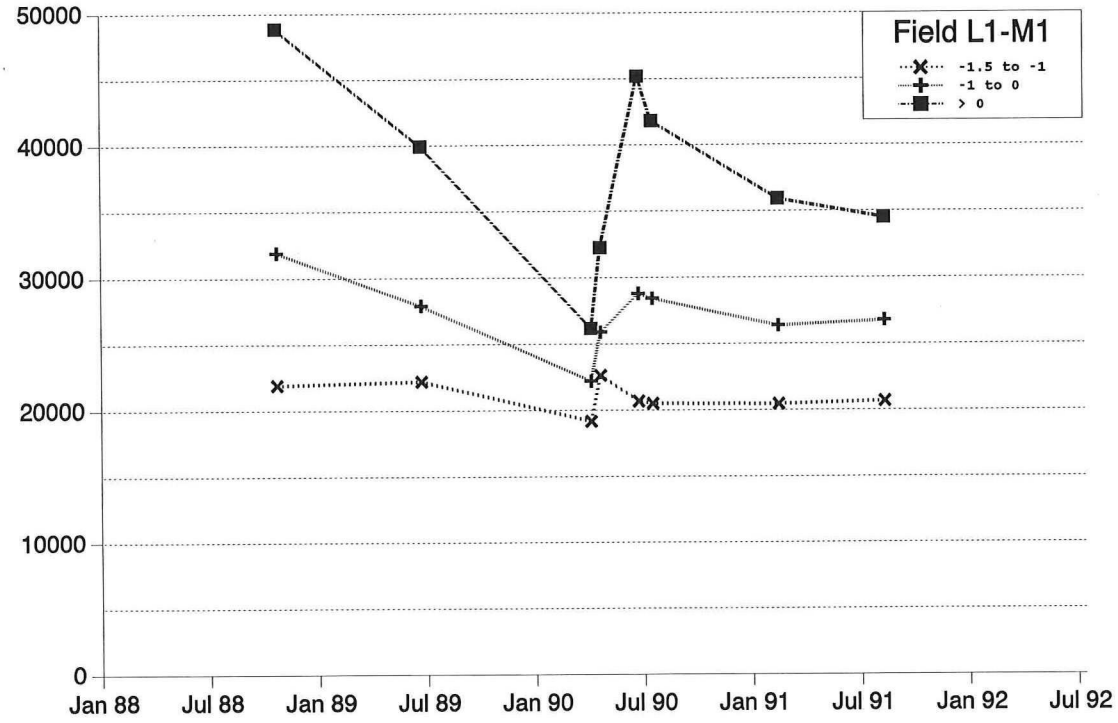

Figure 14 *Volumes between the levels for field L1-M1.*

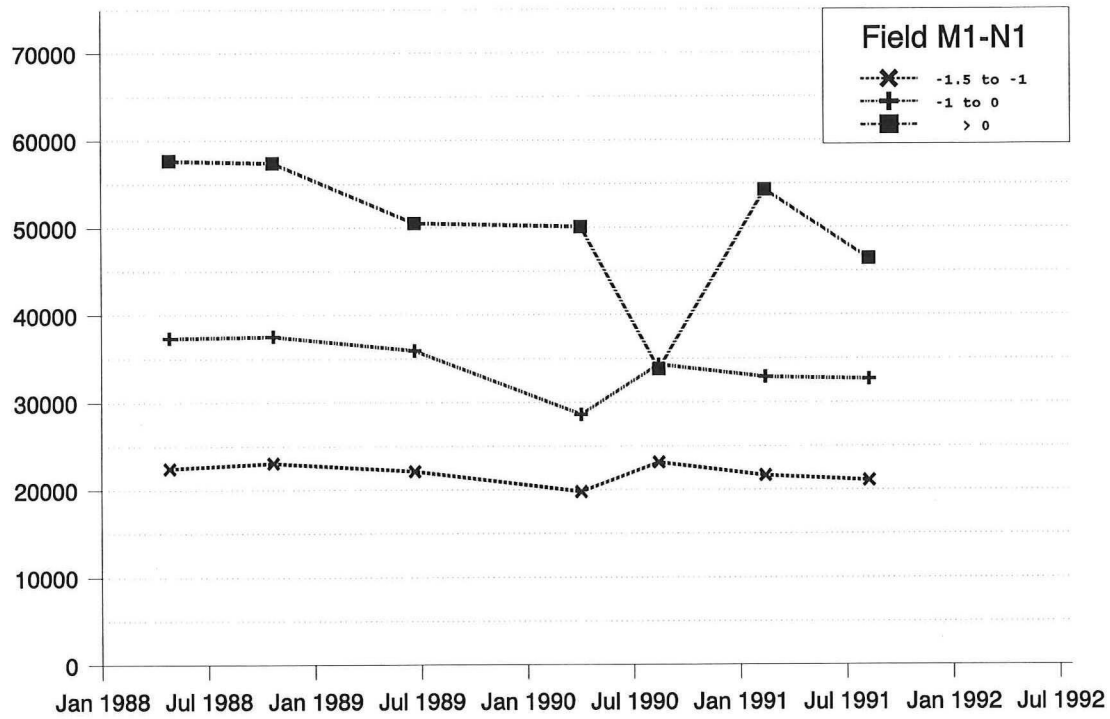

Figure 15 *Volumes between the levels for field M1-N1.*

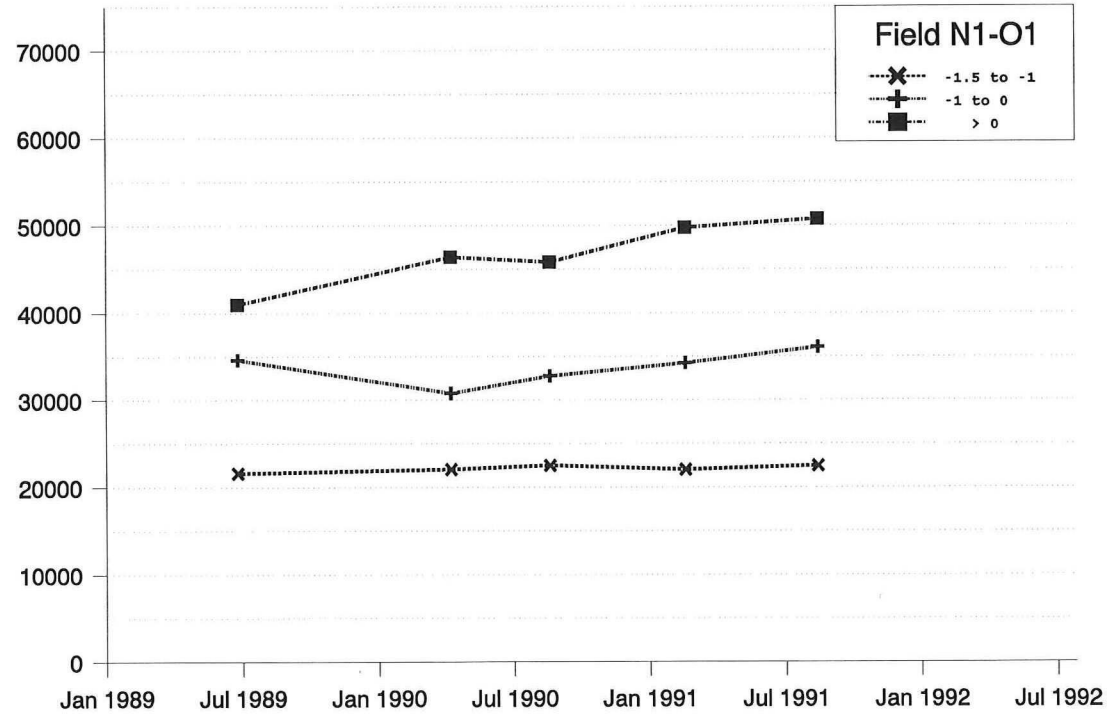

Figure 16 *Volumes between the levels for field N1-O1.*

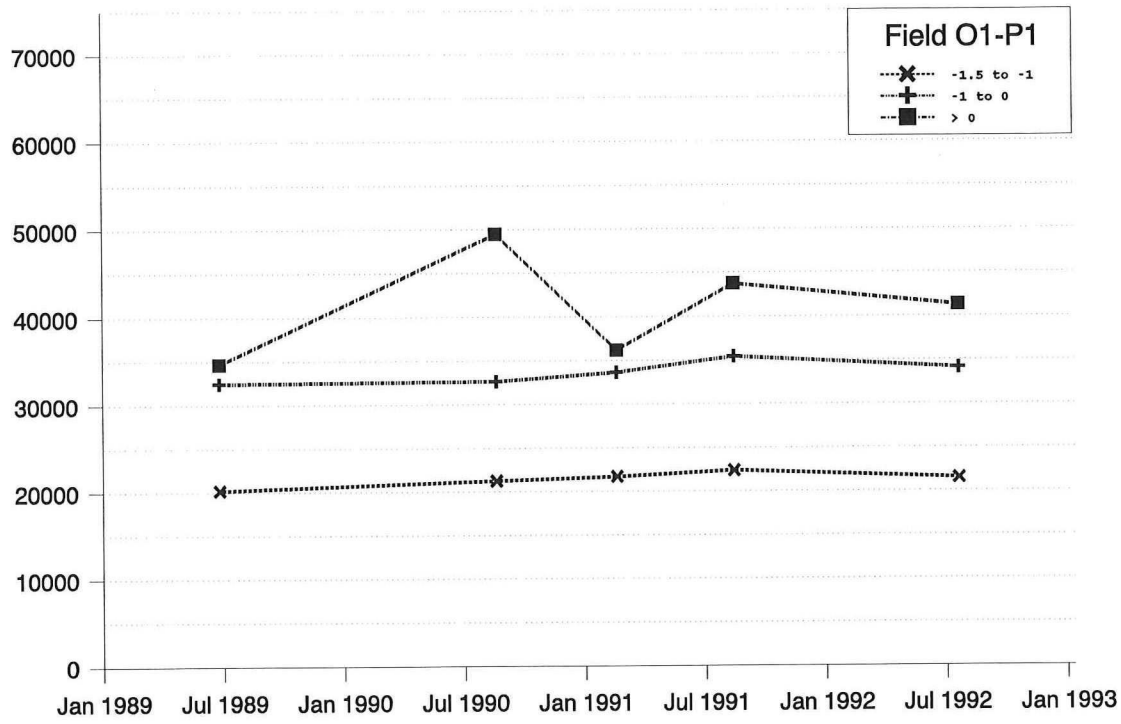

Figure 17 *Volumes between the levels for field O1-P1.*

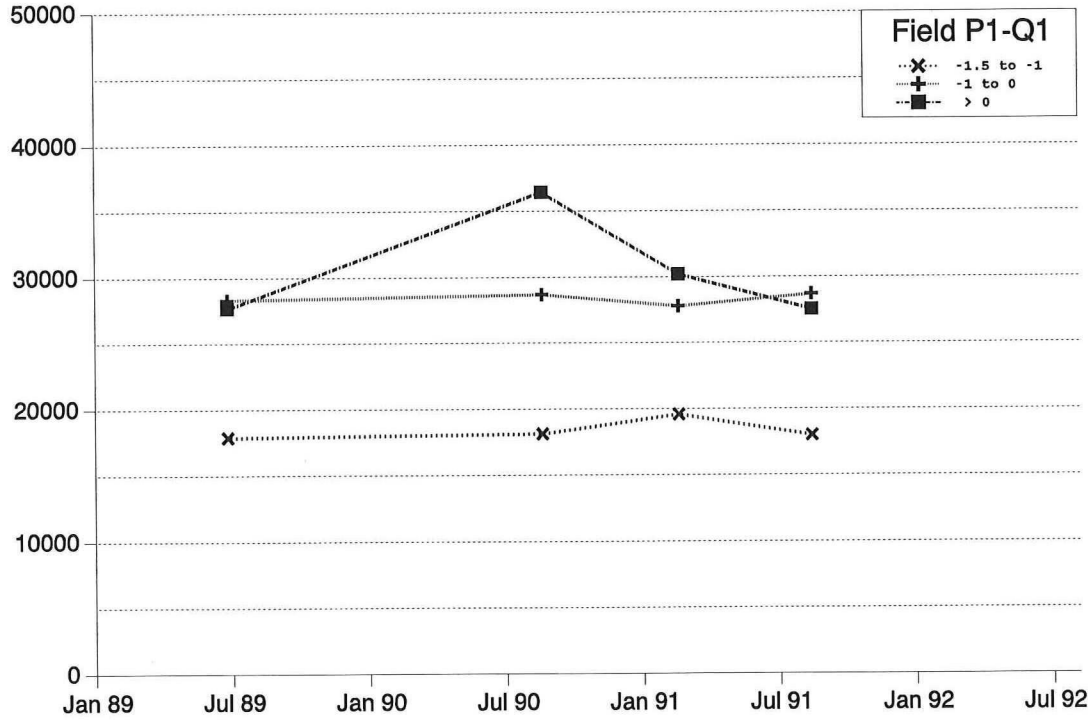

Figure 18 *Volumes between the levels for field P1-Q1.*

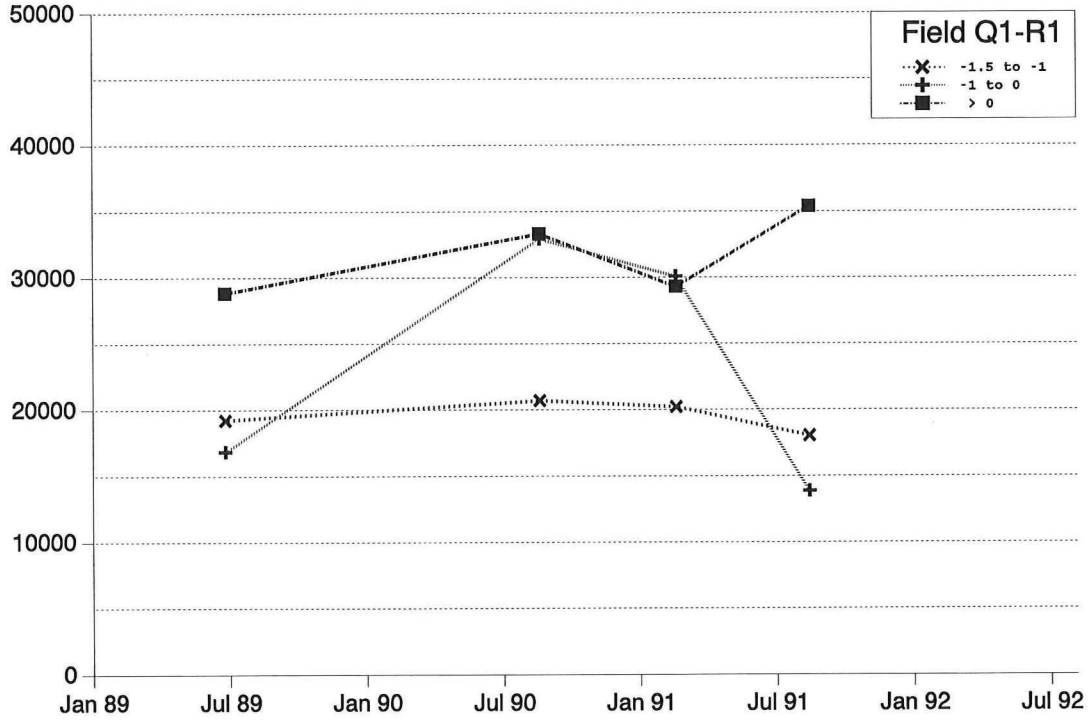

Figure 19 *Volumes between the levels for field Q1-R1.*

The volumes above the levels for groin D to groin R1.

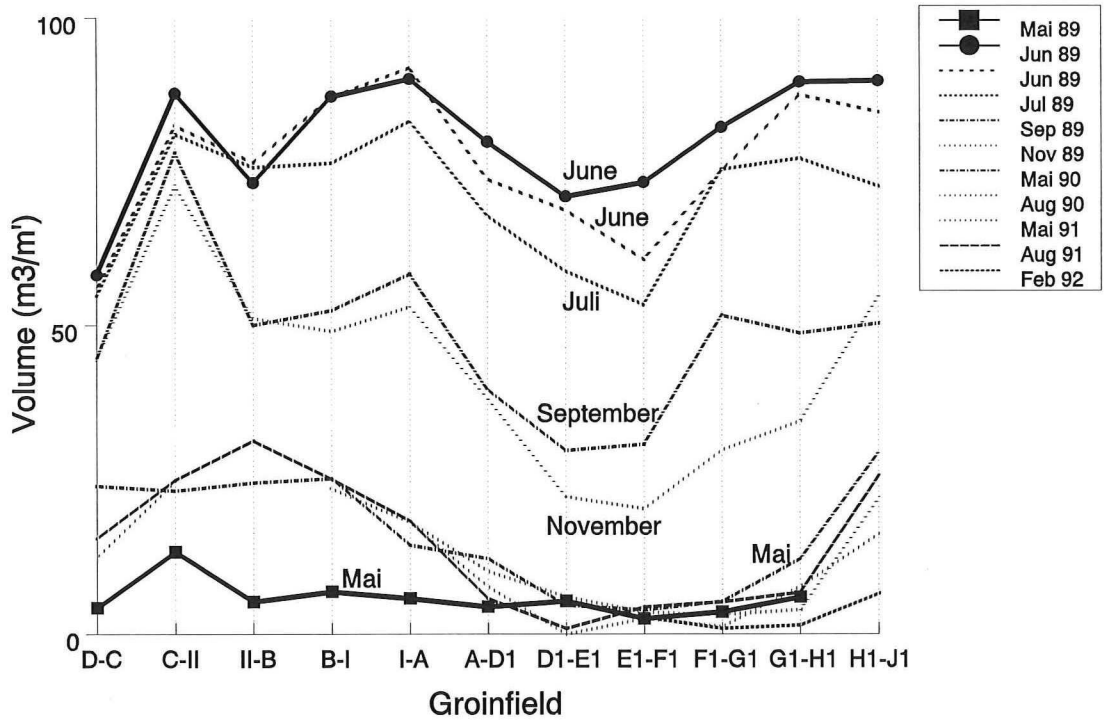

Figure 20 *Volumes above NN+0m, between may 1989 and feb 1992.*

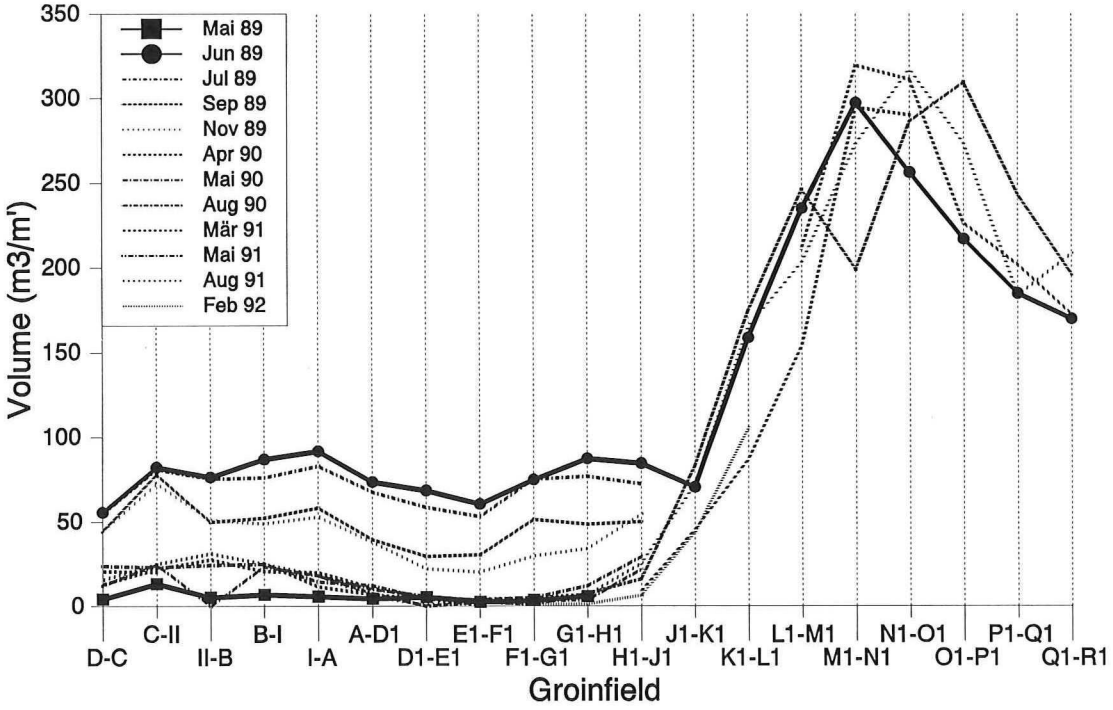

Figure 21 *Volumes above NN-0m, between mei 1989 and feb 1992.*

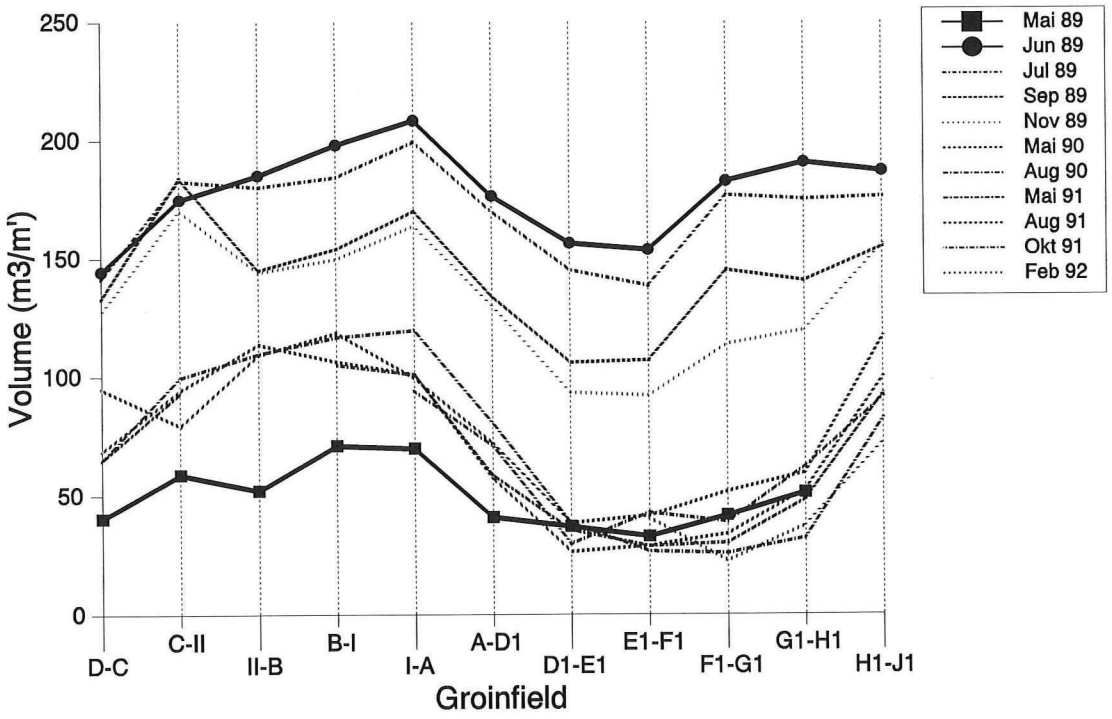

Figure 22 *Volumes above NN-1m, between may 1989 and feb 1992.*

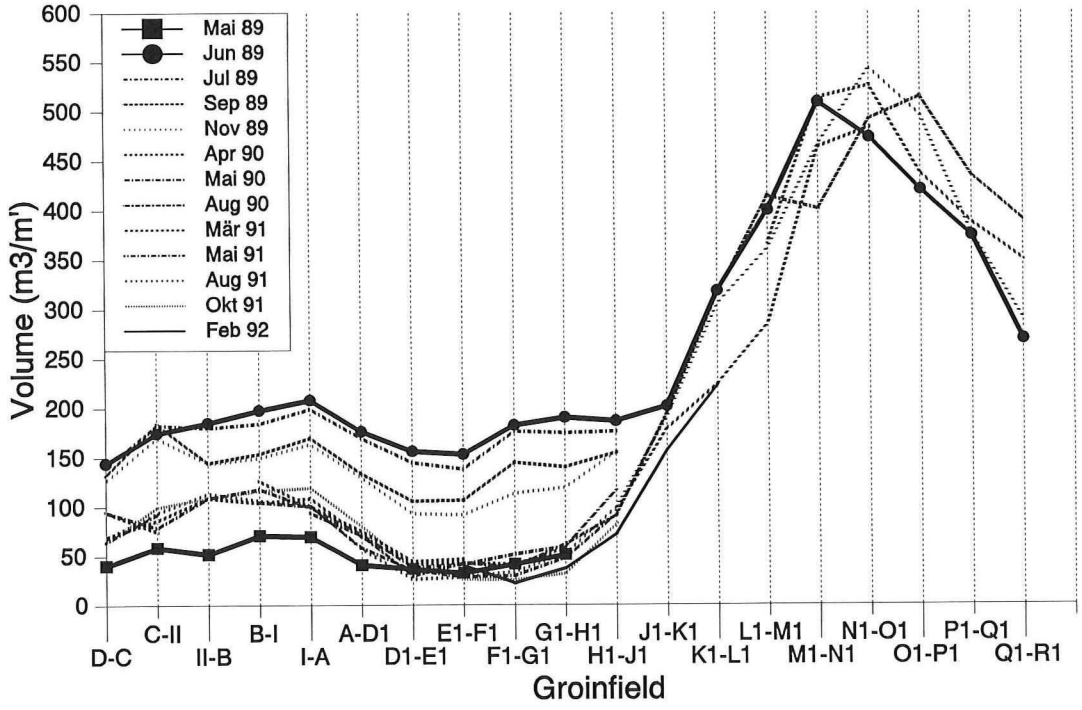

Figure 23 *Volumes above NN-1m, between may 1989 and feb 1992.*

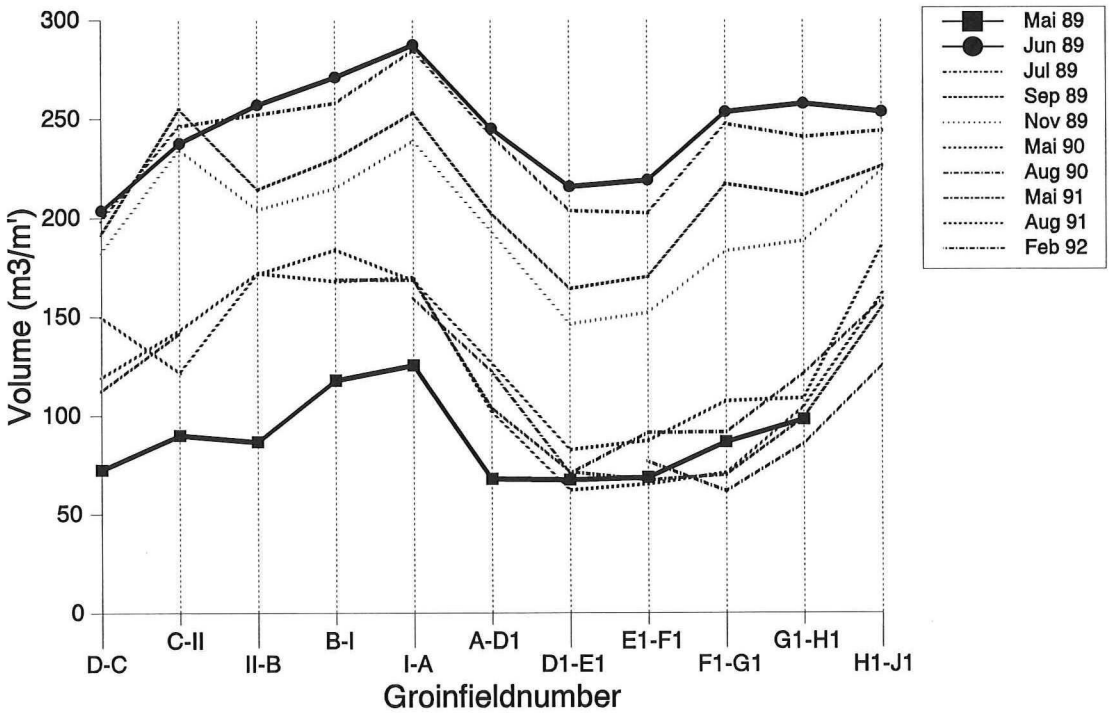

Figure 24 *Volumes above NN-1.5m, between may 1989 and feb 1992.*

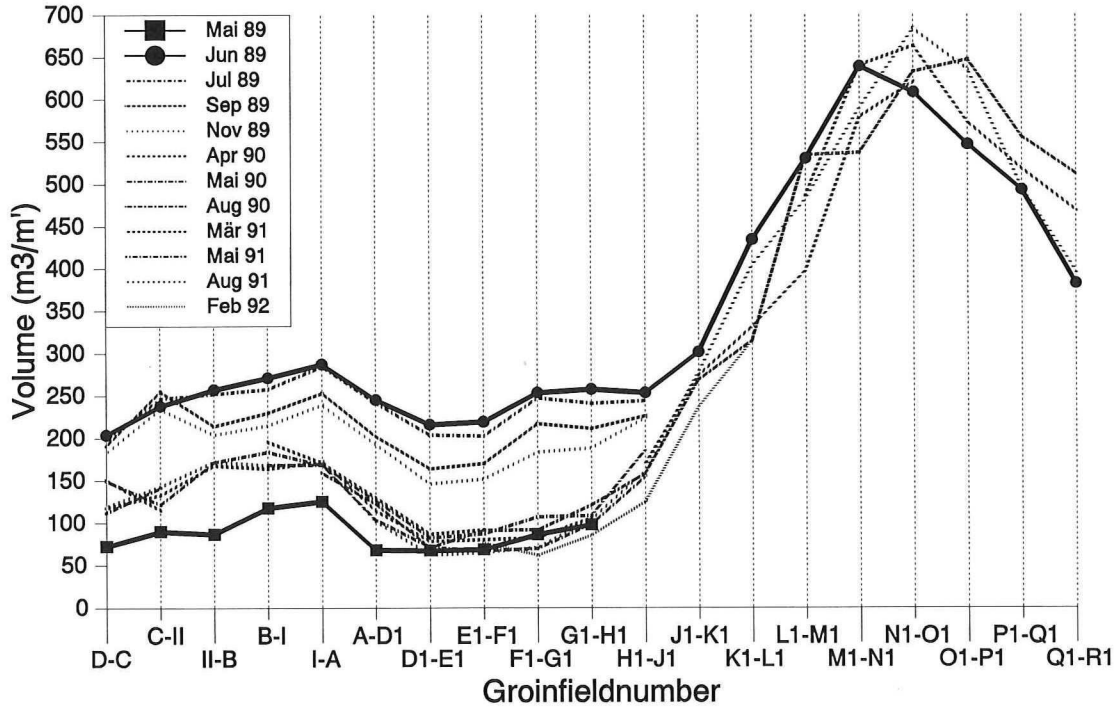

Figure 25 *Volumes above NN-1.5m, between may 1989 and feb 1992.*

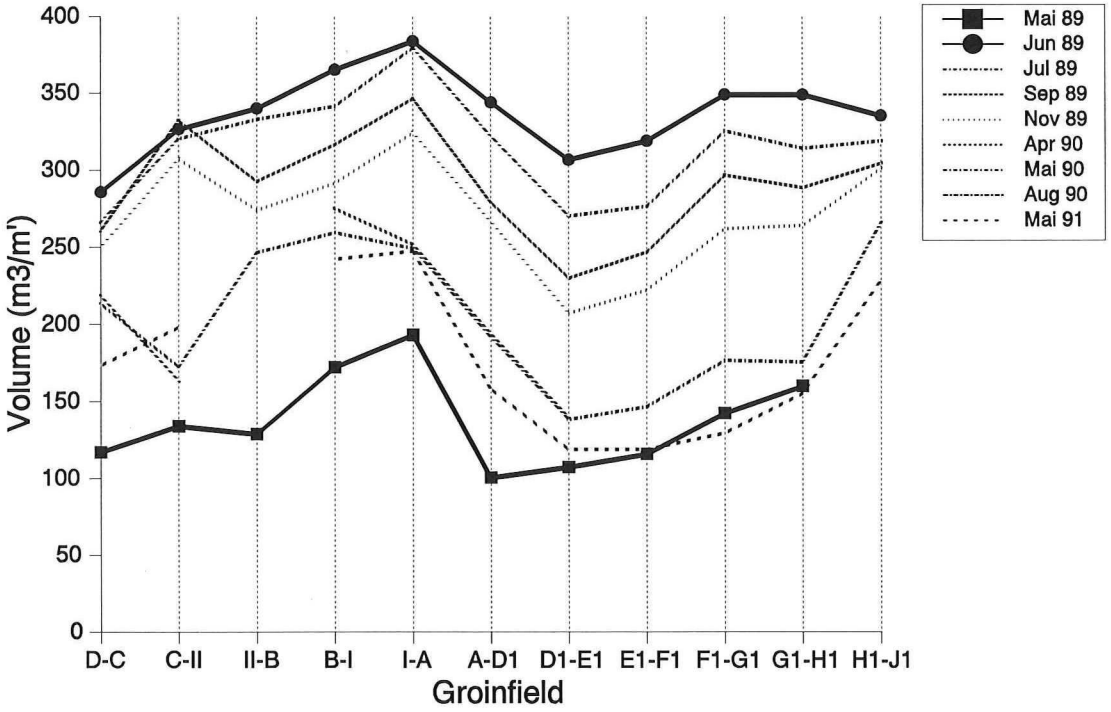

Figure 26 *Volumes above NN-2m, between may 1989 and may 1991.*

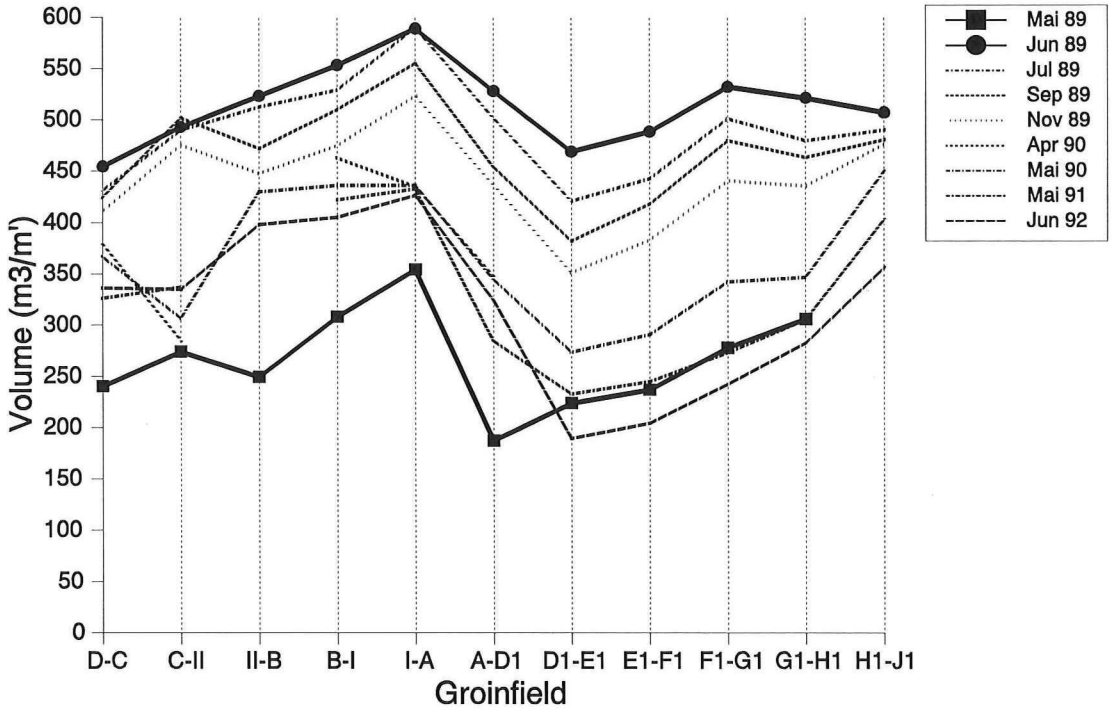

Figure 27 *Volumes above NN-3m, between may 1989 and feb 1991.*

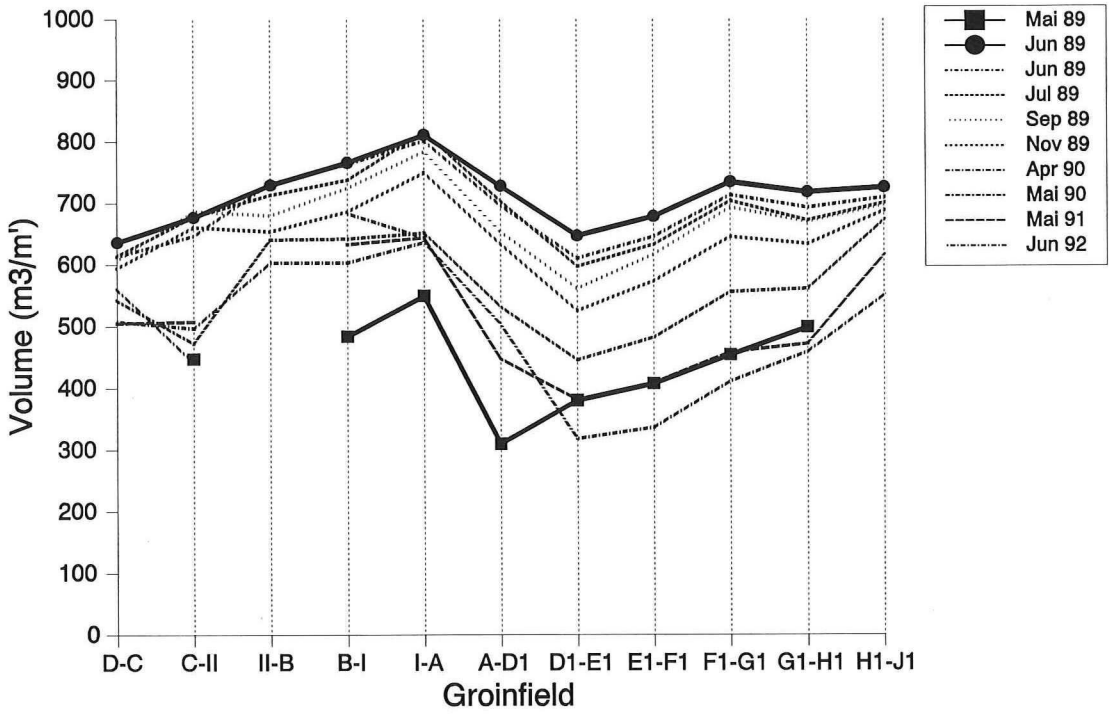

Figure 28 *Volumes above NN-4m, between may 1989 and jun 1992.*

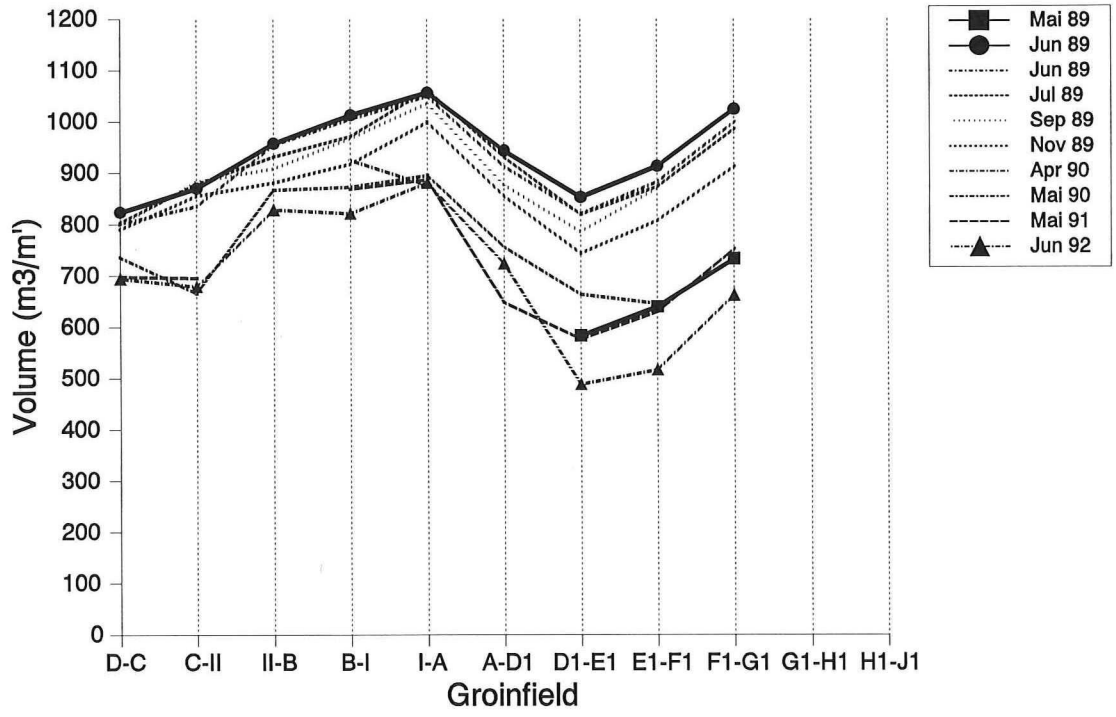

Figure 29 *Volumes above NN-5m, between may 1989 and jun 1992.*

Volumes between the levels pro meter for groin D to R1.

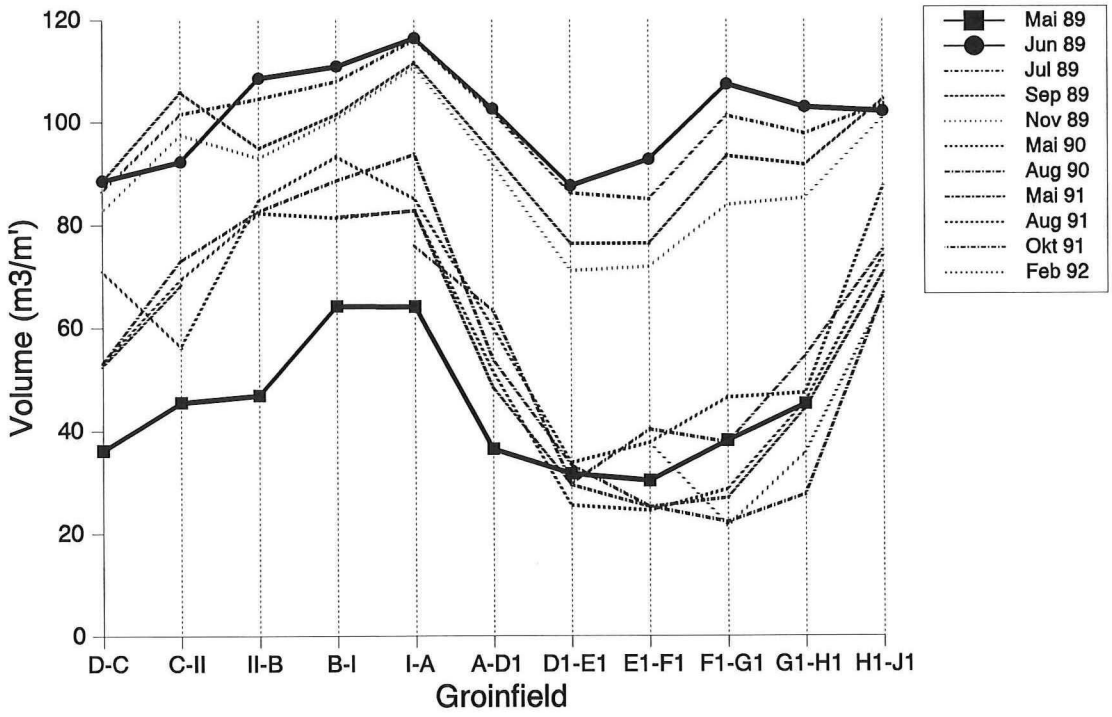

Figure 30 *Volumes between NN+0m and NN-1m.*

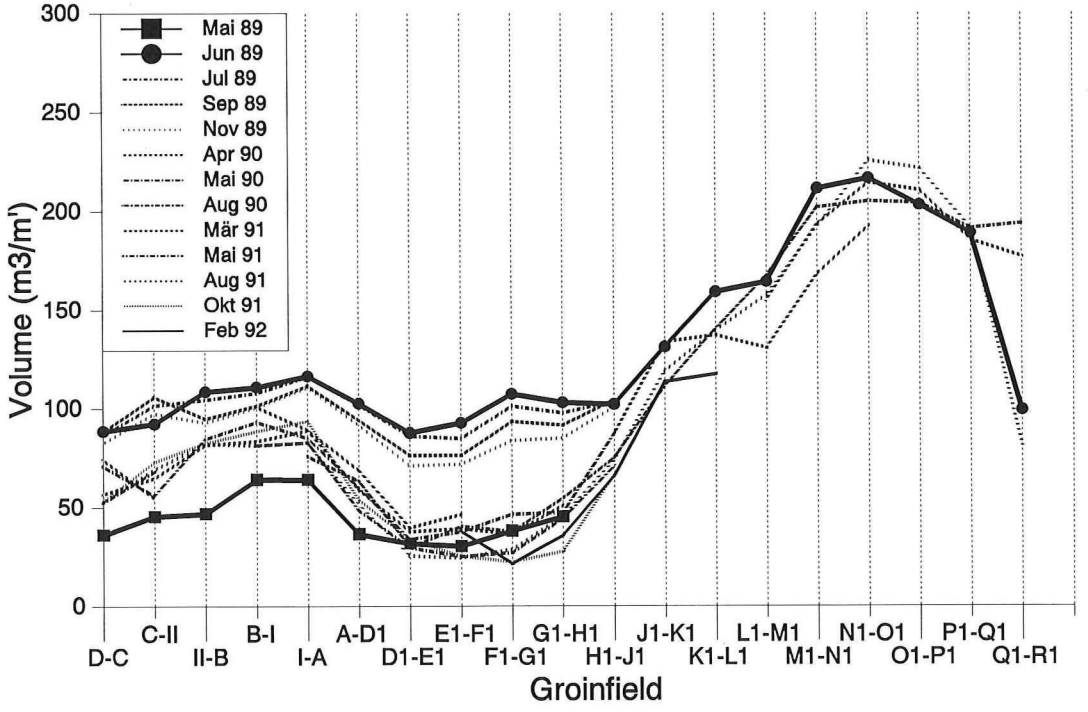

Figure 31 *Volumes between NN+0m and NN-1m.*

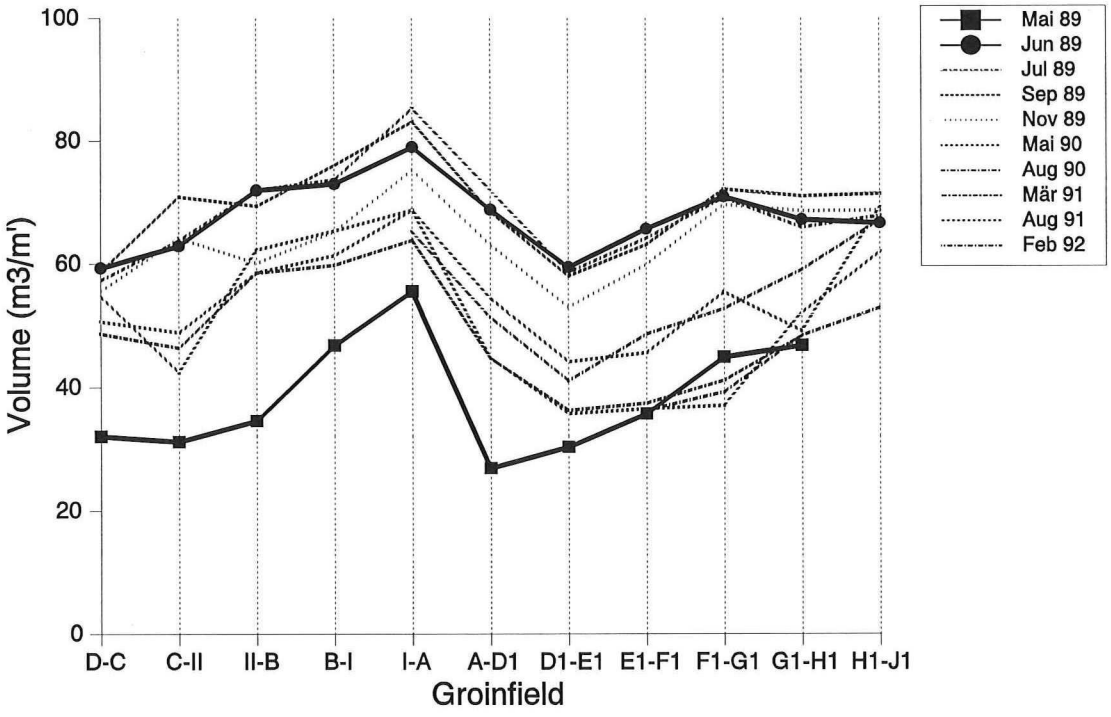

Figure 32 *Volumes between NN-1m and NN-1.5m.*

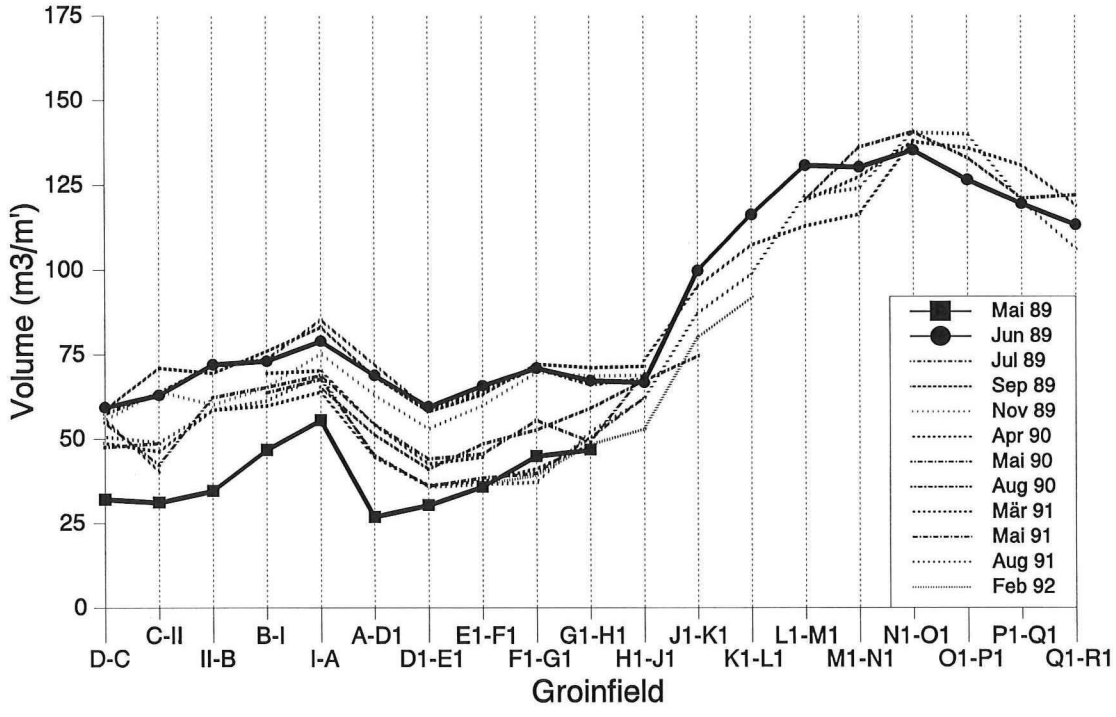

Figure 33 *Volumes between NN-1m and NN-1.5m.*

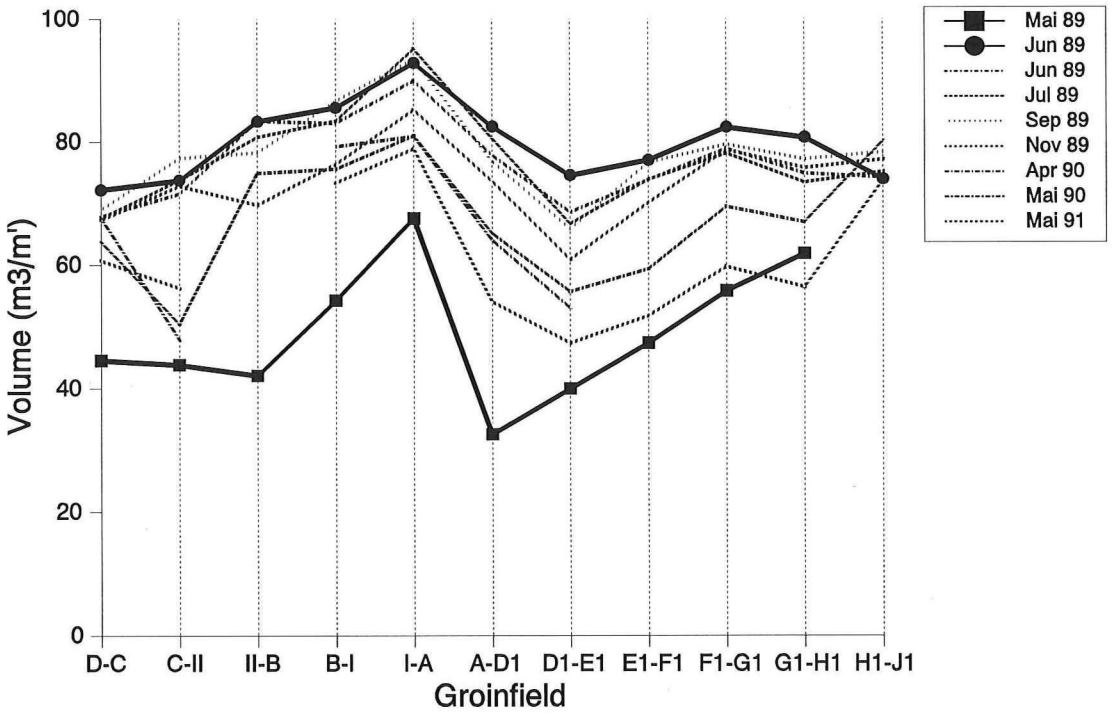

Figure 34 *Volumes between NN-1.5m and NN-2m.*

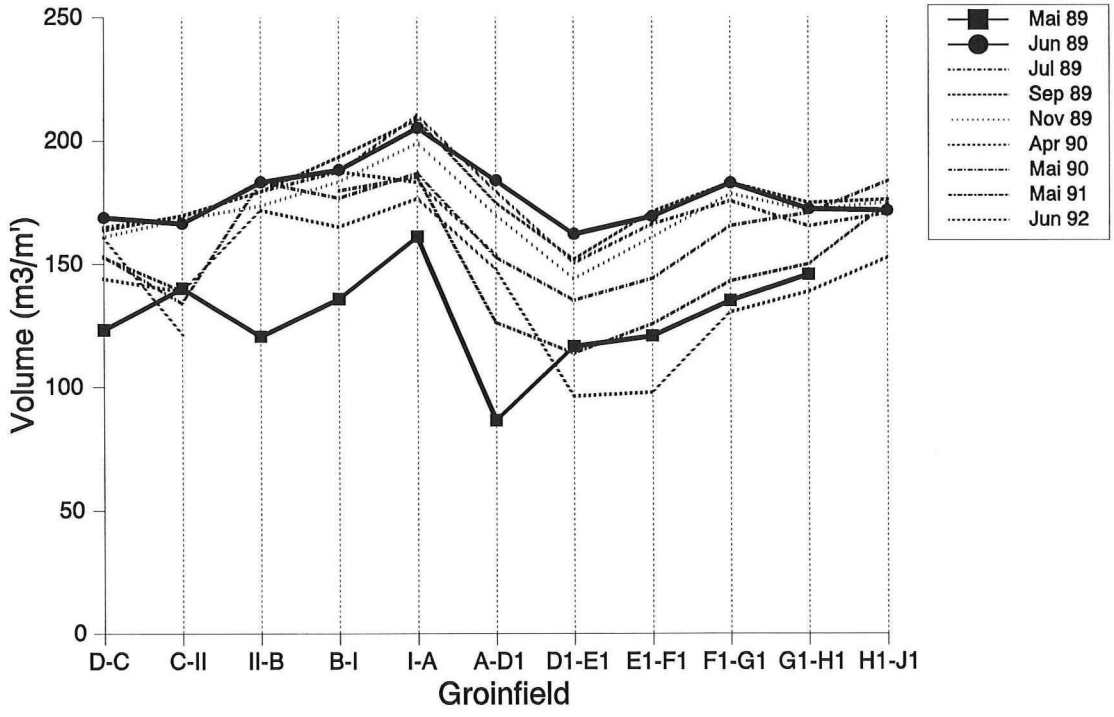

Figure 35 *Volumes between NN-2m and NN-3m.*

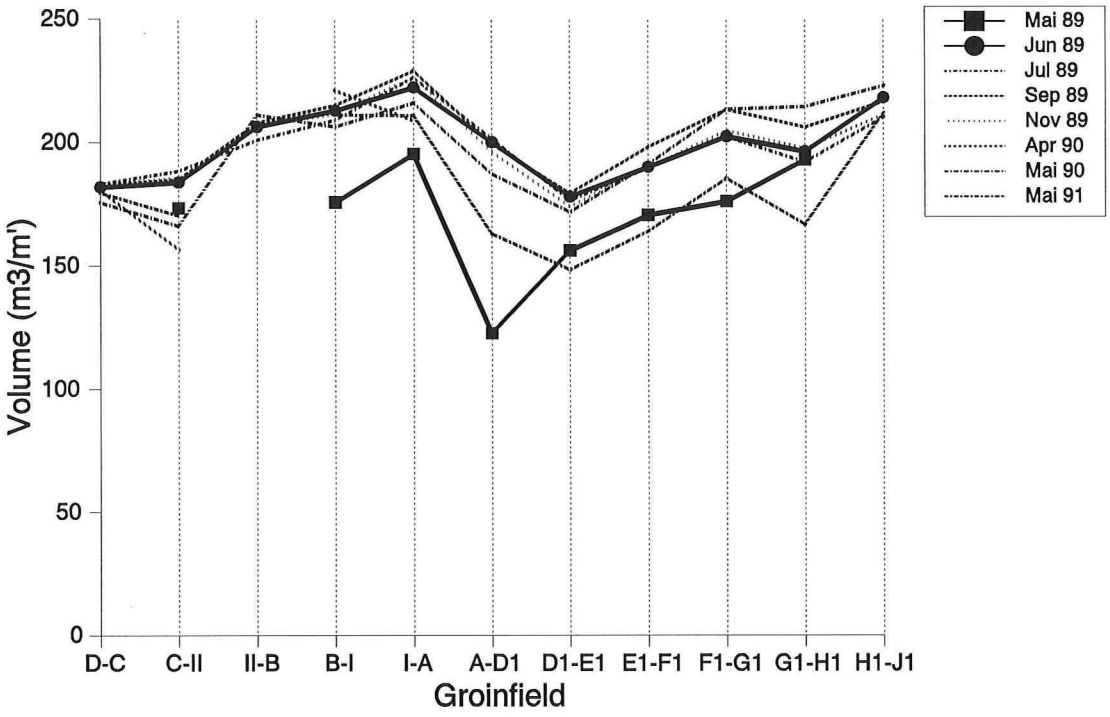

Figure 36 *Volumes between NN-3m and NN-4m.*

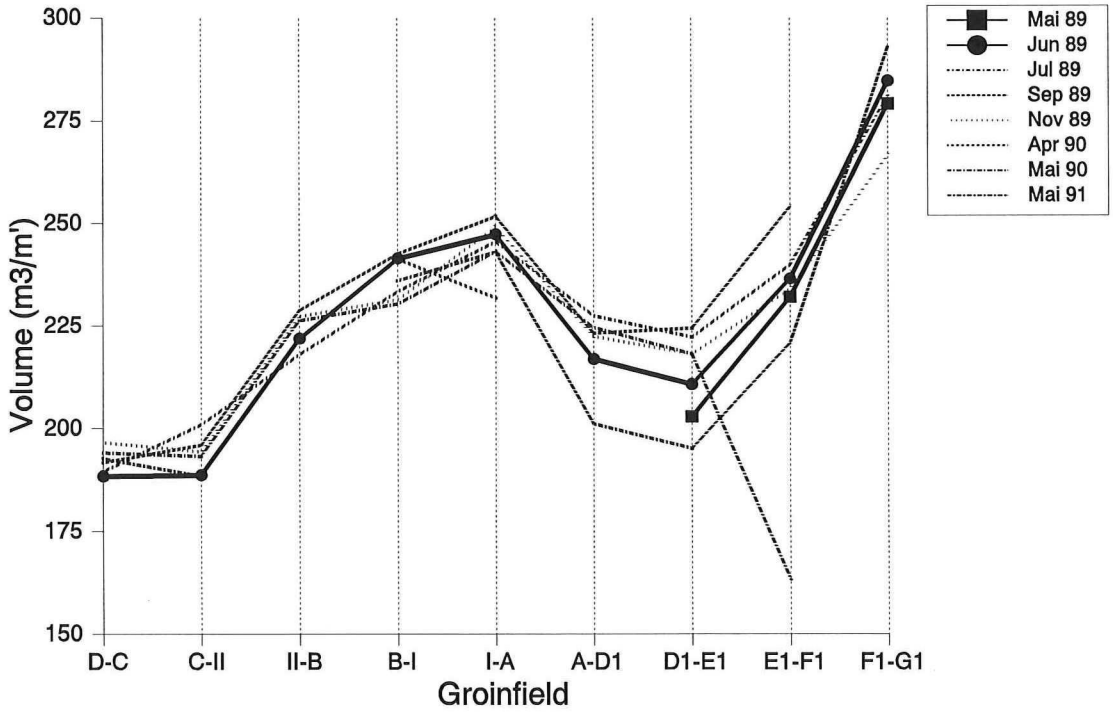

Figure 37 *Volumes between NN-4m and NN-5m.*

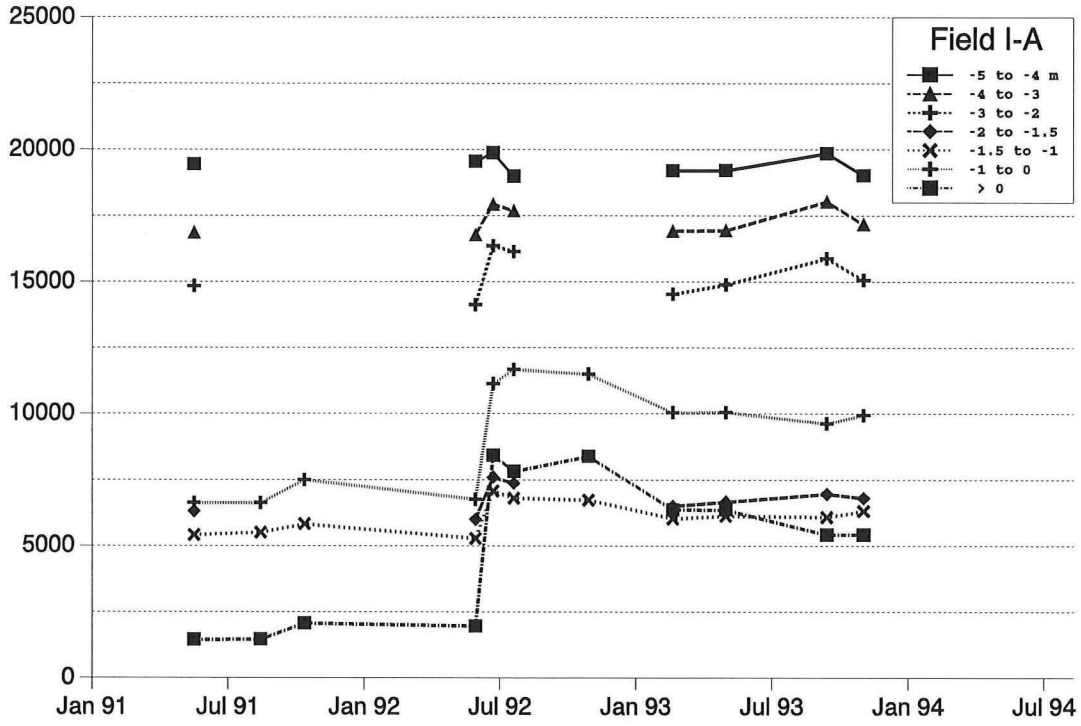

Figure 38 *Volumes between the levels for field ZbI-A*

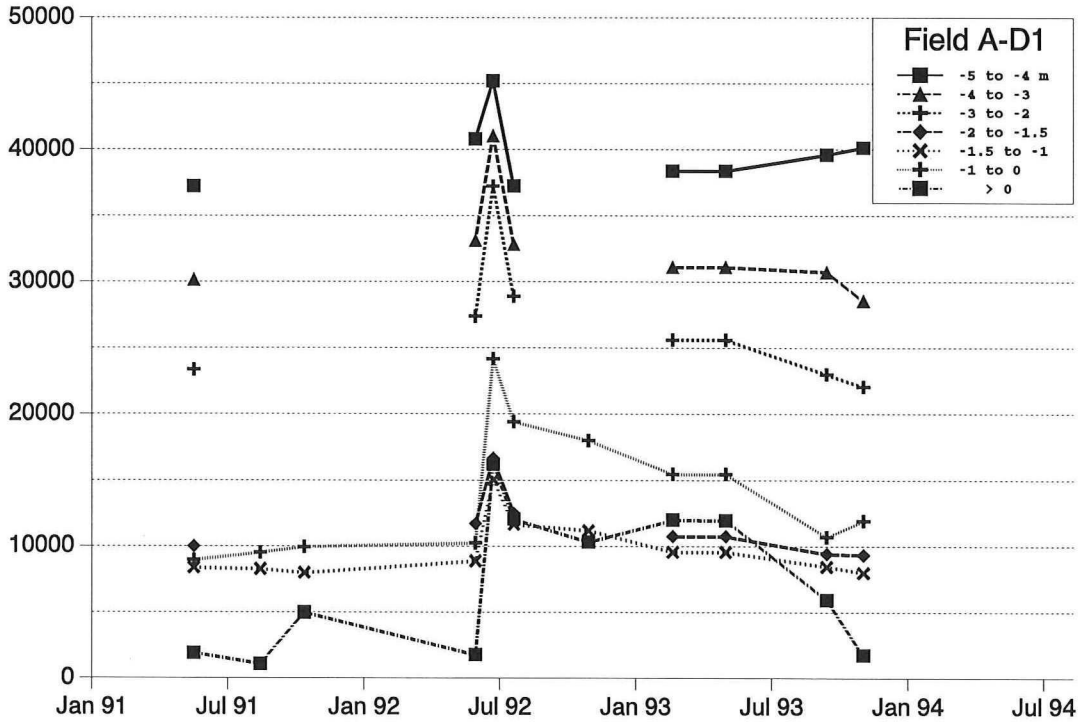

Figure 39 *Volumes between the levels for field A-D1*

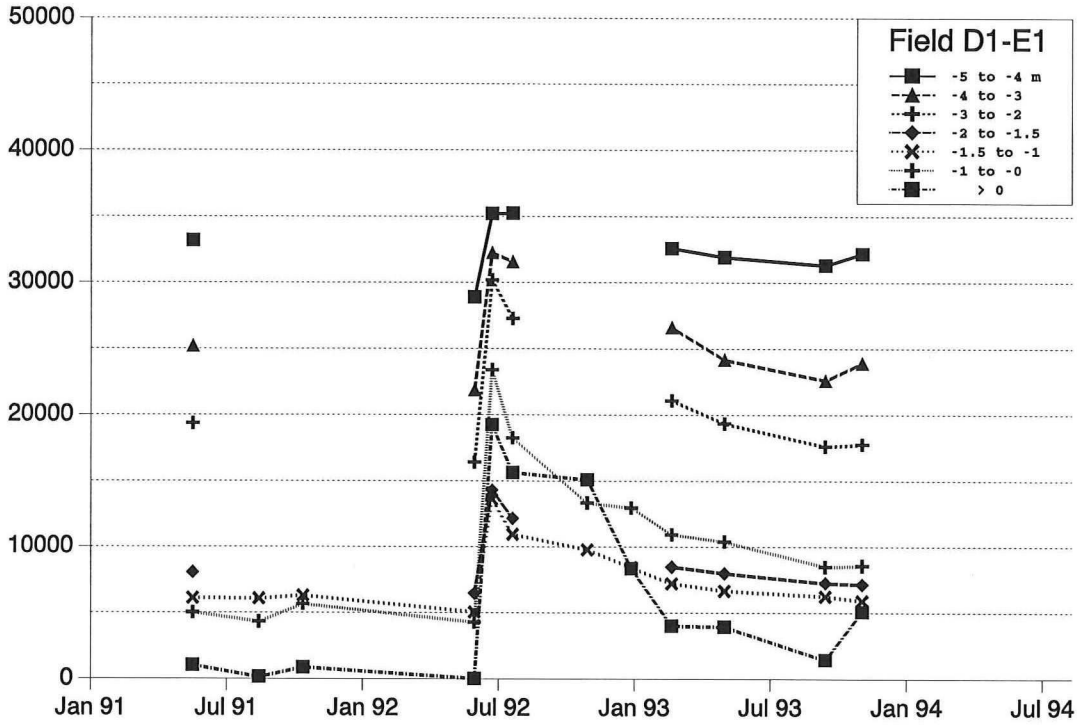

Figure 40*Volumes between the levels for field D1-E1*

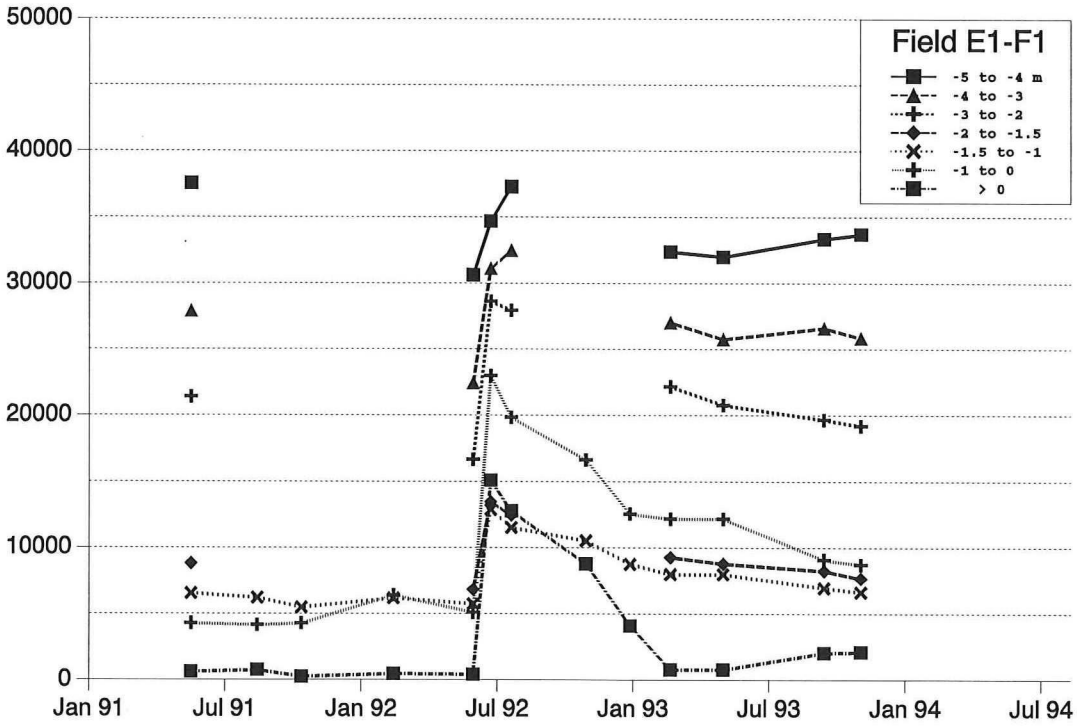

Figure 41*Volumes between the levels for field E1-F1*

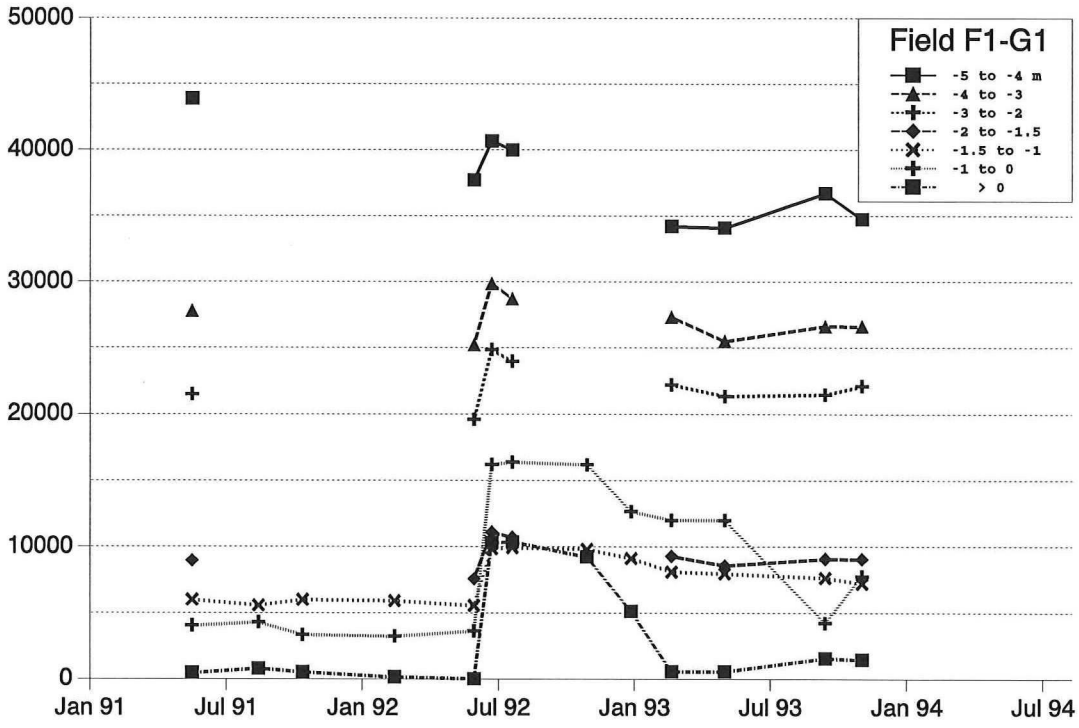

Figure 42 *Volumes between the levels for field F1-G1*

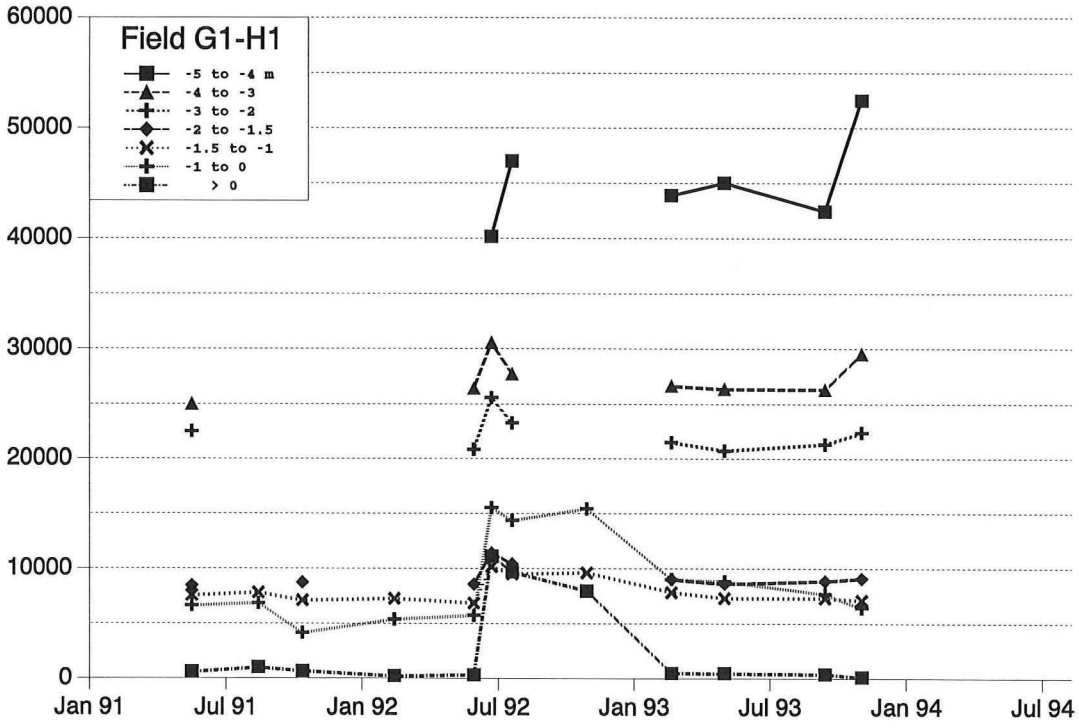

Figure 43 *Volumes between the levels for field G1-H1*

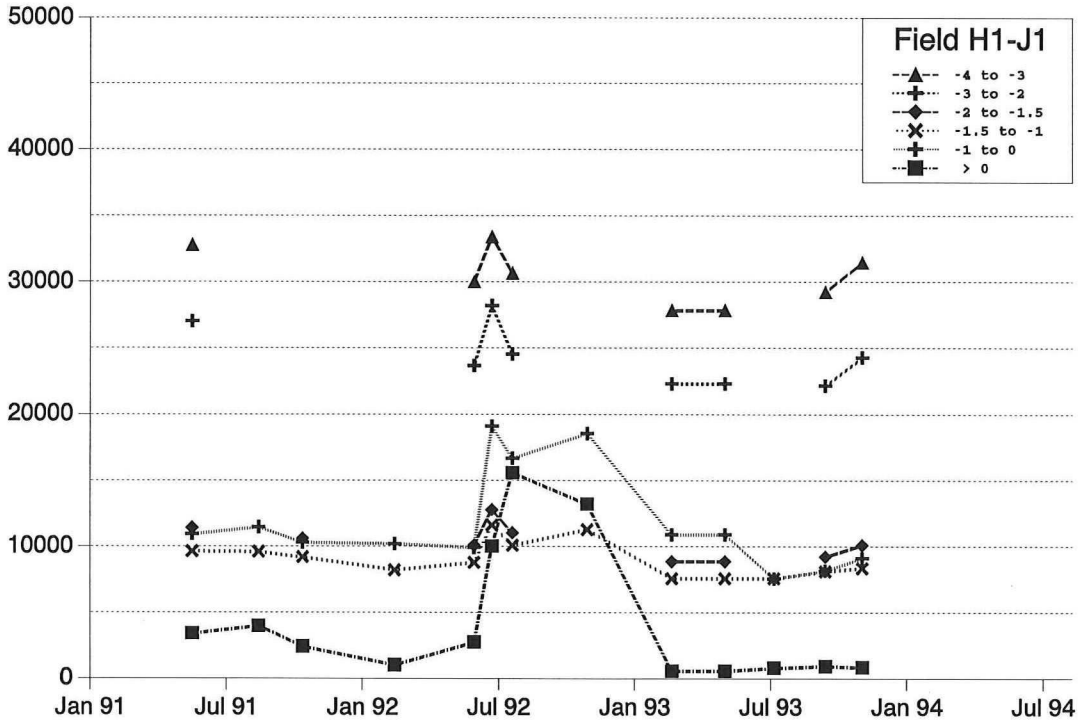

Figure 44*Volumes between the levels for field H1-J1*

Appendix D Example of original volume data

The results of the volume computations are files per groinfield giving the computed volumes above the levels per date. These volumes give the amount of sand above that level in the entire groinfield. As example a part of the file of groinfield D1-E1 is shown below. The first column gives the date of measurement. The integer gives the year of measurement. The fraction gives the part of the year which went by that year up to the moment of measurement. The others the volumes computed above each level. The volumes between two levels have been computed by subtraction of the involving columns. Many times the volumes are computed only down to NN-1.5m. Only just before and a while after the nourishments of 1989 and 1992 the profile measurements are carried out regularly down to NN-5m.

	>NN-5m	>NN-4m	>NN-3m	>NN-2m	>NN-1.5m	>NN-1m	>NN+0m
1980.501	0	0	0	0	10760	6255	1377
1981.430	0	0	0	11685	7208	3818	706
1981.597	0	0	0	0	8756	4391	307
1982.008	0	0	0	0	6228	2415	0
1982.170	0	0	0	0	5991	2142	0
1982.293	0	0	0	0	6611	2789	0
1982.332	0	0	0	0	7620	3935	106
1982.600	0	0	0	0	35089	24952	9125
1982.767	0	0	0	0	28633	19079	5496
1983.011	0	0	0	0	24837	16653	4380
1983.742	0	0	0	0	14588	6929	297
1984.279	0	0	0	0	10005	4097	378
1984.411	106346	68550	40497	18782	10555	4735	513
1985.375	144118	96802	60583	33246	21933	13340	3016
1985.822	0	0	0	0	18410	10930	1887
1986.493	0	0	0	24673	15065	7653	787
1987.411	0	0	0	0	14280	7071	772
1987.740	0	0	0	0	16169	8699	1224
1988.329	0	0	0	0	11435	5251	609
1988.822	0	0	0	0	11990	5722	432
1989.384	99064	64584	38046	18239	11446	6285	908
1989.430	144894	109915	79683	52111	39438	27832	12057
1989.477	139535	103719	74412	48331	36669	26559	11677
1989.534	139279	101505	71541	45943	34601	24623	9987
1989.682	133571	95421	64942	39090	27891	18025	5050
1989.904	126371	89291	59711	35216	24863	15853	3779
1990.301	0	0	0	23777	14760	7517	767
1990.411	112803	75731	46529	23507	14040	6534	796
1990.575	0	0	0	20558	12047	5062	2
1990.822	0	0	0	19678	11820	5472	71
1991.247	0	0	0	0	13354	7180	780
1991.411	97957	64787	39565	20208	12151	6038	1025
1991.658	0	0	0	0	10570	4483	158
1991.822	0	0	0	0	12838	6535	876
1992.460	83001	54107	32211	15819	9348	4306	25
1992.526	168149	132951	100708	70523	56246	42668	19255
1992.603	151044	115814	84236	56952	44809	33868	15623
1992.882	0	0	0	0	38181	28408	15087
1993.044	0	0	0	0	29721	21292	8351
1993.195	110971	78378	51761	30669	22179	14949	4020
1993.392	104482	72562	48372	29015	21013	14339	3947
1993.767	94987	63682	41068	23456	16193	9939	1448